



Univerza v Ljubljani  
Biotehniška fakulteta  
petinsedemdesetletnica

---

Znanost o življenju - znanje za življenje

III

Doktorski  
dan

Bi(●)znanosti

zbornik prispevkov

---

L j u b l j a n a

juni j ■ 2022

## **Tretji doktorski dan Bi(o)znanosti?**

Zbornik prispevkov

Ljubljana, 2022

## **Tretji doktorski dan Bi(o)znanosti?**

### **Zbornik prispevkov**

#### **Založnik zbornika:**

Biotehniška fakulteta  
Jamnikarjeva 101  
1000 Ljubljana

**Uredniki zbornika:** Jure Mravlje, Maja Hostnik, Iva Zahija, Amela Kujović, Pia Starič, Zala Brajnik

#### **Organizacijski odbor:**

Jure Mravlje, Maja Hostnik, Amela Kujović, Pia Starič, Iva Zahija, Zala Brajnik, Vesna Ješe Janežič  
in Programski Svet Bioznanosti

#### **Datum in kraj dogodka:**

7. junij 2022, Biotehniška fakulteta

**Tehnično urejanje zbornika:** Jure Mravlje, Maja Hostnik, Iva Zahija

**Zbornik recenziranih prispevkov** (Recenzirali člani PS Bioznanosti).

**Število strani:** 82

#### **Naklada:**

Elektronska publikacija

#### **Publikacija je dostopna na povezavi:**

<https://repozitorij.uni-lj.si/IzpisGradiva.php?id=137102>

Kataložni zapis o publikaciji (CIP) pripravili v Narodni in univerzitetni knjižnici v Ljubljani

COBISS.SI-ID 110463491

ISBN 978-961-6379-62-5 (PDF)

# KAZALO

## AGRONAMIJA/AGRONOMY

**Vojnovič A. et al:** Spectral responses of three potato (*Solanum tuberosum* L.) cultivars subjected to water-restriction stress in greenhouse..... 1

## AGROŽIVILSKA MIKROBIOLOGIJA/MICROBIOLOGY

**Ramić D. et al:** Targeting biofilm-forming features of *Campylobacter jejuni* with ethanolic extract of *Lavandula angustifolia* ‘Super Blau’ waste material ..... 9

## BIOLOGIJA/BIOLOGY

**Mravlje J. et al:** Decontamination of *Fusarium graminearum* from buckwheat grains with low-pressure cold plasma treatment..... 16

**Rigg R. et al:** It’s the method that counts: Improving estimates of grey wolf abundance in Slovakia ..... 25

## BIOTEHNOLOGIJA/BIOTECHNOLOGY

**Petek B. et al:** Identification of new keratinolytic bacterial isolates by 16S rRNA gene sequencing, FAMES analysis and whole genome sequencing ..... 35

## UPRAVLJANJE GOZDNIH EKOSISTEMOV/MANAGING FOREST ECOSYSTEMS

**Šmidovnik T. and Grošelj P:** Comparison of DEMATEL and WINGS method ..... 41

## ZNANOST O CELICI/CELL SCIENCES

**Kunčič K. et al:** Ultrastructure of septate junctions in arthropod epithelia: comparative analysis of junctions in the hindgut and digestive glands of *Porcellio scaber*..... 48

**Žugec M. and Potokar M.:** Experimental models for studying migratory potential of astrocytes ..... 56

## ZNANOST O ŽIVALIH/ANIMAL SCIENCE

**Pečjak M. et al:** Effect of vitamins E, C and selenium supplementation on gut fermentative activity and gut histology of broiler chickens exposed to cyclic heat stress ..... 65

## ŽIVILSTVO/FOOD SCIENCE

**Mencin M. and Terpinč P.:**Effect of enzymatic treatment on phenolics content and antioxidant activity from spelt (*Triticum spelta* L.) seeds..... 74

## AGRONOMIJA/AGRONOMY

### Spectral responses of three potato (*Solanum tuberosum* L.) cultivars subjected to water-restriction stress in greenhouse

Ana VOJNOVIĆ<sup>1\*</sup>, Janez LAPAJNE<sup>2</sup>, Uroš ŽIBRAT<sup>2</sup>, Matej KNAPIČ<sup>2</sup>, Peter DOLNIČAR<sup>1</sup>, Vladimir MEGLIČ<sup>1</sup>

<sup>1</sup> Agricultural Institute of Slovenia, Crop Science Department, Ljubljana, Slovenia

<sup>2</sup> Agricultural Institute of Slovenia, Plant Protection Department, Ljubljana, Slovenia

\*corresponding author: [ana.vojnovic@kis.si](mailto:ana.vojnovic@kis.si)

### Spectral responses of three potato (*Solanum tuberosum* L.) cultivars under water-restriction stress in greenhouse

**Abstract:** Drought stress is one of the most important abiotic factors reducing crop yields. It affects various morphological, physiological and biochemical processes. Potato (*Solanum tuberosum* L.) is sensitive to water deficit. The aim of our research was to evaluate the spectral response of three potato cultivars under well-watered and water-restriction conditions in a greenhouse experiment. Hyperspectral imaging in the visible and near infrared (VNIR, 400-1000 nm) and shortwave infrared (SWIR, 1000-2500 nm) spectral regions was used to obtain spectral signatures of individual plants. We achieved classification accuracy of up to 81% in distinguishing water regimes and cultivars. The study demonstrates the usefulness of hyperspectral imaging for assessing drought occurrence and distinguishing cultivars. The results are valuable for future work in breeding programmes.

**Key words:** cultivar differentiation; drought stress; hyperspectral imaging; pot experiment remote sensing; *Solanum tuberosum* (L.)

### Spektralni odziv treh sort krompirja (*Solanum tuberosum* L.) pod sušnim stresom v rastlinjaku

**Izveček:** Sušni stres je eden najpomembnejših abiotskih dejavnikov, ki vplivajo na količino pridelka. Izpostavljenost rastlin suši vpliva na različne morfološke, fiziološke in biokemične procese. Krompir (*Solanum tuberosum* L.) je občutljiv na pomanjkanje vode. Namen naše raziskave je bil ovrednotiti spektralni odziv treh sort krompirja pri dobro in slabše zalitih rastlinah v kontroliranih razmerah v rastlinjaku. Za pridobivanje spektralnih podpisov posameznih rastlin smo izvedli hiperspektralno slikanje v vidnem in bližnjem infrardečem (VNIR, 400-1000 nm) in kratkovalovnem infrardečem območju spektra. Pri razlikovanju vodnih režimov in sort smo dosegli do 81 % klasifikacijske natančnosti. Raziskava dokazuje uporabnost hiperspektralnega slikanja za zaznavanje pojava suše in razlikovanje sort. Rezultati bodo uporabni v prihodnjem delu v žlahtniteljskih programih.

**Ključne besede:** daljinsko zaznavanje; hiperspektralno slikanje; lončni poskus; razlikovanje sort; *Solanum tuberosum* (L.); sušni stress

## 1 INTRODUCTION

The potato is one of the world's most important food crops. It is grown in a variety of landscapes, as a high production crop in agriculturally rich parts of the world as well as in harsher environments, such as small farms in the Andean highlands and other similarly remote areas with limited access to agricultural inputs (George et al., 2017; Monneveux et al., 2013). Potatoes (*Solanum tuberosum* L.) are susceptible to water deficit, although some varieties show more drought tolerance (Obidiegwu et al., 2015). Therefore, potato production will likely be affected by climate change. Higher temperatures, changes in water availability and precipitation, and biotic stress factors, such as pests and diseases have negative impact on crop yields and production (Kleinwechter et al., 2016). Drought stress is one of the main abiotic factors reducing crop yields (Hirut et al., 2017). As multidimensional stress it affects several morphological, physiological and biochemical processes (George et al., 2017).

Hyperspectral imaging (HSI) is a non-invasive technique for detection of various stressors, which affect plant health. Stress causes the activation of plant defense mechanisms, which act by changing biophysical and biochemical constituent of plant's tissue (Thomas et al., 2018). Furthermore, these changes manifest as modifications of spectral characteristics. In HSI, sensors capture reflected light, with high spectral resolution, in numerous spectral bands. Typically, it incorporates at least 20 bands, of width 5-20 nm, explicitly distributed throughout the spectrum (Moghimi et al., 2018). Consequently, a lot of spectral bands are acquired at each capture, where bands positions and its range depend on specifications of HSI camera used (Moghadam et al., 2017). The distribution described by discrete spectral bands (i.e. the reflectance at each spectral band) is called spectral signature, and is unique for different objects and materials.

Well-adapted and tolerant cultivars of crops are needed to avoid losses in crop production, due to climate change. However, successful breeding of tolerant cultivars requires a better understanding of plant adaptation to stress and the development of effective phenotyping techniques. The aim of this study was to assess the spectral response of three potato cultivars to a water-restriction stress under greenhouse conditions. We expect more pronounced differences among cultivars and treatments later in season. Findings will be also valuable for future work in breeding programme of the Agricultural institute of Slovenia (AIS).

## 2 MATERIALS AND METHODS

### 2.1. Experimental setup

We conducted the greenhouse experiment from April to August 2020 at the Agricultural Institute of Slovenija (Ljubljana, Slovenia) in a chamber with controlled environmental conditions ( $T = 21\text{ }^{\circ}\text{C}/15\text{ }^{\circ}\text{C}$ ,  $\text{RH} = 60\%$ , photoperiod 14 h light/10 h dark). Three potato cultivars were used in this study: 'KIS Krka' (late, drought tolerant), 'KIS Savinja' (mid-early, sensitive to moderately drought-tolerant) and 'KIS Vipava' (early, drought sensitive). For each cultivar, we used 20 plants, grown from tubers in 5-litre pots filled with *Sphagnum* peat substrate (Potgrond H, Klassmann). At the beginning of the treatment, about five weeks after planting, each pot was watered to field capacity and weighed. The plants were divided into two groups, well-watered conditions (more than 87% of the weight of the saturated substrate) and water-restricted conditions (60–70% of the weight of the saturated substrate). The treatment

lasted for four full weeks. Thereafter, all plants were watered to saturation of the substrate for four more weeks until the experiment was completed. Hyperspectral images were taken twice during the experiment, in Session 1 and Session 2, respectively two and four weeks after the start of the treatment.

## 2.2. Data acquisition

Hyperspectral images were acquired in the VNIR (visible to near infrared) and SWIR (short-wave infrared) spectral regions by using Hyspex pushbroom cameras VNIR-1600 (400–988 nm, 160 bands, bandwidth 3.6 nm) and SWIR-384 (950–2500 nm, 288 bands, bandwidth 5.4 nm). Both were placed together with calibrated halogen lamps at a 3 m distance from the potato plants. The acquisition was carried out in a dark room where no other light sources were present. This ensured a homogeneous light intensity to capture the reflected light with a high signal-to-noise ratio (SNR). Image acquisition followed previously used method (Žibrat et al., 2021). An example of a hyperspectral image in red-green-blue (RGB) is shown in Figure 1 a). Three potato plants and a calibrated reference panel with 20% reflectance, placed on a background with low reflectance (< 5%), were scanned simultaneously. The reference panel was used to convert the radiometrically calibrated radiance image into a reflectance image, i.e. its pixels were normalized to a range between zero and one. We adopted the conversion process and the methods for extracting the spectral signatures from a paper by Lapajne et al., 2022. In this way, a dataset of mean reflectance signatures was created, with each signature representing one potato plant.

Several subsets were created from the complete dataset, e.g. KIS Krka, where only the spectral signatures of the KIS Krka cultivar were considered. Similarly, subsets were created for the cultivars KIS Savinja and KIS Vipava. In each total of 14 potato plants were included, of which half belonged to well-watered and other half to water-restriction treatment. In addition, all subsets were combined to obtain the metrics of a merged subset. In order to be able to compare the results between the two sessions, the subsets and the performance assessments were carried out separately for both. Different subsets were also created to evaluate the effectiveness of classification algorithm of differentiation between different cultivars. More specifically, between three potato cultivars: KIS Krka, KIS Savinja and KIS Vipava. Cultivars were equally represented in all created subsets, so 7 of each were considered in analysis. The metrics were first calculated for well-watered and water-restriction treatment separately and then for their combination. As with the treatment classification, the performance evaluation was carried out independently for each session.

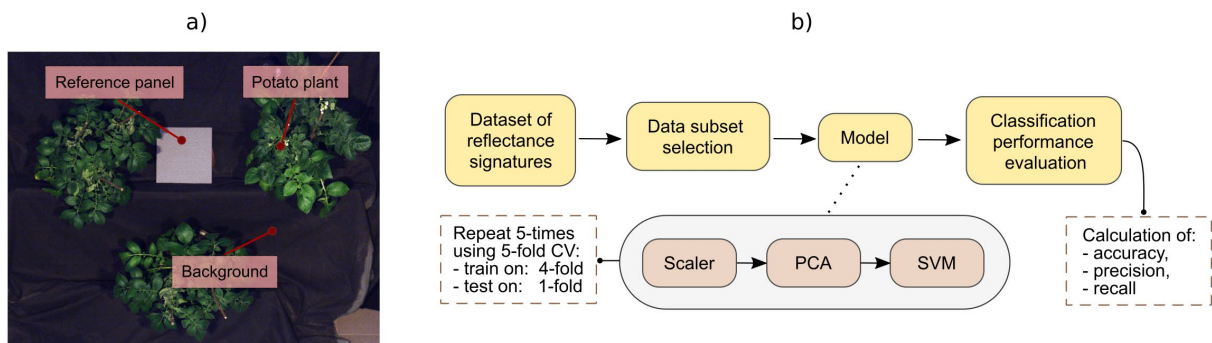


**Figure 1:** a) Hyperspectral image represented in RGB spectrum and b) analysis pipeline.

### 2.3. Analysis

In this study, the analysis is based on the performance of classification algorithm, classifying spectral signatures. The pipeline of methods used is shown schematically in Figure 1 b). Depending on the problem under study, a specific subset of signatures was selected for analysis. Each signature was assigned a ground truth label based on prior knowledge about the corresponding potato plant. Furthermore, the signatures were split in a 5-fold repeated and 5-fold stratified cross-validation (CV). In this way, the hyperparameters of the model were optimized and various metrics: accuracy, precision and recall were calculated. The model consisted of Scaler, Principal component analysis (PCA) and Support vector machines (SVM). Scaler was used to standardize the spectral bands by zeroing their mean and scaling them to a unit variance. PCA was applied to the standardized signatures to reduce the dimensionality space and remove collinearity between adjacent spectral bands (Sawant & Prabukumar, 2020). SVM was chosen for classification as it is one of the most commonly used algorithms in HSI for agricultural purposes (Moghadam et al., 2017; Walton et al., 2019). Hyperparameters of SVM and PCA were optimized during CV step. In SVM, kernel was Radial basis function, the parameter C was optimized in the range between 100 and 1e+6, and the kernel coefficient sigma was optimized in the range between 1e-8 and 0.01. For PCA, the number of principal components was optimized in a range between 1 and 10. The model with the best hyperparameters was used to calculate the classification metrics, i.e. accuracy, precision and recall.

## 3 RESULTS AND DISCUSSION

### 3.1. Spectral signatures

The spectral signatures are shown in Figure 2. It can be seen that plants under water restriction have lower reflectance values in the visible and NIR regions of the spectrum, indicating changes in pigment structure. In addition, KIS Krka also showed lower reflectance values in the SWIR part of the spectrum. In other regions, no significant differences between well-watered and water-restriction treatments were observed. This is consistent with observations on tomato plants under drought (Susič et al., 2018). The spectral ranges in the NIR and SWIR are associated with chemical and physical properties such as carbohydrates, proteins, cellulose and water content (Li et al., 2015; Qiao et al., 2007; Yin et al., 2017).

All cultivars showed more pronounced differences in spectral signatures in Session 1 compared to Session 2. To objectively confirm the visually associated results, we also calculated the Euclidean distances between the two signatures. For Session 1 we obtained 0.117 for KIS Krka, 0.054 for KIS Savinja and 0.056 for KIS Vipava, and for Session 2 0.340 for KIS Krka, 0.122 for KIS Savinja and 0.103 for KIS Vipava. The calculated distances more than doubled for all cultivars between imaging sessions. Moreover, the highest value was obtained for KIS Krka, which was twice as high in Session 1 and three times as high in Session 2, compared to the other two cultivars. The results support our assumption that the changes are most pronounced in Session 2 and that KIS Krka shows the greatest changes when exposed to drought.

HSI data have high redundancy, since it exploits several closely related spectral bands. In classification, it is especially severe when only particular spectral regions change between different classification classes (Sawant & Prabukumar, 2020). To mitigate this problem, we

used PCA to transform the wavelength features into directions of highest variances. Upon examination, we found that the variance described by only the first two principal components exceeded 90% of total variance of the data. Moreover, the first principal component explained at least 60% and second at least 30% of total variance. It exceeded 99% when 10 or more principal components were kept. Therefore, we decided to use maximum of 10 components for classification. PCA also allows us to identify the most important spectral bands by selecting variables according to the magnitude of their loadings (Lapajne et al., 2022).

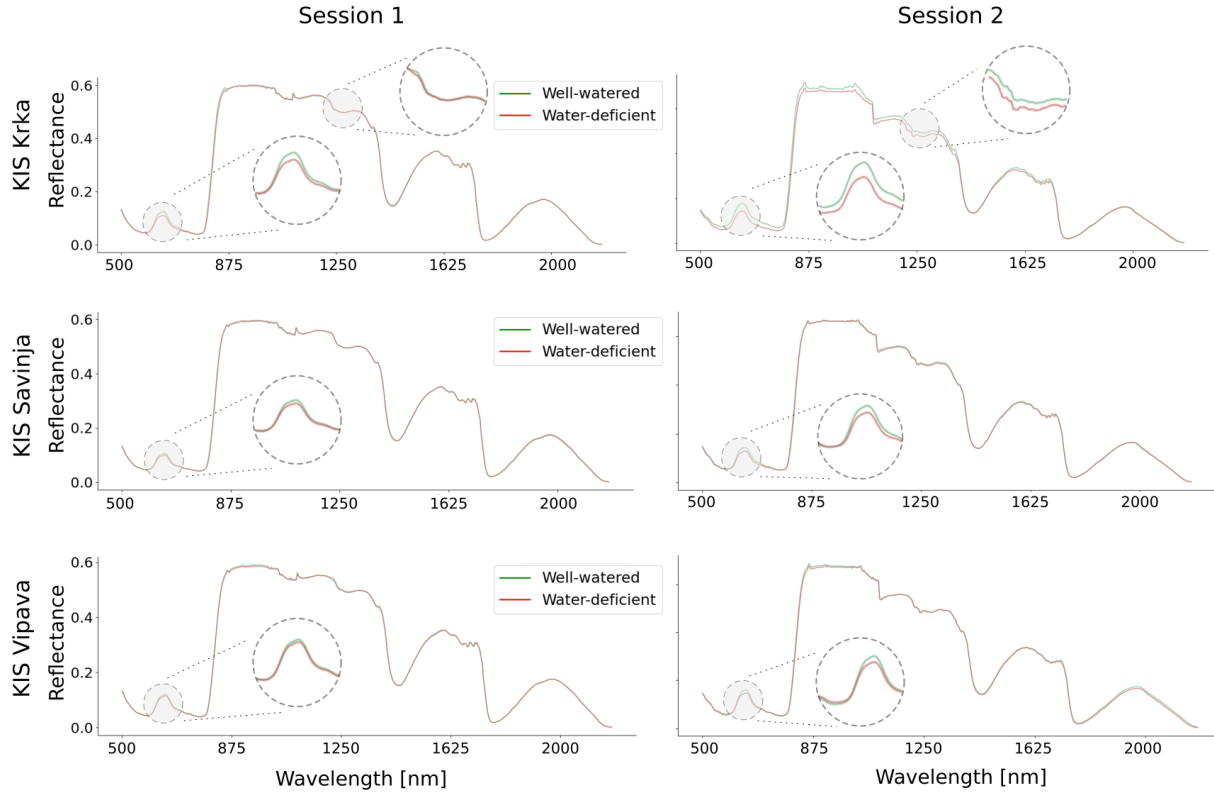


**Figure 2:** Spectral signatures for varieties KIS Krka, KIS Savinja and KIS Vipava for Session 1 and Session 2. The spectral signatures are shown separately for all three cultivars, two treatments and two sessions. Sub-graphs are arranged in a grid, with rows and columns representing cultivars and sessions, respectively. In each graph, an average spectral signature is shown in green for well-watered plants and in red for plants subjected to water-restriction treatment. The most important parts of the spectrum are shown enlarged to show where the difference between the spectral signatures is most pronounced.

### 3.2. Classification performance

Detection of water stress status using hyperspectral imaging achieved an overall success rate of 68%. Overall classification accuracy was higher in Session 2, for all cultivars (Table 1). For KIS Krka the accuracy was 2% higher, for KIS Savinja 7% and for KIS Vipava 10%. The best accuracy of 81% was achieved in Session 2 for the cultivar KIS Krka, and the worst, 57%, for the cultivar KIS Vipava in Session 1. The accuracy achieved was 54% for Session 1 and 67% for Session 2 when all three subsets were pooled.

Discrimination between cultivars was more accurate later in the season (Session 2) and less clear for the water-restriction treatment (Table 2). Consequently, the best result of 81% was obtained in Session 2 for well-watered plants. In addition, accuracy of less than 50% was achieved in both sessions for water-restriction treatment. We suspect that this is due to the

stress to which potato plants were exposed, which shaded spectral differences between cultivars. Interestingly, the accuracy was higher than 70% when both treatments were combined. We think the reason may be the model over-fit on the data or more accurately positioned classification boundaries in case of pooled data by the model. We could confirm our assumption by using a larger dataset, split to training and testing datasets. With plant and leaf senescence reflectance characteristics change (Merzlyak et al., 1999). These changes are associated with the redistribution of resources and the degradation of pigments. In general, the progression of such changes is accelerated in plants under drought, where chlorophyll content is normally reduced (Susič et al., 2018).

**Table 1:** Identification of water stress for all cultivars and both imaging sessions.

Subset	Session	Accuracy	Precision	Recall
KIS Krka	1	0.79	0.78	0.81
	2	0.81	0.75	0.81
KIS Savinja	1	0.65	0.61	0.66
	2	0.72	0.69	0.75
KIS Vipava	1	0.57	0.52	0.57
	2	0.67	0.63	0.69
Pooled	1	0.54	0.54	0.54
	2	0.67	0.70	0.67

**Table 2:** Identification of potato cultivars for both imaging sessions.

Subset	Session	Accuracy	Precision	Recall
Well-watered	1	0.64	0.56	0.67
	2	0.81	0.80	0.82
Water-deficient	1	0.46	0.35	0.45
	2	0.40	0.34	0.41
Pooled	1	0.74	0.77	0.74
	2	0.71	0.75	0.70

#### 4 CONCLUSIONS

In this study, we showed that it is possible to distinguish between different potato cultivars and comparatively accurately detect their watering status. We achieved a classification accuracy of up to 81% for the differentiation of water regime and cultivars. In both cases, classification performance was better later in the season, in Session 2. Better accuracy in discriminating cultivars was achieved in well-watered plants. Classification success in discriminating between treatments was better when the spectral signatures of a single cultivar were used.

The results are valuable for future work in breeding programs. This study also gives a better insight into the potential of remote sensing to assess abiotic stress in potato and the advantages of its use as a non-destructive method for phenotyping. The study was conducted with a small data set and further studies are needed to fully exploit the potential of hyperspectral imaging to better understand the response of different potato cultivars to drought stress.

## ACKNOWLEDGEMENT

The authors acknowledge the financial support from the Slovenian Research Agency (research core funding No. P4-0072 (Agrobiodiversity) and Young researcher grant: A. Vojnović, contract number 1000-21-0401) and by European Union Horizon 2020 Grant Agreement No. 771367 within Ecobreed project.

## 5 REFERENCES

- George, T. S., Taylor, M. A., Dodd, I. C., & White, P. J. (2017). Climate Change and Consequences for Potato Production: a Review of Tolerance to Emerging Abiotic Stress. *Potato Research*, 60(3–4), 239–268. <https://doi.org/10.1007/s11540-018-9366-3>
- Hirut, B., Shimelis, H., Fentahun, M., Bonierbale, M., Gastelo, M., & Asfaw, A. (2017). Combining ability of highland tropic adapted potato for tuber yield and yield components under drought. *PLoS ONE*, 12(7), 1–22. <https://doi.org/10.1371/journal.pone.0181541>
- Kleinwechter, U., Gastelo, M., Ritchie, J., Nelson, G., & Asseng, S. (2016). Simulating cultivar variations in potato yields for contrasting environments. *Agricultural Systems*, 145, 51–63. <https://doi.org/10.1016/j.agsy.2016.02.011>
- Lapajne, J., Knapič, M., & Žibrat, U. (2022). Comparison of Selected Dimensionality Reduction Methods for Detection of Root-Knot Nematode Infestations in Potato Tubers Using Hyperspectral Imaging. *Sensors*, 22(1). <https://doi.org/10.3390/s22010367>
- Li, X., Sun, C., Zhou, B., & He, Y. (2015). Determination of Hemicellulose, Cellulose and Lignin in Moso Bamboo by Near Infrared Spectroscopy. *Scientific Reports*, 5(June), 1–11. <https://doi.org/10.1038/srep17210>
- Merzlyak, M. N., Gitelson, A. A., Chivkunova, O. B., & Rakitin, V. Y. (1999). Non-destructive optical detection of leaf senescence and fruit ripening. *Physiologia Plantarum*, 106(1), 135–141.
- Moghadam, P., Ward, D., Goan, E., Jayawardena, S., Sikka, P., & Hernandez, E. (2017). Plant disease detection using hyperspectral imaging. *DICTA 2017 - 2017 International Conference on Digital Image Computing: Techniques and Applications, 2017-Decem*, 1–8. <https://doi.org/10.1109/DICTA.2017.8227476>
- Moghimi, A., Yang, C., & Marchetto, P. M. (2018). Ensemble Feature Selection for Plant Phenotyping: A Journey from Hyperspectral to Multispectral Imaging. *IEEE Access*, 6, 56870–56884. <https://doi.org/10.1109/ACCESS.2018.2872801>
- Monneveux, P., Ramírez, D. A., & Pino, M. T. (2013). Drought tolerance in potato (*S. tuberosum* L.). Can we learn from drought tolerance research in cereals? *Plant Science*, 205–206, 76–86. <https://doi.org/10.1016/j.plantsci.2013.01.011>
- Obidiegwu, J. E., Bryan, G. J., Jones, H. G., & Prashar, A. (2015). Coping with drought: Stress and adaptive responses in potato and perspectives for improvement. *Frontiers in Plant Science*, 6(JULY), 1–23. <https://doi.org/10.3389/fpls.2015.00542>
- Qiao, J., Ngadi, M. O., Wang, N., Gariépy, C., & Prasher, S. O. (2007). Pork quality and marbling level assessment using a hyperspectral imaging system. *Journal of Food Engineering*, 83.

- Sawant, S. S., & Prabukumar, M. (2020). A survey of band selection techniques for hyperspectral image classification. *Journal of Spectral Imaging*, 9, 1–18. <https://doi.org/10.1255/jsi.2020.a5>
- Susič, N., Žibrat, U., Širca, S., Strajnar, P., Razinger, J., Knapič, M., Vončina, A., Urek, G., & Gerič Stare, B. (2018). Discrimination between abiotic and biotic drought stress in tomatoes using hyperspectral imaging. *Sensors and Actuators, B: Chemical*, 273(June), 842–852. <https://doi.org/10.1016/j.snb.2018.06.121>
- Thomas, S., Kuska, M. T., Bohnenkamp, D., Brugger, A., Alisaac, E., Wahabzada, M., Behmann, J., & Mahlein, A. K. (2018). Benefits of hyperspectral imaging for plant disease detection and plant protection: a technical perspective. *Journal of Plant Diseases and Protection*, 125(1), 5–20. <https://doi.org/10.1007/s41348-017-0124-6>
- Walton, N. S., Sheppard, J. W., & Shaw, J. A. (2019). Using a genetic algorithm with histogram-based feature selection in hyperspectral image classification. *GECCO 2019 - Proceedings of the 2019 Genetic and Evolutionary Computation Conference*, 1364–1372. <https://doi.org/10.1145/3321707.3321748>
- Yin, W., Zhang, C., Zhu, H., Zhao, Y., & He, Y. (2017). Application of near-infrared hyperspectral imaging to discriminate different geographical origins of Chinese wolfberries. *PLoS ONE*, 12(7).
- Žibrat, U., Gerič Stare, B., Knapič, M., Susič, N., Lapajne, J., & Širca, S. (2021). Detection of root-knot nematode meloidogyne luci infestation of potato tubers using hyperspectral remote sensing and real-time pcr molecular methods. *Remote Sensing*, 13(10). <https://doi.org/10.3390/rs13101996>

## AGROŽIVILSKA MIKROBIOLOGIJA/MICROBIOLOGY

### Targeting biofilm-forming features of *Campylobacter jejuni* with ethanolic extract of *Lavandula angustifolia* ‘Super Blau’ waste material

Dina RAMIĆ<sup>1\*</sup>, Iztok DOGŠA<sup>2</sup>, Sonja SMOLE MOŽINA<sup>1</sup>

<sup>1</sup> University of Ljubljana, Biotechnical Faculty, Department of Food Science and Technology, Chair of Biotechnology, Microbiology and Food Safety, Ljubljana, Slovenia

<sup>2</sup> University of Ljubljana, Biotechnical Faculty, Department of Microbiology, Chair of Microbial Ecology and Physiology, Ljubljana, Slovenia

\*corresponding author: [dina.ramic@bf.uni-lj.si](mailto:dina.ramic@bf.uni-lj.si)

#### Targeting biofilm-forming features of *Campylobacter jejuni* with ethanolic extract of *Lavandula angustifolia* ‘Super Blau’ waste material

**Abstract:** *Campylobacter jejuni* is a biofilm-forming, multi-resistant pathogenic bacterium that is widely distributed throughout the food production chain and causes gastrointestinal diseases in humans. Properties important for biofilm formation, such as intercellular signalling, motility and adhesion to different abiotic surfaces, allow *C. jejuni* protection and survival outside its natural habitat. It is necessary to find the right approach to control *C. jejuni* biofilm formation that will reduce the risk that it poses to public health and the food industry. Agri-food by-products present promising bioactives which can be used to control *C. jejuni* biofilms. To test this, we have prepared and tested antimicrobial activity of ethanolic extract from *Lavandula angustifolia* ‘Super Blau’ waste material (LWM) gained after hydrodistillation process of essential oil against *C. jejuni* NCTC 11168 intercellular signalling, motility and adhesion. Indeed, antibacterial activity of LWM was confirmed, with minimal inhibitory concentration 1 mg/mL. We have also confirmed activity against *C. jejuni* intercellular signalling [ $> (30 \pm 2) \%$ ], anti-motility activity ( $> 50 \%$ ) and anti-adhesion activity ( $> 1 \log_{10}$  CFU/mL) of LWM at subinhibitory concentration (0.25 mg/mL). The results confirm the bioactivity of tested ethanolic extract opening the opportunity for further application in *C. jejuni* biofilm control.

**Key words:** adhesion; biofilm control; *Campylobacter jejuni*; intercellular signalling; motility; *Lavandula angustifolia* waste material

#### Obvladovanje filmotvornih lastnosti bakterij *Campylobacter jejuni* z etanolnimi izvlečki odpadnega materiala sivke *Lavandula angustifolia* ‘Super Blau’

**Izveček:** *Campylobacter jejuni* je večkratno odporna, patogena in filmotvorna bakterija, ki je razširjena po celotni živilsko-prehranski oskrbovalni verigi, ter povzroča bolezni prebavil pri ljudeh. Lastnosti, pomembne za tvorbo biofilma, kot so medcelična signalizacija, gibljivost in pritrjevanje na različne abiotične površine, omogočajo zaščito in preživetje *C. jejuni* zunaj naravnega gostitelja. Potrebno je poiskati primerne načine nadzora filmotvornosti bakterij *C.*

*jejuni*, ki bodo zmanjšali tveganje v celotni živilsko-prehranski oskrbovalni verigi. Agroživilski stranski proizvodi predstavljajo obetavne bioaktivne učinkovine, ki jih je mogoče uporabiti za nadzor biofilmov bakterij *C. jejuni*. Da bi to preverili, smo pripravili in preizkusili protimikrobno delovanje etanolnega izvlečka iz odpadnega materiala *Lavandula angustifolia* 'Super Blau' (LWM), pridobljenega po postopku hidrodestilacije eteričnega olja in sicer proti medcelični signalizaciji, gibljivosti in adheziji *C. jejuni* NCTC 11168. Dejansko je bila potrjena antibakterijska aktivnost LWM z minimalno inhibitorno koncentracijo 1 mg/mL. Potrdili smo tudi aktivnost proti medceličnemu signaliziranju *C. jejuni* [ $> (30 \pm 2) \%$ ], aktivnost proti gibljivosti ( $> 50 \%$ ) in proti adheziji aktivnost ( $> 1 \log_{10}$  CFU/mL) LWM pri subinhibitorni koncentraciji (0.25 mg/mL). Rezultati potrjujejo bioaktivnost testiranega etanolnega ekstrakta, ki odpira možnost za nadaljnjo uporabo pri nadzoru biofilmov *C. jejuni*.

**Ključne besede:** *Campylobacter jejuni*; gibljivost; nadzor biofilma; medcelično signaliziranje; odpadni material iz *Lavandula angustifolia*; pritrjevanje

## 1 INTRODUCTION

*Campylobacter jejuni* are one of the most important causative agents of human gastrointestinal diseases since 2005. They are widely distributed throughout whole food production chain and can be found from farm to fork. Many domestic animals are their natural hosts, so the ingestion of undercooked meat or contaminated milk are main sources of the infection (EFSA, 2021). Cross-contamination of food products is also possible, which brings hygiene measures of the food industry into question (Galié et al., 2018). Moreover, *C. jejuni* is biofilm-forming and multi-resistant bacterium making their control even harder, as biofilms are coordinated, functional communities of bacterial cells, which protect bacteria from various environmental stressors. To form biofilms, *C. jejuni* use properties, such as universal intercellular signalling with AI-2 signalling molecules, motility and initial attachment. Additionally, *C. jejuni* can form single-cellular biofilms and multi-cellular biofilms, which enhance its survival (Püning et al., 2021). The burning question of *C. jejuni* control is how to prevent their biofilm formation.

Various approaches are used to control *Campylobacter* in the food production chain, but none of them is fully effective. They include many physical and chemical interventions, the latter, however, raises consumer concerns about unnecessary chemicals in the environment (Carrascosa et al., 2021). It is obvious that new approaches need to be tested and selected. Nowadays, conventional approaches are being replaced with new naturally occurring alternatives, which are recognized as safe (GRAS) and have a broad spectrum of antimicrobial activity. Plant formulations of different origin present an inexhaustible source of bioactive compounds, including agri-food by-products which are known to contain different phytochemicals. Reuse of agri-food by-products in the fight against pathogenic bacteria can be useful also for solving one of the major problems – disposal of agro-food waste (de Elguea-Culebras et al., 2022; Taghian Dinani and van der Goot, 2022).

In this study, *Lavandula* waste material, gained after hydrodistillation of essential oil, was used to produce ethanolic extract (LWM), which was further tested for *C. jejuni* biofilm control. In order to control *C. jejuni* biofilm formation, its critical properties need to be targeted, including

intercellular signalling, motility and adhesion. We assume that motility and adhesion will be decreased if the reduction of the intercellular signalling will be achieved.

## 2 MATERIALS AND METHODS

### 2.1 *Lavandula* waste material and ethanolic extracts preparation

Waste material, gained after hydrodistillation process of essential oil, was from *Lavandula angustifolia* 'Super Blau'. Ethanolic extracts from *Lavandula* waste material (LWM) were prepared by 4 h to 6 h ethanol extraction (Soxhlet extraction) of 20 g dried flowers in 150 mL 96% ethanol. After extraction, ethanol was evaporated and extracts were concentrated in a rotary evaporator (Laborota 4000; Heidolph Instruments, Germany), at 40 °C and 175 mbar pressure, and stored at 4 °C.

### 2.2 Bacterial strains and growth conditions

*Campylobacter jejuni* NCTC 11168 (National Collection of Type Culture), *C. jejuni* 11168 $\Delta$ *luxS* (Plummer, 2012) and biosensor strain *Vibrio harveyi* MM30 (Bassler et al., 1997) were used in this study. The strains were stored at -80 °C in 20% glycerol and 80% Mueller Hinton (MH) broth or autoinducer bioassay (AB) medium. First, *C. jejuni* NCTC 11168 and *C. jejuni* 11168 $\Delta$ *luxS* were sub-cultured on Karmali agar or MH agar supplemented with 30 mg/L kanamycin, respectively, for 24 h under micro-aerobic atmosphere (85% N<sub>2</sub>, 5% O<sub>2</sub>, 10% CO<sub>2</sub>) at 42 °C. Secondly, the strains were cultivated in MH broth at same conditions. After incubation, OD<sub>600</sub> was adjusted at 0.1 (~ 10<sup>7</sup> CFU/mL). 100-fold diluted cultures were used in performed experiments.

### 2.3 Determination of minimal inhibitory concentration (MIC) for LWM

To determine MIC values for LWM formulations against *C. jejuni* NCTC 11168 and *C. jejuni* 11168 $\Delta$ *luxS* we followed the same principles as described in (Ramić et al., 2021). It is of main importance to determine MIC for LWM in planktonic cultures to elect subinhibitory concentrations (1/4 MIC) which were used for further experiments. By the use of subinhibitory concentrations, effect on growth can be avoided and the effect on bacterial properties can be achieved.

### 2.4 Biosensor-based assay – determination of LWM effect on *C. jejuni* intercellular signalling

*V. harveyi* MM30 was used for biosensor assay in order to test the effect of LWM at subinhibitory concentrations on *C. jejuni* intercellular signalling. *Campylobacter jejuni* 11168 $\Delta$ *luxS* was used as negative control, as this strain does not produce AI-2 signalling molecules (Plummer, 2012). *C. jejuni* NCTC 11168 and *C. jejuni* 11168 $\Delta$ *luxS* were cultivated in MH broth or MH broth supplemented with LWM at subinhibitory concentrations under the conditions described in section 2.2. After incubation, cultures were filtrated through 0.2  $\mu$ m syringe filters, to gain cell-free supernatant (CFS) where no bacteria were present. CFS were stored at -80 °C until further experiments. To determine the effect of LWM on *C. jejuni*

intercellular signalling same protocol was used as described in (Šimunović et al., 2020), with some minor modifications. 96-well white microtiter plates with transparent bottom were used and OD<sub>600</sub> for *V. harveyi* MM30 was measured. Bioluminescence was expressed as relative luminescence units (RLU) and measurements were normalized with OD<sub>600</sub> to gain normalized response of *V. harveyi* MM30 (RLU/ OD<sub>600</sub>).

### 2.5 Anti-motility assay

Anti-motility assays was performed as described by Ramić et al. (2021). *C. jejuni* NCTC 11168 was cultivated in MH broth supplemented with LWM in subinhibitory concentrations under the conditions described in section 2.2, afterwards 1 µL of overnight culture was inoculated to the middle of plated soft agar (0.4 %). The plates were incubated for 48 h in a micro-aerobic atmosphere at 42 °C. After this incubation, the diameters of the swarming colonies were measured. The untreated culture was the negative control.

### 2.6 Anti-adhesion assay

To perform anti-adhesion assay, the same principles were used as described before (Ramić et al., 2021). Briefly, adhesion of *C. jejuni* NCTC 11168 was tested in 96-well polystyrene microtiter plates (Nunc 266 120 polystyrene plates; Nunc, Denmark) under the treatment with LWM at subinhibitory concentration. The untreated culture was the negative control. The adhesion of cells was examined as CFU/mL after 24h incubation, as previously described (Šikić Pogačar et al., 2016).

### 2.7 Statistical analysis

All of the experiments were carried out in triplicates as three or more independent experiments. The data are expressed as means ±standard deviation, with analysis using Origin 2018 (OriginLab, Northampton, USA). Statistical analysis was performed in IBM SPSS Statistics 23 (Statsoft Inc., Tulsa, USA). To determine distribution of data Kolmogorov-Smirnov test of normality was performed and statistical significances were determined using Student-t test for two independent means. Results were accepted as significant at *p*-value <0.05.

## 3 RESULTS AND DISCUSSION

Currently we are running out of antimicrobial agents that are effective against bacterial planktonic and biofilm cells. Natural products are promising alternatives which can replace synthetic chemicals in different industries, including food, pharmaceutical, and medical industries. Agri-food industrial by-products are of great interest nowadays, representing an interesting and cheap source of potentially functional bioactive ingredients with particular antimicrobial and antioxidant activities. About 1500 tons of *Lavandula* essential oil is produced annually, resulting in high amounts of waste material which remains after essential oil distillation and is still bioactive (Kivrak, 2018). Therefore, in this study we wanted to prepare and test antimicrobial activity of ethanolic extract from *Lavandula angustifolia* ‘Super Blau’ waste material (LWM) gained after hydrodistillation process of essential oil against *C. jejuni*

NCTC 11168 and its properties important for biofilm formation, i.e. intercellular signalling, motility and adhesion.

Antibacterial activity of LWM against *C. jejuni* was confirmed and MIC was 1 mg of LWM per 1 mL of MH broth. This is moderate and comparable anti-*Campylobacter* activity with other ethanolic extracts originated from postdistillation thyme waste, pinot noir grape skins and seeds, and juniper fruit waste (Klančnik et al., 2017; Šikić Pogačar et al., 2016). It was necessary to determine MIC because in further experiments subinhibitory concentration was used. The chosen concentration was 0.25 mg/mL, the first concentration that did not influence the growth of *C. jejuni*, but affected only its properties.

To test the activity of LWM against *C. jejuni* intercellular signalling, indirect biosensor approach was used with *V. harveyi* MM30 biosensor strain. *C. jejuni* was cultivated with LWM at subinhibitory concentration, afterwards CFS was prepared and added to *V. harveyi* MM30. We confirmed that LWM significantly reduced *C. jejuni* intercellular signalling ( $p < 0.05$ ) for  $(30 \pm 2) \%$  (Figure 1). Consistent with our study, activity against *C. jejuni* intercellular signalling was confirmed for different ethanolic extracts prepared from postdistillation waste material of *Achillea millefolium*, *Urtica dioica*, *Origanum* sp., *Euodia ruticarpa* (Bezek et al., 2016; Šimunović et al., 2020). It is assumed that plant formulations may affect activity of receptor protein or synthase, production of signalling molecules, and degradation of the signalling molecules (Kalia, 2013).

Intercellular signalling, motility and adhesion are interrelated properties important for biofilm formation (Plummer, 2012). Deletion of the *luxS* gene, which synthesizes AI-2, leads to the reduction of motility and adhesion (Elvers and Park, 2002; Reeser et al., 2007), so reduction of *C. jejuni* intercellular signalling can also lead to the reduction of motility and adhesion, which was in this study confirmed. Indeed, LWM had statistically significant anti-motility and anti-adhesion effect ( $p < 0.05$ ), with the reduction of motility for more than 50% and the reduction of adhesion for more than  $1 \log_{10}$  CFU/mL (Figure 1). In our previous study, we have confirmed on molecular level that *L. angustifolia* essential oil decreased gene expression of *C. jejuni* locomotion system (Ramić et al., 2021), which is important for *C. jejuni* motility and adhesion, so it can be expected that LWM had similar effect. Combination of the reduction of *C. jejuni* intercellular signalling with the reduction of motility and adhesion, can lead to the effective reduction of biofilm formation and further spreading of these bacteria throughout whole food production chain increasing food and public health safety.

#### 4 CONCLUSIONS

We have confirmed bioactivity of LWM against *C. jejuni*, one of the leading food-borne pathogen, which suggests that such waste material can be re-used as antimicrobial agent. Our assumption that the reduction of intercellular signalling will lead to the reduction of motility and adhesion was confirmed. Therefore, further efforts can be directed towards search for different agri-food by-products, that can be used as innovative antimicrobials for alternative approaches, which can target bacterial properties important for biofilm formation.

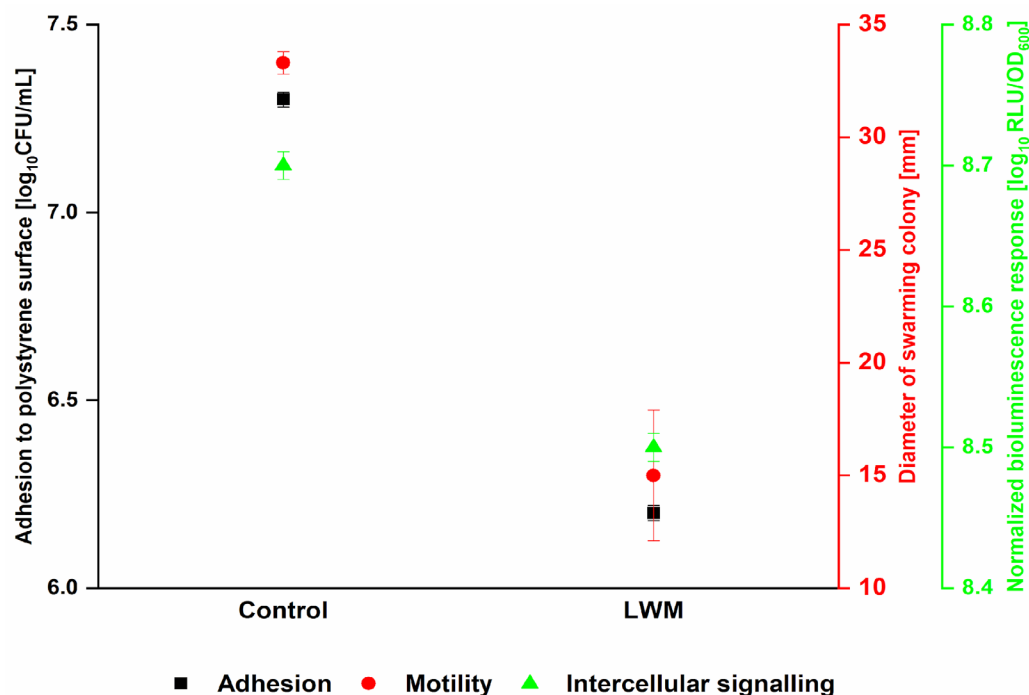


**Figure 1:** Adhesion ( $\log_{10}$  CFU/mL), motility (mm) and intercellular signalling ( $\log_{10}$  RLU/OD<sub>600</sub>) of *Campylobacter jejuni* NCTC 11168 cultivated without or with the addition of LWM at subinhibitory concentration (0.25 mg/mL). Average values are shown  $\pm$ SD.

## 5 REFERENCES

- Bassler, B. L., Greenberg, E. P., & Stevens, A. M. (1997). Cross-species induction of luminescence in the quorum-sensing bacterium *Vibrio harveyi*. *Journal of Bacteriology*, 179(12), 4043–4045. <https://doi.org/10.1128/JB.179.12.4043-4045.1997>
- Bezek, K., Kurinčič, M., Knauder, E., Klančnik, A., Raspor, P., Bucar, F., & Smole Možina, S. (2016). Attenuation of adhesion, biofilm formation and quorum sensing of *Campylobacter jejuni* by *Euodia ruticarpa*. *Phytotherapy Research*, 30(9), 1527–1532. <https://doi.org/10.1002/PTR.5658>
- Carrascosa, C., Raheem, D., Ramos, F., Saraiva, A., & Raposo, A. (2021). Microbial biofilms in the food industry-A comprehensive review. *Int. J. Environ. Res. Public Health*, 18. <https://doi.org/10.3390/ijerph18042014>
- de Elguea-Culebras, G. O., Bravo, E. M., & Sánchez-Vioque, R. (2022). Potential sources and methodologies for the recovery of phenolic compounds from distillation residues of Mediterranean aromatic plants. An approach to the valuation of by-products of the essential oil market – A review. *Industrial Crops and Products*, 175, 114261. <https://doi.org/10.1016/J.INDCROP.2021.114261>
- Elvers, K.T., Park, S.F. (2002). Quorum sensing in *Campylobacter jejuni*: detection of a luxS encoded signalling molecule. *Microbiology (Reading, England)*, 148(Pt 5), 1475–1481. <https://doi.org/10.1099/00221287-148-5-1475>
- Galié, S., García-Gutiérrez, C., Miguélez, E. M., Villar, C. J., & Lombó, F. (2018). Biofilms in the food industry: Health aspects and control methods. In *Frontiers in Microbiology* (Vol. 9, Issue MAY, p. 898). Frontiers Media S.A.

<https://doi.org/10.3389/fmicb.2018.00898>

- Kalia, V. C. (2013). Quorum sensing inhibitors: An overview. *Biotechnology Advances*, 31(2), 224–245. <https://doi.org/10.1016/J.BIOTECHADV.2012.10.004>
- Klančnik, A., Šikić Pogačar, M., Trošt, K., Tušek Žnidarič, M., Mozetič Vodopivec, B., Smole Možina, S. (2017). Anti-Campylobacter activity of resveratrol and an extract from waste Pinot noir grape skins and seeds, and resistance of *Campylobacter jejuni* planktonic and biofilm cells, mediated via the CmeABC efflux pump. *Journal of Applied Microbiology*, 122(1), 65–77. <https://doi.org/10.1111/jam.13315>
- Klančnik, A., Šimunović, K., Sterniša, M., Ramić, D., Smole Možina, S., & Bucar, F. (2021). Anti-adhesion activity of phytochemicals to prevent *Campylobacter jejuni* biofilm formation on abiotic surfaces. In *Phytochemistry Reviews* (Vol. 20, Issue 1, pp. 55–84). Springer Science and Business Media B.V. <https://doi.org/10.1007/s11101-020-09669-6>
- Plummer, P.J. (2012). LuxS and quorum-sensing in *Campylobacter*. *Frontiers in Cellular and Infection Microbiology*, 2, 22. <https://doi.org/10.3389/FCIMB.2012.00022>
- Püning, C., Su, Y., Lu, X., & Götz, G. (2021). Molecular mechanisms of *Campylobacter* biofilm formation and quorum sensing. In *Current Topics in Microbiology and Immunology* (Vol. 431, pp. 293–319). Springer Science and Business Media Deutschland GmbH. [https://doi.org/10.1007/978-3-030-65481-8\\_11](https://doi.org/10.1007/978-3-030-65481-8_11)
- Ramić, D., Bucar, F., Kunej, U., Dogša, I., Klančnik, A., Smole Možina, S. (2021). Antibiofilm potential of *Lavandula* preparations against *Campylobacter jejuni*. *Applied and Environmental Microbiology*, 87(19), 1–18. <https://doi.org/10.1128/AEM.01099-21>
- Reeser, R. J., Medler, R. T., Billington, S. J., Jost, B. H., & Joens, L. A. (2007). Characterization of *Campylobacter jejuni* biofilms under defined growth conditions. *Applied and Environmental Microbiology*, 73(6), 1908–1913. <https://doi.org/10.1128/AEM.00740-06>
- Šikić Pogačar, M., Klančnik, A., Bucar, F., Langerholc, T., Smole Možina, S. (2016). Anti-adhesion activity of thyme (*Thymus vulgaris* L.) extract, thyme post-distillation waste, and olive (*Olea europea* L.) leaf extract against *Campylobacter jejuni* on polystyrene and intestine epithelial cells. *Journal of the Science of Food and Agriculture*, 96(8), 2723–2730. <https://doi.org/10.1002/jsfa.7391>
- Šimunović, K., Ramić, D., Xu, C., Smole Možina, S. (2020). Modulation of *Campylobacter jejuni* motility, adhesion to polystyrene surfaces, and invasion of int407 cells by quorum-sensing inhibition. *Microorganisms*, 8(1). <https://doi.org/10.3390/microorganisms8010104>
- Taghian Dinani, S., van der Goot, A. J. (2022). Challenges and solutions of extracting value-added ingredients from fruit and vegetable by-products: a review. <https://doi.org/10.1080/10408398.2022.2049692>
- The European Union One Health 2020 Zoonoses Report. (2021). *EFSA Journal*, 19(12). <https://doi.org/10.2903/j.efsa.2021.6971>

## BIOLOGIJA/BIOLOGY

### Decontamination of *Fusarium graminearum* from buckwheat grains with low-pressure cold plasma treatment

Jure MRAVLJE <sup>1\*</sup>, Marjana REGVAR <sup>1</sup>, Miran MOZETIČ <sup>2</sup>, Katarina VOGEL-MIKUŠ <sup>1,2</sup>

<sup>1</sup> University of Ljubljana, Biotechnical Faculty, Department of Biology, Ljubljana, Slovenia

<sup>2</sup> Jozef Stefan Institute, Ljubljana, Slovenia

\*corresponding author: [jure.mravlje@bf.uni-lj.si](mailto:jure.mravlje@bf.uni-lj.si)

### Decontamination of *Fusarium graminearum* from buckwheat grains with low-pressure cold plasma treatment

**Abstract:** Fungi from genera *Fusarium* are important phytopathogens that commonly infect crops in the field. Besides causing the decay of plants, many of them are also capable of producing mycotoxins, which can negatively affect our health. The aim of this study was to test cold plasma (CP) treatment for decontamination of *F. graminearum* from buckwheat grains. We used a large-scale custom-made inductively coupled radio frequency plasma system operating under vacuum conditions. We tested two exposure times, 45 and 90 s, and found a 20% and almost 90% reduction in grain contamination, compared to the control, respectively. The longer CP treatment time also significantly suppressed the fungal growth rate. In addition, both CP treatments decreased the germination of buckwheat grains, making this kind of CP treatment applicable in post-harvest (food and feed storage) but not in pre-harvest processes.

**Key words:** fungi; decontamination; cold plasma; *Fusarium*; buckwheat; plant production

### Uporaba nizko-tlačne hladne plazme za dekontaminacijo zrn ajde okuženih z glivo *Fusarium graminearum*

**Izveček:** Glive iz rodu *Fusarium* so pomembni fitopatogeni, ki pogosto okužujejo pridelke na polju. Poleg tega da povzročajo propad rastlin, so mnoge vrste sposobne sinteze mikotoksinov, ki negativno vplivajo na naše zdravje. Namen te študije je bil testirati metodo obdelave s hladno plazmo (HP) za dekontaminacijo glive *F. graminearum* na zrnih ajde. Uporabili smo velik, po meri narejen induktivno sklopljen plazemski sistem z radio frekvenčnim generatorjem, ki deluje v vakuumu. Testirali smo dve časovni izpostavitvi, 45 in 90 s ter ugotovili zmanjšano kontaminacijo zrnja ajde in sicer za 20 % oziroma 90 % v primerjavi s kontrolo. Daljša izpostavitvev HP je prav tako pomembno znižala stopnjo glivne rasti. Vendar pa sta obe časovni izpostavitvi HP hkrati tudi zmanjšali delež kalitve zrnja ajde, zato bi tovrstna obdelava s HP bila uporabna za namene shranjevanja zrnja po žetvi (v prehranske namene), ne pa za nadaljnjo setev na polje.

**Ključne besede:** glive; dekontaminacija; hladna plazma; *Fusarium*; ajda; rastlinska proizvodnja

## 1 INTRODUCTION

Crop grains are frequently infected with fungal propagules, originating either from field or storage (Christensen, 1957) and affecting their quality by suppressing germination or causing spoilage of stored grains (Halloin, 1983). They can also act as primary inoculum for later fungal diseases (Kay & Owen, 1973; Rioux et al., 2014), negatively impacting the whole plant production process. As for most cereals and pseudocereals, fungi present the leading cause of buckwheat diseases at all stages, from germination to harvest and post-harvest stages. Especially problematic are field fungi and soil parasites that can cause the decay of grains or the later rotting of the seedlings (Milevoj, 1989). Among them are *Fusarium* species, which represent one of the most economically important genera of phytopathogenic fungi that naturally contaminate many cereal grains (Ferrigo et al., 2016). They are widespread pathogens on small-grain cereals worldwide, causing root, stem, and ear rot and resulting in major reductions in crop yield (Bottalico & Perrone, 2002). *Fusarium* species are frequently isolated from buckwheat grains and associated with many diseases (Kalinova et al., 2004; Milevoj, 1989; Mills & Wallace, 1971; Singh et al., 1984). Besides being plant pathogens, they are also problematic as many fungi from the genus *Fusarium* can produce toxic secondary metabolites – mycotoxins, which are harmful to humans and animals. Their ingestion can induce acute intoxication, causing severe sickness or even death, or chronic effects (genotoxic and mutagenic), even carcinogenic in some cases (Fung & Clark, 2004). Mycotoxins from the genus *Fusarium* have traditionally been associated with temperate cereal crops as these fungi require somewhat lower temperatures for growth and mycotoxin production compared to some other mycotoxigenic fungi (Placinta et al., 1999). The most important and widespread groups of mycotoxins in small-grain cereals produced by *Fusarium* spp. include trichothecenes (such as deoxynivalenol (DON), nivalenol (NIV), T-2 toxin and HT-2 toxin), zearalenone (ZEN), moniliformin (MON) and fumonisins (Bottalico & Perrone, 2002; Placinta et al., 1999). Amongst them, DON, ZEA and fumonisins are believed to be three of the five most agriculturally-important fungal toxins. DON is probably the most widely distributed mycotoxin in food and feed, as it occurs almost wherever cereal crops are grown (Miller, 1995). *Fusarium* diseases that affect cereal crops are caused by several individual *Fusarium* species or, more commonly, different co-occurring species (Ferrigo et al., 2016). One of the most problematic diseases caused by *Fusarium* species worldwide is the “*Fusarium* head blight (FHB)” of small-grain cereals, also from the mycotoxicological point of view due to the potential accumulation of mycotoxins in grains intended for foods and feeds (Bottalico & Perrone, 2002). FHB is associated with moderate temperatures and the presence of high humidity in grain-growing regions, and although there are many different *Fusarium* species associated with FHB, the primary and most aggressive causal agent of FHB worldwide is *F. graminearum* (Ferrigo et al., 2016). This species is most prevalent in southern Europe, and can produce many different mycotoxins, including DON, NIV, and ZEN (Bottalico & Perrone, 2002; Ferrigo et al., 2016).

Traditionally, seeds and grains are treated by fungicides, which is still the most effective and widely used method to prevent and suppress fungal growth (Mancini & Romanazzi, 2014). However, all these chemical substances leave undesirable residues and negatively impact the environment and human health; therefore, new technologies are needed in light of reducing the usage of pesticides. The emerging use of cold plasma technology offers promising solutions for the decontamination of fungi and their toxins (Mravlje et al., 2021a). Cold plasma (CP) is an ionised gas, also referred to as the fourth state of matter, consisting of electrons, atoms, ions,

radicals, and other molecules coexisting with UV photons and visible light (Piel, 2010). All these components give CP unique properties, and although it has no net charge, it conducts electricity (Tendero et al., 2006). CP is generated by applying energy to a gas, either as thermal or electrical energy (Conrads & Schmidt, 2000). The beforementioned active chemical species in CP have efficient antimicrobial properties and can be utilised for surface sterilisation, e.g., decontamination of fungi from the surface of the grains (Mravlje et al., 2021a).

This research aimed to test surface decontamination of Common buckwheat (*Fagopyrum esculentum* Moench) grains artificially infected with *F. graminearum*. Common buckwheat is a traditional crop grown in Slovenia, and much of Europe and Asia often referred to as an alternative crop. It has numerous positive and beneficial effects on human health, as it has a very high nutritional value (rich in proteins and phenolics) (Kreft et al., 2020) and is gluten-free, therefore safe for consumption by celiac patients (Skerritt, 1986). And since the interest in functional foods is growing, buckwheat production is again rapidly increasing in Europe and worldwide, as it is also suitable for organic farming due to its modest growing demands (Popović et al., 2014). All these properties make buckwheat an excellent alternative crop in the light of increasing trends towards sustainable and environmentally friendly agriculture, which also tends to limit the use of chemical fertilisers and pesticides. And because fungal infections possess a significant threat to (pseudo) cereals and their products meant for foods and feeds, new approaches are needed to eliminate their growth on grains, one of such could be the use of CP technology.

## 2 MATERIALS AND METHODS

### 2.1 Origin of Buckwheat Grains

Grains were obtained from Rangus Mill (Šentjernej, Slovenia, about 230 m a.s.l.). They were harvested in 2019 and stored under suitable conditions (in a dry and dark environment at room temperature) until the experiments were performed in 2022.

### 2.2 Grain Contamination Procedure

First, the pre-decontamination process was performed to eliminate the possible growth of naturally occurring microorganisms on the grains' surface. Grains were initially surface sterilised with 30 % hydrogen peroxide for 20 min and then rinsed three times with sterile distilled water. Grains were then dried under a laminar flow overnight. A pure isolate of *Fusarium graminearum* (FG; strain NAX03, obtained from our collection of buckwheat fungal isolates) was grown on 2% Potato Dextrose Agar (PDA) at room temperature (24 °C) in the dark for 7 days. Spores of *F. graminearium* were obtained by adding 5 mL of sterile distilled water mixed with one drop of Tween80 and scraping a 7-day-old culture of fungus growing on PDA. The spore suspension was estimated to be  $10^4$ /mL via counting under the microscope using a Neubauer chamber (Zhang et al., 2020). Surface sterilised buckwheat grains were immersed in this spore suspension and vigorously shaken using a rotary shaker for 20 min. Afterwards they were air-dried overnight in sterile Petri dishes in a laminar flow hood.

### 2.3 Cold Plasma Treatment of Grains

CP treatment of buckwheat grains was carried out in a low-pressure cold plasma system with an inductively coupled RF-generator described in (Mravlje et al., 2021b), using pure oxygen as a feeding gas. CP treatment times were 0 (control group), 45, and 90 seconds. Immediately after CP treatment, grains were packed in sterile PVC bags to prevent contamination from the environment.

### 2.4 Decontamination Test

For the cultivation of fungi, we used the direct agar plate (“Ulster”) method to evaluate grain contamination and fungal growth level. Sterile Petri dishes (diameter of 70 mm) containing 2% PDA supplemented with the antibiotic chloramphenicol (50 mg L<sup>-1</sup>) were used. For each group of grains, five buckwheat grains were placed in a circle evenly distributed around 2 cm from the edge of the dish. Three groups of grains were tested: the control group (grains contaminated with FG and not treated with CP), 45 s and 90 s CP grains previously infected with FG. For each group of grains, the test was performed in fifteen replicants. Plates were incubated at a temperature of 24 °C in dark conditions for one week. After one week, the percentage of contaminated grains (CG) was calculated according to Equation 1.

$$(1) \text{ CG (\%)} = (\text{number of colonised grains}) / (\text{total number of grains}) \times 100$$

Also, the average level of fungal growth was measured (expressed in mm<sup>2</sup>) around each grain using the free software program ImageJ. Based on these measurements, the average fungal growth area (FGA) around grain was calculated according to Equation 2:

$$(2) \text{ FGA (mm)} = (\sum \text{ surface of fungal growth areas around the contaminated grains [mm]}) / (\text{number of contaminated grains})$$

### 2.4 Germination Test

In germination tests, 20 grains from each group were placed into Petri dishes (diameter 70 mm) with two layers of filter paper and moistened with 3 mL of distilled water. For each group of grains, the germination test was performed in five replicates. The grains were incubated in plant growth chambers at 22 °C, with 60% humidity, in the dark. The germinated grains were counted after one week and the germination percentage (GP%) was calculated according to Equation 3.

$$(3) \text{ GP (\%)} = (\text{number of germinated grains}) / (\text{total number of grains}) \times 100$$

### 2.5 Statistical Analysis

All results reported are expressed as mean ± standard error (SE). Statistical significance between groups of grains (different treatments) was determined using a one-way analysis of variance (ANOVA) with Duncan’s post hoc test (using Statistica StatSoft version 7). The significance level was considered at a p-value of less than 0.05.

## 3 RESULTS AND DISCUSSION

CP treatment of contaminated buckwheat grains infected with FG significantly affected the degree of fungal contamination (Figure 1). After 45 s CP treatment, around 80% of grains

remained contaminated with FG, while after 90 s CP treatment, only 5% of grains were still infected with FG (Figure 2a). The CP treatment not only reduced the percentage of contaminated grains but also resulted in a lower average fungal growth area around each grain (Figure 2b). After 45 s CP treatment, the average fungal growth area was comparable to the control group, whereas after 90 s CP treatment, the average fungal growth area was less than 10% of the control group. To our best knowledge, there have been only a few publications about decontamination of *Fusarium* sp. on grains with CP treatment. The majority of authors used the atmospheric-pressure dielectric barrier discharge (DBD) type of cold plasma (Homa et al., 2021; Šerá et al., 2019; Świecimska et al., 2020; Zahoranová et al., 2016; Zahoranová et al., 2018), so the results are hard to compare with ours.

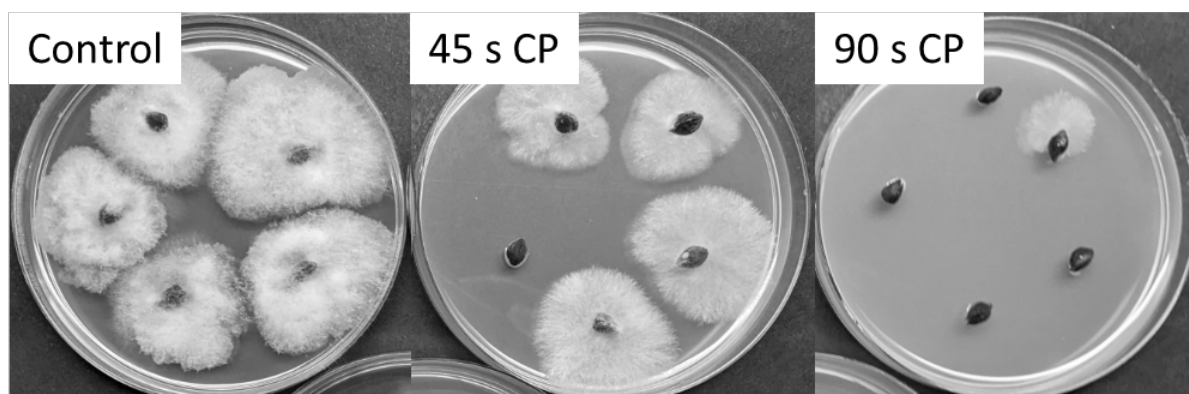


**Figure 1:** A representative photograph of *Fusarium graminearum* growth around buckwheat grains on PDA medium after 1-week of cultivation in control, 45 s and 90 s CP treated grains.

The contamination with *F. culmorum* reduced to around 70% of initial contamination after 30 s CP treatment and to less than 5% after 60 s CP treatment in artificially wheat seeds (A. Zahoranová et al., 2016). After 90 s CP treatment, growth of both *F. culmorum* and *F. nivale* was completely inhibited. Similarly was confirmed for artificially contaminated maize seeds, where *F. culmorum* was inhibited entirely after 120 s CP treatment (Zahoranová et al., 2018). It was also demonstrated that CP is efficient in the decontamination of *Fusarium* spp. on pine seeds (Šerá et al., 2019; Świecimska et al., 2020). Already a few second CP treatment times can reduce the infection with *F. circinatum*, while 60 s treatment time led to complete inhibition (Šerá et al., 2019). Similarly was found in the case of pine seeds contaminated *F. oxysporum*, where almost complete decontamination (more than 90% efficiency) was observed already after 3 s CP treatment time (Świecimska et al., 2020). Recently, there has been some research about the effects of plasma-activated water (PAW) on *F. graminearum* decontamination (Guo et al., 2022). They showed that PAW is an effective disinfection procedure against *F. graminearum*. It reduced spore germination and fungal growth *in vitro* (in suspension) and disease symptoms on wheat spikelets *in vivo*.

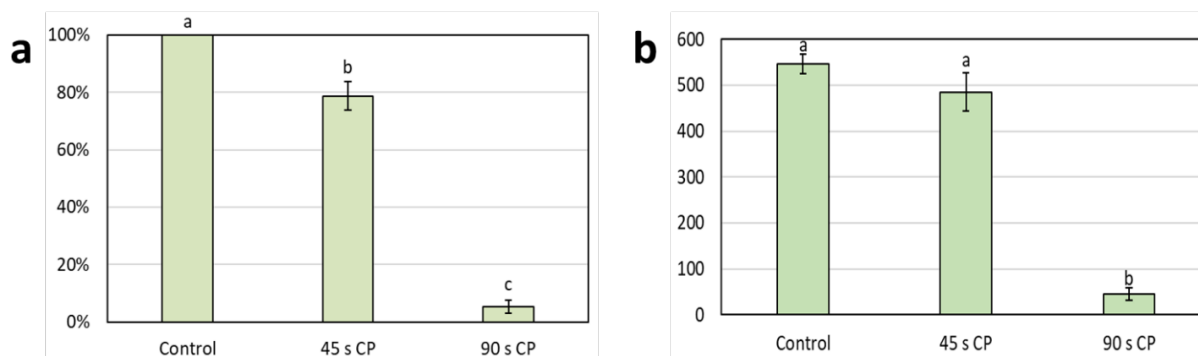


**Figure 2:** Fungal contamination in control, 45 s and 90 s CP treated buckwheat grains expressed as: (a) percentage (%) of contaminated grains (N=75); (b) average area of fungal growth around a single grain (N depends on the number of contaminated grains: 75 in control, 62 in 45 s CP treatment, and 9 in 90 s CP treatment). Different letters indicate statistically significant differences between groups of grains.

CP treatment of buckwheat grains also resulted in lower germination (Table 1). In the control group germination was 96%, while after 45 s CP treatment, it decreased to 73% and after 90 s CP treatment, only around one-third of control grains still germinated.

**Table 1:** Germination percentage (%) in control, 45 s and 90 s CP treated buckwheat grains after one week (N=100). Different letters indicate statistically significant differences between groups of grains.

Treatment	Germination [%]
Control group	96,0 ± 2,4 <sup>a</sup>
45 s CP treatment	73,0 ± 4,6 <sup>b</sup>
90 s CP treatment	27,0 ± 5,1 <sup>c</sup>

It is almost impossible to compare the effects of our CP system on the germination of different seeds and grains with the published data, as the type of plasma apparatus and the parameters of the plasma treatment having a significant impact on the obtained results, are very diverse amongst various studies (Šerá et al., 2019). It was shown that there were significant differences in germination and early growth of buckwheat grains when treated with a different type of plasma apparatus (Šerá et al., 2012). However, also the majority of other authors who examined CP treatment for *Fusarium* spp. decontamination efficacy observed a reduction in seed germination with prolonged CP treatment time: after 60 s in wheat (Zahoranová et al., 2016) and 120 s in maize (Zahoranová et al., 2018). As for pine seeds, which are a lot smaller, treatments longer than 10 s caused decreased germination and almost complete cessation after 60 s treatment (Šerá et al., 2019; Świecimska et al., 2020).

#### 4 CONCLUSIONS

The results reported in this study present the first evidence of a low-pressure cold plasma use for the inactivation of artificially contaminated buckwheat grains. We demonstrated that already shorter CP treatment times (45 s) significantly reduce the degree of contamination with *Fusarium graminearum*. Longer CP treatment times (90 s) reduced contamination to less than 10% of control and substantially suppressed the growth of surviving fungi. In addition, longer CP treatment times decreased the germination of buckwheat grains, so the CP treatment as used in our study would be applicable for treating buckwheat for foods and feeds but not for further sowing.

## ACKNOWLEDGEMENT

The authors acknowledge the financial support from the Slovenian Research Agency (ARRS) within the framework of research programs P1-0212 (Plant biology) and P2-0082 (Thin-film structures and plasma surface engineering), projects (J1-3014 and N1-0105) and young researcher grant (Jure Mravlje).

## 5 REFERENCES

- Bottalico, A., & Perrone, G. (2002). Toxigenic *Fusarium* species and mycotoxins associated with head blight in small-grain cereals in Europe. *European Journal of Plant Pathology*, *108*(7), 611–624. <https://doi.org/10.1023/A:1020635214971>
- Christensen, C. M. (1957). Deterioration of Stored Grains by Fungi. *Botanical Review*, *23*(2), 108–134.
- Conrads, H., & Schmidt, M. (2000). Plasma generation and plasma sources. *Plasma Sources Science and Technology*, *9*(4), 441–454. <https://doi.org/10.1088/0963-0252/9/4/301>
- Ferrigo, D., Raiola, A., & Causin, R. (2016). *Fusarium* toxins in cereals: Occurrence, legislation, factors promoting the appearance and their management. *Molecules*, *21*(5). <https://doi.org/10.3390/molecules21050627>
- Fung, F., & Clark, R. F. (2004). Health effects of mycotoxins: A toxicological overview. *Journal of Toxicology - Clinical Toxicology*, *42*(2), 217–234. <https://doi.org/10.1081/CLT-120030947>
- Guo, J., Wang, J., Xie, H., Jiang, J., Li, C., Li, W., Li, L., Liu, X., & Lin, F. (2022). Inactivation effects of plasma-activated water on *Fusarium graminearum*. *Food Control*, *134*. <https://doi.org/10.1016/j.foodcont.2021.108683>
- Halloin, J. M. (1983). *Deterioration Resistance Mechanisms in Seeds*. 335–339.
- Homa, K., Barney, W. P., Davis, W. P., Guerrero, D., Berger, M. J., Lopez, J. L., Wyenandt, C. A., & Simon, J. E. (2021). Cold plasma treatment strategies for the control of *fusarium oxysporum* f. sp. *basilici* in sweet basil. *HortScience*, *56*(1), 42–51. <https://doi.org/10.21273/HORTSCI15338-20>
- Kalinova, J., Voženilkova, B., & Moudry, J. (2004). Occurrence of *Fusarium* spp and bacteria on surface of buckwheat achenes (*Fagopyrum esculentum* Moench). *Proceedings of the 9th International Symposium on Buckwheat, January 2004*, 491–493.
- Kay, J. G., & Owen, H. (1973). Transmission of *Rhynchosporium secalis* on barley grain. *Transactions of the British Mycological Society*, *60*(3), 405–411. [https://doi.org/10.1016/s0007-1536\(73\)80025-7](https://doi.org/10.1016/s0007-1536(73)80025-7)
- Kreft, I., Zhou, M., Golob, A., Germ, M., Likar, M., Dziedzic, K., & Luthar, Z. (2020). Breeding buckwheat for nutritional quality. *Breeding Science*, *70*(1), 67–73. <https://doi.org/10.1270/jsbbs.19016>
- Mancini, V., & Romanazzi, G. (2014). Seed treatments to control seedborne fungal pathogens of vegetable crops. *Pest Management Science*, *70*(6), 860–868. <https://doi.org/10.1002/ps.3693>
- Milevoj, L. (1989). Buckwheat diseases. In I. Kreft (Ed.), *Fagopyrum (Buckwheat newsletter)*

(Vol. 9, pp. 31–40). Biotehniška fakulteta.

- Miller, J. D. (1995). Fungi and mycotoxins in grains: Implication for stored product research. *Journal of Stored Products Research*, 31(1), 1–16. [https://ac.els-cdn.com/0022474X9400039V/1-s2.0-0022474X9400039V-main.pdf?\\_tid=b51cfb5d-6589-4fbd-af12-d4e48122268b&acdnat=1548347680\\_9e581aef0cc8da1a253b927646de1f62](https://ac.els-cdn.com/0022474X9400039V/1-s2.0-0022474X9400039V-main.pdf?_tid=b51cfb5d-6589-4fbd-af12-d4e48122268b&acdnat=1548347680_9e581aef0cc8da1a253b927646de1f62)
- Mills, J. T., & Wallace, H. A. H. (1971). Microflora of buckwheat seed, changes in storage and effect of seed treatments on seedling emergence. *Canadian Plant Disease Survey*, 51(4), 154–158.
- Mravlje, J., Regvar, M., Starič, P., Mozetič, M., & Vogel-Mikuš, K. (2021). Cold plasma affects germination and fungal community structure of buckwheat seeds. *Plants*, 10(5). <https://doi.org/10.3390/plants10050851>
- Mravlje, J., Regvar, M., & Vogel-Mikuš, K. (2021). Development of cold plasma technologies for surface decontamination of seed fungal pathogens: Present status and perspectives. *Journal of Fungi*, 7(8). <https://doi.org/10.3390/jof7080650>
- Piel, A. (2010). Plasma Physics. In *Springer* (Vol. 53, Issue 9). <https://doi.org/10.1017/CBO9781107415324.004>
- Placinta, C. M., Mello, J. P. F. D., & Macdonald, A. M. C. (1999). A review of worldwide contamination of cereal grains and animal feed with *Fusarium* mycotoxins. *Animal Feed Science and Technology*, 78, 21–37.
- Popović, V., Sikora, V., Berenji, J., Filipović, V., Dolijanović, Ž., Ikanović, J., & Dončić, D. (2014). Analysis of buckwheat production in the world and Serbia. *Ekonomika Poljoprivrede*, 61(1), 53–62. <https://doi.org/10.5937/ekopolj1401053p>
- Rioux, R. A., Shultz, J., Garcia, M., Willis, D. K., Casler, M., Bonos, S., Smith, D., & Kerns, J. (2014). *Sclerotinia homoeocarpa* Overwinters in turfgrass and is present in commercial seed. *PLoS ONE*, 9(10). <https://doi.org/10.1371/journal.pone.0110897>
- Šerá, B., Zahoranová, A., Bujdáková, H., & Šerý, M. (2019). Disinfection from pine seeds contaminated with *fusarium circinatum* nirenberg & O'Donnell using non-thermal plasma treatment. *Romanian Reports in Physics*, 71(1), 1–12.
- Šerá, Božena, Gajdová, I., Černák, M., Gavril, B., Hnatiuc, E., Kováčik, D., Kříha, V., Sláma, J., Šerý, M., & Špatenka, P. (2012). How various plasma sources may affect seed germination and growth. *Proceedings of the International Conference on Optimisation of Electrical and Electronic Equipment, OPTIM, May*, 1365–1370. <https://doi.org/10.1109/OPTIM.2012.6231880>
- Singh, P. N., Sindhu, I. R., & Singhal, G. (1984). Fungi recorded from seeds and seedlings of *Fagopyrum esculentum*. In *Journal of Indian Botanical Society* (Vol. 63, Issue 3, pp. 236–243).
- Skerritt, J. H. (1986). Molecular Comparison of Alcohol-Soluble Wheat and Buchwheat Proteins. *Cereal Chemistry*, 63(4), 365–369.
- Świecimska, M., Tulik, M., Šerá, B., Golińska, P., Tomeková, J., Medvecká, V., Bujdáková, H., Oszako, T., Zahoranová, A., & Šerý, M. (2020). Non-thermal plasma can be used in disinfection of scots pine (*Pinus sylvestris* L.) seeds infected with *fusarium oxysporum*. *Forests*, 11(8), 1–11. <https://doi.org/10.3390/fl1080837>

- Tendero, C., Tixier, C., Tristant, P., Desmaison, J., & Leprince, P. (2006). Atmospheric pressure plasmas: A review. *Spectrochimica Acta - Part B Atomic Spectroscopy*, 61(1), 2–30. <https://doi.org/10.1016/j.sab.2005.10.003>
- Zahoranová, A., Henselová, M., Hudecová, D., Kaliňáková, B., Kováčik, D., Medvecká, V., & Černák, M. (2016). Effect of Cold Atmospheric Pressure Plasma on the Wheat Seedlings Vigor and on the Inactivation of Microorganisms on the Seeds Surface. *Plasma Chemistry and Plasma Processing*, 36(2), 397–414. <https://doi.org/10.1007/s11090-015-9684-z>
- Zahoranová, Anna, Hoppanová, L., Šimončicová, J., Tučeková, Z., Medvecká, V., Hudecová, D., Kaliňáková, B., Kováčik, D., & Černák, M. (2018). Effect of Cold Atmospheric Pressure Plasma on Maize Seeds: Enhancement of Seedlings Growth and Surface Microorganisms Inactivation. *Plasma Chemistry and Plasma Processing*, 38(5), 969–988. <https://doi.org/10.1007/s11090-018-9913-3>
- Zhang, M., Gu, L., Zheng, P., Chen, Z., Dou, X., Qin, Q., & Cai, X. (2020). Improvement of cell counting method for Neubauer counting chamber. *Journal of Clinical Laboratory Analysis*, 34(1), 1–6. <https://doi.org/10.1002/jcla.23024>

## It's the method that counts: Improving estimates of grey wolf abundance in Slovakia

Robin RIGG<sup>1\*</sup>, Barbara BOLJTE<sup>1</sup>, Maja JELENČIČ<sup>1</sup>, Marjeta KONEC<sup>1</sup>, Tomaž SKRBINŠEK<sup>1</sup>

<sup>1</sup> University of Ljubljana, Biotechnical Faculty, Biology Department, Ljubljana, Slovenia

\* corresponding author: [info@slovakwildlife.org](mailto:info@slovakwildlife.org)

### It's the method that counts: Improving estimates of grey wolf abundance in Slovakia

**Abstract:** Obtaining reliable data on key population parameters is fundamental to wildlife management. In Slovakia, there has been considerable controversy regarding the status of the grey wolf (*Canis lupus*). Estimates of abundance based on hunters' reports differ by an order of magnitude from those of environmentalists and both lack replicable scientific methodology. We used noninvasive genetic sampling, microsatellite genotyping and mark-recapture modelling to estimate numbers of wolves in the Liptov region (1,988 km<sup>2</sup>) and compared our results with official hunting statistics compiled from hunters' reports. We genotyped samples (n=698) at 16 canine unlinked autosomal microsatellite loci and the Amelogenin locus for sex determination. Using the Capwire mark-recapture model we obtained, for the first time in Slovakia, a statistically robust estimate of wolf abundance: 49 individuals (40–69, 95% CI) in c.14% of occupied wolf range in 2015/16. Comparable results for the following two seasons indicated the population to be stable or slightly increasing. Official hunting statistics were more than 5-times greater than our genetic mark-recapture estimates. We conclude that the choice of method has a major influence on the reliability of population size estimation. This is of paramount importance for monitoring and conservation of protected species such as the wolf.

**Key words:** *Canis lupus*; Carpathians; citizen science; noninvasive genetic sampling; population monitoring

## 1 INTRODUCTION

Reliable estimation of population size is fundamental to effective wildlife management and conservation (Lancia et al., 1996). Member States of the European Union (EU) are legally obliged by Article 11 of Council Directive 92/43/EEC (the 'Habitats Directive') to monitor species of Community interest, including large carnivores such as the grey wolf (*Canis lupus*), to assess whether they are at 'favourable conservation status' (Epstein et al., 2016).

Slovakia is an important range state of the Carpathian wolf population in Central Europe (Kutal & Rigg, 2008). In this country, the wolf is listed in Annex V of the Habitats Directive, which allows hunting through quotas, provided this does not harm the species' conservation status, but the obligation to conduct surveillance still applies (Trouwborst & Fleurke, 2019). A dearth of systematic, objective and reliable monitoring has resulted in the status of the population being disputed by diverse interest groups (Rigg, 2008). Estimates of abundance based on hunters' reports are an order of magnitude higher than those of environmentalists, and both

lack a replicable scientific methodology. When objective data are lacking, population estimates can be highly inaccurate (Moqanaki et al., 2018) and may reflect the personal position or agenda of the author (Skrbinšek et al., 2019), particularly when a highly controversial species such as the wolf is considered. Moreover, diverse interest groups may generate disparate information, fuelling social conflicts (Rigg et al., 2014).

The European Commission opened an infringement process against Slovakia in 2013 (no. 2013/4081) due to the uncertainty of wolf conservation status and concerns about the impact hunting quotas may have been having on the wolf population in the West Carpathians. A national wolf management plan was subsequently adopted (Antal et al., 2016) which prescribed methods for monitoring, but state authorities have yet to produce statistically robust estimates of key population parameters at management-relevant scales. There is a clear need to implement an appropriate programme of monitoring involving key stakeholders in the co-generation of data through ‘citizen science’ (cf. Aceves-Bueno et al., 2015) in order to reach agreement on the status of the population.

Monitoring large carnivores is difficult and resource-demanding due to their relatively low population densities, large home ranges and cryptic behaviour (Gibbs, 2000). However, advances in technology and data processing during the last 30 years have provided powerful new tools to estimate population size more accurately and reliably. Molecular genetics have revolutionised wildlife research and monitoring (Frankham et al., 2002). Noninvasive genetic sampling enables the study of live animals without the need to handle or observe them directly (Schwartz & Monfort, 2008). High-resolution marker systems such as short tandem repeats (‘microsatellites’) are used to identify species, gender, individual and kinship (Ellegren, 2004), while genetic mark-recapture techniques generate robust estimates of population size (Lukacs & Burnham, 2005, Mumma et al., 2015).

In order to address the controversy over wolf conservation status in Slovakia, we developed a project utilising state-of-the-art research methods to obtain robust estimates of population size in a model area. This began as a one-year pilot action financed by the European Commission (contract no. 07.0307/2013/654446/SER/B.3) and implemented as a collaborative effort of the Slovak Wildlife Society, the Slovak Hunting Association, Forests of the Slovak Republic state enterprise, the State Nature Conservancy and the University of Ljubljana (Rigg et al., 2014). A one-off ‘snapshot’ of the population subsequently evolved into continuous monitoring using a combination of noninvasive genetic sampling, microsatellite genotyping and mark-recapture modelling with the support of crowdfunding and volunteer citizen scientists. Here, we present results from the first five sampling seasons and compare them with official hunting statistics.

## 2 MATERIALS AND METHODS

### 2.1 Sample collection and storage

Fieldwork was conducted in the Liptov region of northern Slovakia (1,988 km<sup>2</sup>). A total of 698 noninvasive genetic samples were collected during five sampling seasons (1<sup>st</sup> July to 30<sup>th</sup> June) in 2013–2018 by project staff, trained ‘citizen scientists’, students, national park zoologists and rangers, professional foresters and hunters. Volunteers were trained in noninvasive sample collection. Sampling was passive (without use of lures) and conducted mostly in winter, when

samples tend to be better preserved (Lucchini et al., 2002) and are more easily found whilst following tracks in snow, thereby reducing individual capture heterogeneity and sampling of non-target species (Marucco et al., 2011). We focused on fresh samples to minimise DNA degradation and thereby maximise genotyping success rates (Santini et al., 2007).

Scat samples were collected in 5 ml flasks filled with DETs preservation buffer which preserves the target DNA and makes samples simpler to transport since it is non-toxic and non-combustible. Urine samples in seasons 2013/14–2015/16 were collected in 50 ml flasks filled with EDTA-Ethanol-NaOH mixture designed to preserve the target DNA. Since the 2016/17 season DETs buffer was also used for urine samples. Urine and scat samples were kept frozen at -20 °C prior to analysis. Hair samples were collected in paper envelopes and stored at room temperature in re-sealable plastic bags with desiccant (silica). Saliva was collected using commercial kits forensic swabs with desiccant (FLOQSwabs®, Copan Flock Technologies, Brescia, Italy).

Each sample tube or resealable plastic bag was fitted with a label for field data entry to keep collection data with samples. Estimated age of scat was also recorded, as we found this to have considerable effect on expected amplification success (Skrbinšek, 2020). For samples collected while snow-tracking, we also recorded the number of animals in the group.

## 2.2 DNA extraction, amplification and genotyping

Sample handling and analysis adhered to strict regimes to avoid any possibility of contamination. We used a dedicated laboratory for DNA extraction from noninvasive samples where we enforced strict rules regarding movement of personnel, equipment and material. Upon entry in the laboratory, data about each sample were entered into a relational database and barcodes were used to track samples through the genotyping process and eliminate manual data entry. Each critical step in analysis was photo-documented to allow back-checking for errors and negative controls were used throughout.

DNA extraction was done using a specifically developed magnetic-beads based protocol for noninvasive samples. Pipette tips with aerosol barriers were used for all liquid transfers. From 2015 we used a pipetting robot, combined with barcode reading, for DNA extraction and to organise samples and prepare them for analysis, which reduces the probability of pipetting errors to close to zero.

In the first screening process, each sample was amplified with the full genotyping PCR protocol twice and analysed on an automatic sequencer (Applied Biosystem ABI 3130xl Genetic Analyzer). Samples that yielded PCR product were genotyped up to eight times at 16 canine unlinked autosomal microsatellite loci (AHT137, AHT171, AHT260, AHTk211, AHTk253, CXX279, FH2054, FH2848, INRA21, INU030, INU055, REN162C04, REN169D01, REN169O18, REN247M23, REN54P11) in one PCR multiplex and the Amelogenin locus for sex determination. We followed recommended procedures to minimise genotyping errors (Waits et al., 2001, Waits & Paetkau, 2005, Broquet et al., 2007, Lampa et al., 2013). After each genotyping run, reliability was checked with the Reliotype maximum-likelihood approach (Miller et al., 2002). Genotypes with reliability  $\geq 0.98$  were accepted.

## 2.3 Individual ID and pedigree reconstruction

MisBase software (Skrbinšek, unpublished) was used to assess if genotypes matched those from other samples or known individuals. Samples with genotype reliability below the 0.98 threshold were accepted if they matched a reliably genotyped sample as the probability of a reliable match to a reliably genotyped sample in the presence of errors is marginal. If a sample was not matched to another reliable sample, the analysis was repeated up to eight times until reliability reached 0.98 or else it was discarded. If the quality index of a sample (Miquel et al., 2006) was below 0.4, the unmatched samples were also discarded since the DNA quality was too low to provide a reliable genotype.

Since the number of microsatellite markers used was large relative to the expected number of animals in the study area, some mismatch between samples that looked like being caused by allelic dropout was tolerated, but no direct incompatibilities (i.e. different alleles between samples) were allowed. To avoid the problem of incorrect individual assignment due to false alleles (Taberlet et al., 1996), we set a minimum threshold of two clear observations of an allele in separate PCRs / sequencer runs before the allele was considered 'true'. In case of doubt, samples were reanalysed until the problem was resolved. We also calculated probability of identity and probability of identity for siblings for each locus to determine the power of our locus panel to distinguish between individuals (Waits et al., 2001).

Genetic data from individuals identified in the noninvasive sampling formed the basis for pedigree reconstruction to distinguish between wolf family groups ('packs'). Program COLONY (Jones & Wang, 2010) was used, which enables efficient use of available data by assigning parentage and sibship in the same model. We performed three long runs with full-likelihood analysis method in each analysis, running analysis in multiple processor cores (between four and 16) to keep processing times reasonable. We checked for convergence between runs and before accepting results we checked if they made spatial sense in a Geographic Information System (GIS).

#### 2.4 Abundance estimation

Population size in the study area was estimated with the Capwire mark-recapture model (Miller et al., 2005) implemented using the 'capwire' R package (Pennell, 2013). This model was designed specifically for noninvasive genetic sampling, is quite robust to capture heterogeneity (unequal probability of capture success) and allows for continuous sampling in a single session, which fits well with how our samples were collected. We analysed each sampling season separately to avoid serious violation of the population closure assumption.

Prior to running the models, we removed auto-correlated samples from the data (i.e. if multiple samples were collected from the same animal in the same tracking session, only a single sample was retained). We also removed the few animals not related to any family groups in the study area since they were probably dispersing young individuals or 'floaters' (Mech & Boitani, 2003), whose capture probability would have been different to resident wolves. These animals were later added to the final result to obtain a total population size estimate. We ran three different models: equal capture probability (ECM), two-innate rates (TIRM) and partitioning (PART). We ran tests to check which model provided the best fit for the data. We ran the models for all animals together and separately for each sex.

#### 2.5 General data analysis

When not stated otherwise, all data management and analysis was done in R Data Analysis Environment (R Core Team, 2018). Spatial analyses and mapping were performed in ArcGIS 10.3.1 (ESRI) or QGIS 3.8.2.

### 3 RESULTS AND DISCUSSION

We collected 90–242 (mean = 140) noninvasive samples per sampling season: 49% of them urine, 45% scat, 3% saliva, 1.5% hair and 1.5% blood. PCR product was obtained from 68.8% of all samples. Overall, we obtained putative wolf genotypes from 415 samples, a yield of 59.5% of all samples collected.

We detected 12–44 different wolf genotypes during each sampling season, representing a minimum count of individuals in the study area. The panel of loci used to distinguish between individuals had considerable power: the probability of two unrelated animals sharing the same genotype was  $9.25 \times 10^{-11}$ , and the same probability for siblings was  $1.1 \times 10^{-4}$ , making incorrect assignments highly unlikely.

Insufficient sample sizes and a high number of autocorrelated samples (e.g. collected from the same individual while following snow tracks) precluded mark-recapture modelling in 2013/14 and 2014/15, but we were able to produce meaningful mark-recapture estimates for the subsequent three seasons. For resident animals (family groups), we estimated 46 individuals (37–66, 95% CI) in 2015/16, 53 (42–64) in 2016/17 and 46 (31–73) in 2017/18. During each season, 3–7 detected individuals were not closely related to any known family group. When these ‘non-residents’ are included, our estimates for the total number of wolves in the study area were 49 (40–69) in 2015/16, 57 (46–68) in 2016/17 and 53 (38–80) in 2017/18 (Table 1).

**Table 1:** Wolf population size estimates for Liptov, Slovakia. Capture-mark recapture (CMR) estimates were performed for resident animals, i.e. members of family groups (‘packs’). Total estimates (with 95% confidence intervals) also include non-resident individuals, which were detected (genotyped) in the study area but were not related to any known family group.

Sampling season	Sex	Samples used	Genotypes residents	CMR estimate of residents (95% CI)	Genotypes non-residents	Total (95% CI)
	All	62	29	46 (37–66)	3	49 (40–69)
2015/16	Males	29	13	24 (15–36)	2	26 (17–38)
	Females	33	16	26 (19–43)	1	27 (20–44)
	All	80	40	53 (42–64)	4	57 (46–68)

2016/17	Males	46	22	27 (22–35)	3	30 (25–38)
	Females	34	18	26 (18–38)	1	27 (19–39)
	All	44	27	46 (31–73)	7	53 (38–80)
2017/18	Males	32	18	27 (18–41)	3	30 (21–44)
	Females	12	9	24 (10–80)	4	28 (14–84)

Our results indicate that wolf numbers in the study area were stable or possibly slightly increasing in 2016–2018. This finding is corroborated by a reported expansion of total occupied wolf range in Slovakia from 13,864 km<sup>2</sup> in 2015 (Antal et al., 2016) to 17,807 km<sup>2</sup> in 2018 (NLC, 2018), suggesting that the population was growing.

Official game statistics for the study area compiled from hunters' reports (NLC, 2020) were 5.1–5.6 times higher than our genetic mark-recapture estimates. It has been previously reported that official game statistics substantially over-estimate numbers of Eurasian lynx (*Lynx lynx*) in Slovakia (Kubala et al., 2017). Wolves and lynx have home ranges of tens to hundreds of square kilometres, so the same animals are subject to being counted multiple times by hunters in neighbouring hunting grounds.

Cost is often a major consideration, and potentially limiting factor, in the implementation of robust monitoring (Stenglein et al., 2010). Our study began as a one-year pilot action, during which unfavourable weather and other factors hindered sampling and hence precluded mark-recapture estimation. With only modest resources to continue, relying on volunteers and crowdfunding, we improved the efficiency and effectiveness of field and laboratory procedures to reduce costs while increasing yield. We succeeded in doubling the proportion of samples from which PCR product was obtained from 41.4% to 83.5% and increased the proportion of useful samples from 39.6% to 74.0%. In effect, we obtained twice as many useful samples and data for the same effort and halved the cost per data point. This enabled us to achieve robust estimates of key population parameters that had previously been lacking in Slovakia.

The benefits and efficacy of well-run citizen science projects are widely acknowledged. For example, Ražen et al. (2020) described an excellent example of how citizen science and stakeholder participation, coordinated by researchers, can be scaled up to achieve high-quality wolf monitoring on a population level. The quality of datasets produced by volunteers can equal or surpass those of professionals (Kosmala et al., 2016). For example, a study in North America found that new recruits were better than experienced observers at collecting noninvasive genetic samples from wolves (Soller et al., 2020).

Trained volunteers were fundamental to our sampling effort and proved to be highly effective. Overall, 86.5% of noninvasive samples from which PCR product was obtained were confirmed as being from the target species. Although greater participation by national park staff in 2016/17 helped us collect substantially more samples than in any other season, the PCR success rate did not increase and the yield of useful samples was lower than in both the preceding and following seasons due to inclusion of more non-target and mixed samples.

#### 4 CONCLUSIONS

We used a combination of noninvasive genetic sampling, microsatellite genotyping and mark-recapture modelling to estimate the number of wolves in the Liptov region of Slovakia. For 3 consecutive sampling seasons, our estimates for late winter were in the range of 49–57 individuals. These are the first statistically robust estimates of abundance obtained from the West Carpathian wolf population. Official hunting statistics substantially over-estimated wolf abundance due to deficiencies in methodology.

A relatively small-scale project such as ours cannot be a substitute for a permanent, state-run programme of national monitoring. Nevertheless, in the absence of adequate surveillance, our findings have helped guide science-based recommendations to conservation authorities and wildlife managers in Slovakia. It is a ‘proof of concept’, demonstrating at the local level the applicability and usefulness of citizen science and molecular genetics for obtaining credible scientific data while building trust among stakeholders and acquiring experience and know-how that could be applied to larger-scale studies.

#### 5 REFERENCES

- Aceves-Bueno, E., Adeleye, A.S., Bradley, D., Brandt, W.T., Callery, P., Feraud, M., ... Tague, C. (2015). Citizen science as an approach for overcoming insufficient monitoring and inadequate stakeholder buy-in in adaptive management: criteria and evidence. *Ecosystems*, 18, 493–506. <https://doi.org/10.1007/s10021-015-9842-4>.
- Antal, V., Boroš, M., Čertíková, M., Ciberej, J., Dóczy, J., Find’o, S., ... Šramka, Š. (2016). Program starostlivosti o vlka dravého (*Canis lupus*) na Slovensku. (Programme of care of the wolf (*Canis lupus*) in Slovakia.) Banská Bystrica: State Nature Conservancy of the Slovak Republic. [in Slovak]
- Broquet, T., Ménard, N., & Petit, E. (2007). Noninvasive population genetics: A review of sample source, diet, fragment length and microsatellite motif effects on amplification success and genotyping error rates. *Conservation Genetics*, 8(1), 249–260.
- Ellegren, H. (2004). Microsatellites: simple sequences with complex evolution. *Nature Reviews Genetics*, 5, 435–445.
- Epstein, Y., López-Bao, J.V., & Chapron, G. (2016). A legal-ecological understanding of favorable conservation status for species in Europe. *Conservation Letters*, 9, 81–88.

- Frankham, R., Ballou, J.D., & Briscoe, D.A. (2002). Introduction to conservation genetics. Cambridge, UK: Cambridge University Press.
- Gibbs, J.P. (2000). Monitoring populations. In L. Boitani & T.K. Fuller (Eds.), *Research techniques in animal ecology: controversies and consequences* (pp. 213–252). New York, NY: Columbia University Press.
- Jones, O.R., & Wang, J. (2010). COLONY: a program for parentage and sibship inference from multilocus genotype data. *Molecular Ecology Resources*, 10(3), 551–555. DOI: 10.1111/j.1755-0998.2009.02787.x.
- Kosmala, M., Wiggins, A., Swanson, A., & Simmons, B. (2016). Assessing data quality in citizen science. *Frontiers in Ecology and the Environment*, 14(10), 551–560. <https://doi.org/10.1002/fee.1436>.
- Kubala, J., Smolko, P., Zimmermann, F., Rigg, R., Tám, B., Il'ko, T., ... Breitenmoser, U. (2017). Robust monitoring of the Eurasian lynx *Lynx lynx* in the Slovak Carpathians reveals lower numbers than officially reported. *Oryx*, 53(3), 548–556.
- Kutal, M., & Rigg, R. (Eds.) (2008). Perspectives of wolves in Central Europe. Proceedings from the conference held on 9th April 2008 in Malenovice, Beskydy Mts. Olomouc, Czech Republic: Hnutí Duha.
- Lampa, S., Henle, K., Klenke, R., Hoehn, M., & Gruber, B. (2013). How to overcome genotyping errors in non-invasive genetic mark-recapture population size estimation—A review of available methods illustrated by a case study. *Journal of Wildlife Management*, 77(8), 1490–1511. DOI: 10.1002/jwmg.604.
- Lancia, R.A., Nichols, J.D., & Pollock, K.H. (1996). Estimating the number of animals in wildlife populations. In T.A. Bookhout (Ed.), *Research and management techniques for wildlife and habitats*, 5<sup>th</sup> edition revised (215–253). Bethesda: The Wildlife Society.
- Lucchini, V., Fabbri, E., Marucco, F., Ricci, S., Boitani, L., & Randi, E. (2002). Noninvasive molecular tracking of colonizing wolf (*Canis lupus*) packs in the western Italian Alps. *Molecular Ecology*, 11, 857–868.
- Lukacs, P.M., & Burnham, K.P. (2005). Review of capture-recapture methods applicable to noninvasive genetic sampling. *Molecular Ecology*, 14(13), 3909–3919.
- Mumma, M.A., Zieminski, C., Fuller, T.K., Mahoney, S.P., Waits, L.P. (2015). Evaluating noninvasive genetic sampling techniques to estimate large carnivore abundance. *Molecular Ecology Resources*, 15(5), 1133–1144. DOI: 10.1111/1755-0998.12390.
- Marucco, F., Boitani, L., Pletscher, D.H., & Schwartz, M.K. (2011). Bridging the gaps between non-invasive genetic sampling and population parameter estimation. *European Journal of Wildlife Research*, 57, 1–13. DOI: 10.1007/s10344-010-0477-7.

- Mech, L.D., & Boitani, L. (2003). Wolf social ecology. In L.D. Mech & L. Boitani (Eds.), *Wolves: behavior, ecology, and conservation* (1–34). *Chicago: University of Chicago Press*.
- Miller, C.R., Joyce, P. & Waits, L.P. (2002). Assessing allelic dropout and genotype reliability using maximum likelihood. *Genetics*, *160*(1), 357–366.
- Miller, C.R., Joyce, P., & Waits, L.P. (2005). A new method for estimating the size of small populations from genetic mark–recapture data. *Molecular Ecology*, *14*(7), 1991–2005. <https://doi.org/10.1111/j.1365-294X.2005.02577.x>.
- Miquel, C., Bellemain, E., Poillot, C., Bessière, J., Durand, A., & Taberlet P. (2006). Quality indexes to assess the reliability of genotypes in studies using noninvasive sampling and multiple-tube approach. *Molecular Ecology Notes*, *6*, 985–988. <http://doi.wiley.com/10.1111/j.1471-8286.2006.01413.x>.
- Moqanaki, E.M., Jiménez, J., Bensch, S, López-Bao, J.V. (2018). Counting bears in the Iranian Caucasus: Remarkable mismatch between scientifically-sound population estimates and perceptions. *Biological Conservation*, *220*, 182–191.
- NLC (2018). Poľovnícka štatistická ročenka Slovenskej republiky 2018. (Hunting statistics yearbook of the Slovak Republic 2018.) Zvolen: Národné lesnícke centrum. [in Slovak]
- NLC (2020). Poľovnícka štatistická. (Hunting statistics.) Zvolen: Národné lesnícke centrum. Retrieved from <https://gis.nlcsk.org/IBULH/PolovStat/PolovStat> [in Slovak]
- Pennell, M.W., Stansbury, C.R., Waits, L.P., & Miller, C.R. (2013). Capwire: a R package for estimating population census size from non-invasive genetic sampling. *Molecular Ecology Resources*, *13*(1), 154–157. <https://doi.org/10.1111/1755-0998.12019>.
- R Core Team (2018). R: A language and environment for statistical computing. R Foundation for Statistical Computing, Vienna. Retrieved from <https://www.R-project.org/>.
- Ražen, N., Kuralt, Ž., Fležar, U., Bartol, M., Černe, R., Kos, I., ... Potočnik, H. (2020). Citizen science contribution to national wolf population monitoring: what have we learned? *European Journal of Wildlife Research*, *66*, 46. <https://doi.org/10.1007/s10344-020-01383-0>.
- Rigg, R. (2008). Početnosť, odstrel a ochrana vlka dravého (*Canis lupus*) v Slovenských Karpatoch – privedla či málo? (Abundance, hunting and protection of the wolf (*Canis lupus*) in the Slovak Carpathians—too much or not enough?) Výskum a ochrana cicavcov na Slovensku, VIII, 200–213. [in Slovak with English summary]
- Rigg, R., Skrbínšek, T. & Linnell, J. (2014). Engaging hunters and other stakeholders in a pilot study of wolves in Slovakia using non-invasive genetic sampling. Report to DG Environment, European Commission, Bruxelles. Contract no. 07.0307/2013/654446/SER/B.

- Santini, A., Lucchini, V., Fabbri, E., & Randi, E. (2012). Ageing and environmental factors affect PCR success in wolf (*Canis lupus*) excremental DNA samples. *Molecular Ecology Notes*, 7(6), 955–961. <https://doi.org/10.1111/j.1471-8286.2007.01829.x>.
- Schwartz, M.K., & Monfort, S.L. (2008). Genetic and endocrine tools for carnivore surveys. In R.A. Long, P. MacKay, W.J. Zielinski & J.C. (Eds.), *Noninvasive survey methods for carnivores* (pp. 238–262). Washington: Island Press.
- Skrbinšek, T., Luštrik, R., Majič-Skrbinšek, A., Potočnik, H., Kljun, F., Jelenčič, M., ... Trontelj, P. (2019). From science to practice: genetic estimate of brown bear population size in Slovenia and how it influenced bear management. *European Journal of Wildlife Research*, 65, 1–15.
- Skrbinšek, T. (2020). Effects of different environmental and sampling variables on the genotyping success in field-collected scat samples: a brown bear case study. *Acta Biologica Slovenica*, 63, 2.
- Soller, J.M., Ausband, D.E., & Szykman Gunther, M. (2020). The curse of observer bias: error in noninvasive genetic sampling. *PLoS ONE*, 15(3), e0229762. <https://doi.org/10.1371/journal.pone.0229762>.
- Stenglein, J.L., Waits, L.P., Ausband, D.E., Zager, P., & Mack, C.M. (2010). Efficient, noninvasive genetic sampling for monitoring reintroduced wolves. *Journal of Wildlife Management*, 74(5), 1050–1058. DOI: 10.2193/2009-305.
- Taberlet, P., Griffin, S., Goossens, B., Questiau, S., Manceau, V., Escaravage, N., ... Bouvet, J. (1996). Reliable genotyping of samples with very low DNA quantities using PCR. *Nucleic Acids Research*, 24, 3189–3194. DOI: 10.1093/nar/24.16.3189.
- Trouwborst, A., & Fleurke, F.M. (2019). Killing wolves legally: exploring the scope for lethal wolf management under European nature conservation law. *Journal of International Wildlife Law & Policy*. DOI: 10.1080/13880292.2019.1686223.
- Waits, L.P., Luikart, G., & Taberlet, P. (2001). Estimating the probability of identity among genotypes in natural populations: Cautions and guidelines. *Molecular Ecology*, 10(1), 249–256.
- Waits, L.P., & Paetkau, D. (2005). Noninvasive genetic sampling tools for wildlife biologists: A review of applications and recommendations for accurate data collection. *Journal of Wildlife Management*, 69(4), 1419–1433.

## BIOTEHNOLOGIJA/BIOTECHNOLOGY

Identification of new keratinolytic bacterial isolates by 16S rRNA gene sequencing, FAMES analysis and whole genome sequencing  
Blaž PETEK<sup>1\*</sup>, Tomaž ACCETTO, Maša ZOREC, Romana MARINŠEK LOGAR

<sup>1</sup> University of Ljubljana, Biotechnical Faculty, Department of Microbiology, Ljubljana, Slovenia

\*corresponding author: [blaz.petek@bf.uni-lj.si](mailto:blaz.petek@bf.uni-lj.si)

### Identification of new keratinolytic bacterial isolates by 16S rRNA gene sequencing, FAMES analysis and whole genome sequencing

**Abstract:** Rapid and efficient identification of microorganisms is very important in various fields of research. In our study, 16 keratinolytic bacterial isolates were identified in three different ways: by 16S rRNA gene sequencing, by membrane fatty acid profiles analysis (FAMES), and by whole genome sequencing. The results showed that identification by 16S rRNA gene sequencing and FAMES analysis was accurate at the genus level (genus *Bacillus*) but not at the species level. Whole genome sequencing was chosen for final identification. Our isolates belong to four different species of the genus *Bacillus* (*Bacillus mycoides*, *Bacillus subtilis*, *Bacillus altitudinis* and *Bacillus wiedmannii*). Core genome analysis showed that the isolates belonged into two major groups (*Bacillus cereus* and *Bacillus subtilis* group).

**Key words:** identification; keratinolytic microorganisms; 16S rRNA gene sequencing; FAMES; whole genome sequencing

### Identifikacija novih keratinolitičnih bakterijskih izolatov s sekvenciranjem gena za 16S rRNA, analizo FAMES in sekvenciranjem celotnega genoma

**Izveček:** Hitra in učinkovita identifikacija mikroorganizmov je zelo pomembna na različnih področjih raziskovanja. V naši raziskavi smo 16 keratinolitičnih bakterijskih izolatov identificirali na tri različne načine: s sekvenciranjem gena za 16S rRNA, z analizo profilov membranskih maščobnih kislin (FAMES) in sekvenciranjem celotnega genoma. Rezultati so pokazali, da je bila identifikacija s sekvenciranjem gena za 16S rRNA in analizo FAMES natančna na nivoju rodu (rod *Bacillus*), ne pa tudi na nivoju vrste. Za dokončno identifikacijo smo izbrali sekvenciranje celotnega genoma. Naši izolati pripadajo štirim različnim vrstam iz rodu *Bacillus* (*Bacillus mycoides*, *Bacillus subtilis*, *Bacillus altitudinis* in *Bacillus wiedmannii*). Analiza jedrnega genoma je pokazala, da so izolati razdeljeni v dve večji skupini (skupini *Bacillus cereus* in *Bacillus subtilis*).

**Ključne besede:** identifikacija; keratinolitični mikroorganizmi; sekvenciranje gena za 16S rRNA; FAMES; sekvenciranje celotnega genoma

## 1 INTRODUCTION

Rapid and easy identification of microorganisms is very important and highly desirable in various research areas. There are many different methods for identification, but some of them are time-consuming, expensive, or require a high level of experience and expertise (Santos et al., 2018). Chemical analyses of bacterial components (fatty acids, proteins), such as MALDI TOF MS, are increasingly used for taxonomic classification of microorganisms. They are rapid, cheap and reliable, but have been mainly used as routine methods for pathogen identification in clinical microbiology laboratories (Sanguinetti & Posteraro, 2016). Bacterial fatty acids are highly genetically conserved because they play an essential role in cell function and structure (Dawyndt et al., 2006). Fatty acid methyl esters (FAMES)-based identifications showed near-perfect identification performance at the genus level, with some necessary optimization for successful identification at the species level. Different chain lengths, positions of double bonds, and binding of functional groups in more than 300 fatty acids already found in bacteria make them very useful taxonomic markers (Dawyndt et al., 2006; Slabbinck et al., 2009).

All microorganisms have at least one copy of the 16S rRNA gene, and it is the most commonly used single target for phylogenetic studies of bacteria and archaea. Some bacterial species may contain multiple 16S rRNA genes that can differ from each other. However, in addition to the presence of variable copy numbers of 16S rRNA genes with sequence variations in their genomes, 16S rRNA gene sequencing alone may be insufficient to reliably identify many microbial species for other reasons: high genetic similarity within specific microorganisms or groups (Sanguinetti & Posteraro, 2016; Church et al., 2020).

Advances in whole genome sequencing (WGS) in recent years have led to a reduction in cost and an increase in the speed of sequencing, with the prospect of reducing the time required to sequence a microbial genome from several days or weeks to only hours. WGS is increasingly being used in clinical microbiology, where it can be used to detect the presence of antimicrobial resistance genes or genes associated with virulence and pathogenicity (Rossen et al., 2018).

In our study, we isolated 116 microbial isolates that showed keratinolytic activity. Only highly keratinolytic isolates (with higher keratinolytic activity than the positive control *Streptomyces fradiae*) were selected for identification and further study. Three different methods were used for identification. For preliminary identification, we used 16S rRNA gene sequencing and FAMES analysis. All isolates were finally identified by WGS. In this paper we present only the results of bacterial identification.

## 2 MATERIALS AND METHODS

### 2.1 Microbial cultures

We used 16 highly keratinolytic bacterial strains isolated from the waste sheep wool compost pile and the soil under the pile. All cultures were grown in a Nutrient broth (Biolife, Italy) at 30 °C and 150 rpm.

### 2.2 DNA isolation and 16S rRNA sequencing

DNA was isolated using the DNeasy UltraClean Microbial Kit (Qiagen, Hilden, Germany). The 16S rRNA genes from 17 bacterial isolates were amplified by PCR using Supercycler SC300T (Kyratec, Queensland, Australia) with primers fd1 (5'-AGAGTTTGATCCTGGCTCAG-3') (Weisburg et al., 1991) and 1492R (5'-TACGGYTACCTTGTTACGACTT-3') (Lane, 1991). 20 µl reaction mixture contained 1 µl of each primer (10 µM), 0.4 µl of dNTP mixture (10 mM each) (Thermo Fischer Scientific, Massachusetts, USA), 1 µl of diluted template DNA, 4 µl of 5× Phusion HF buffer (New England Biolabs, Massachusetts, USA), and 0.2 µl of Phusion HF polymerase (New England Biolabs, Massachusetts, USA). The PCR consisted of initial denaturation at 98 °C for 30 s, 35 cycles of denaturation at 98 °C for 10 s, annealing at 57 °C for 30 s, extension at 72 °C for 45 s, and a final extension at 72 °C for 5 min. The PCR products were analysed by electrophoresis on a 1.2 % (w/v) agarose gel and then purified using the High Pure PCR Product Purification Kit (Roche Diagnostics GmbH, Switzerland). DNA concentration was also measured using the NanoVue Plus spectrophotometer. PCR products were sequenced with the same primers as used for amplification by Microsynth AG (Balgach, Switzerland) at our request. The sequences were compared with the 16S rRNA database of type and reference bacterial strains in the NCBI database.

### 2.3 FAMEs analysis

Selected isolates were grown in tryptic soy broth or agar at 30 °C for 24 h. Colonies were harvested from agar plates, or pellets were collected from the broth. FAMEs were prepared and analysed strictly according to the guidelines of MIDI Inc. (Newark, USA) for their Microbial Identification System (Sasser, 1990) using gas chromatography with flame ionization detector (GC-FID).

### 2.4 Genomic DNA isolation, whole genome sequencing and bioinformatics analysis

DNA was isolated using the DNeasy UltraClean Microbial Kit (Qiagen, Hilden, Germany). Whole genomes were sequenced by Novogene (Beijing, China) using Illumina MiSeq paired-end technology. The quality of raw reads was checked using the FASTQC tool, version 0.11.2 (Andrews et al., 2011-2014). Assembly was done by SPAdes Assembles, version 3.1.1 (Bankevich et al., 2012). Final identification was performed by calculating average nucleotide identity (ANI) (Richter & Rossello-Mora, 2009) for whole genome comparisons with selected *Bacillus* type strains using pyani (Pritchard et al., 2016). Genome annotations were performed using Prokka 1.7 (Seemann, 2014). Core genome analysis was done with Roary tool (Page et al., 2015). Phylogenetic trees were prepared with Molecular Evolutionary Genetics Analysis (MEGA 11) software.

## 3 RESULTS AND DISCUSSION

The results of 16S rRNA gene sequencing showed that all 16 isolates, included in this study belonged to the genus *Bacillus* (Table 1). Identification by FAMEs was also successful only at the genus level (Table 1). According to the similarity dendrogram (Figure 1), prepared from FAMEs profiles analysis all the isolates are divided into three major subgroups. Compared to the WGS results, where isolates were also divided into three subgroups, two (RSRT17, RS3022) from a total of 16 isolates were not correctly grouped, probably because they were

not similar to any FAMES profile stored in database until then. Regardless of the results of Slabnick et al. (2009) who showed that machine learning proves to be very useful for the identification of bacterial species based on FAMES, Santos et al. (2018) achieved successful identification of *Bacillus* strains using gas chromatography only after replacing the originally used FID detector with a vacuum ultraviolet detector (GC-VUV).

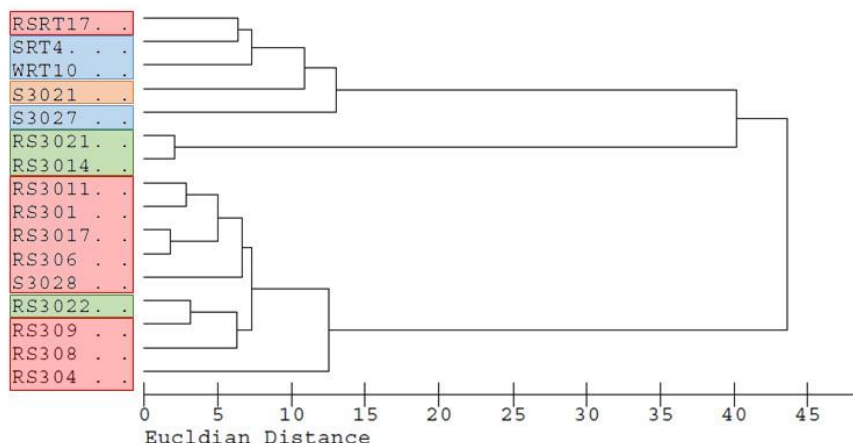


**Figure 1:** Similarity dendrogram resulting from the FAMES analysis. Isolates marked with red colour belong to the species *Bacillus subtilis*, with blue colour to *B. wiedmannii*, with green colour to *B. altitudinis* and with orange colour to *B. mycoides* (based on the WGS).

According to the WGS results (Table 1) our keratinolytic isolates belong to four different *Bacillus* species (*B. mycoides*, *B. subtilis*, *B. altitudinis* and *B. wiedmannii*).

**Table 1:** Comparison of keratinolytic isolates identification by 16S rRNA gene sequencing, FAMES analysis and WGS.

Isolate	16S rRNA gene sequencing	FAMES analysis	Whole genome sequencing
RS301	<i>Bacillus</i>	<i>Bacillus atrophaeus</i> / <i>subtilis</i>	<i>Bacillus subtilis</i>
RS304	<i>Bacillus</i>	<i>Bacillus atrophaeus</i> / <i>subtilis</i>	<i>Bacillus subtilis</i>
RS306	<i>Bacillus</i>	<i>Bacillus atrophaeus</i> / <i>subtilis</i>	<i>Bacillus subtilis</i>
RS308	<i>Bacillus</i>	<i>Bacillus atrophaeus</i> / <i>subtilis</i>	<i>Bacillus subtilis</i>
RS309	<i>Bacillus</i>	<i>Bacillus atrophaeus</i> / <i>subtilis</i>	<i>Bacillus subtilis</i>
RS3011	<i>Bacillus</i>	<i>Bacillus atrophaeus</i> / <i>subtilis</i>	<i>Bacillus subtilis</i>
RS3014	<i>Bacillus</i>	<i>Bacillus pumilus</i> / <i>megaterium</i>	<i>Bacillus altitudinis</i>
RS3017	<i>Bacillus</i>	<i>Bacillus atrophaeus</i> / <i>subtilis</i>	<i>Bacillus subtilis</i>
RS3021	<i>Bacillus</i>	<i>Bacillus pumilus</i> / <i>megaterium</i>	<i>Bacillus altitudinis</i>
RS3022	<i>Bacillus</i>	<i>Bacillus atrophaeus</i> / <i>subtilis</i>	<i>Bacillus altitudinis</i>
RSRT17	<i>Bacillus</i>	<i>Bacillus cereus</i> / <i>mycoides</i>	<i>Bacillus subtilis</i>
S3021	<i>Bacillus</i>	<i>Bacillus cereus</i> / <i>mycoides</i>	<i>Bacillus mycoides</i>
S3027	<i>Bacillus</i>	<i>Bacillus mycoides</i> / <i>cereus</i>	<i>Bacillus wiedmannii</i>
S3028	<i>Bacillus</i>	<i>Bacillus atrophaeus</i> / <i>Virgibacillus pantothenicus</i>	<i>Bacillus subtilis</i>
SRT4	<i>Bacillus</i>	<i>Bacillus cereus</i>	<i>Bacillus wiedmannii</i>
WRT10	<i>Bacillus</i>	<i>Bacillus cereus</i>	<i>Bacillus wiedmannii</i>

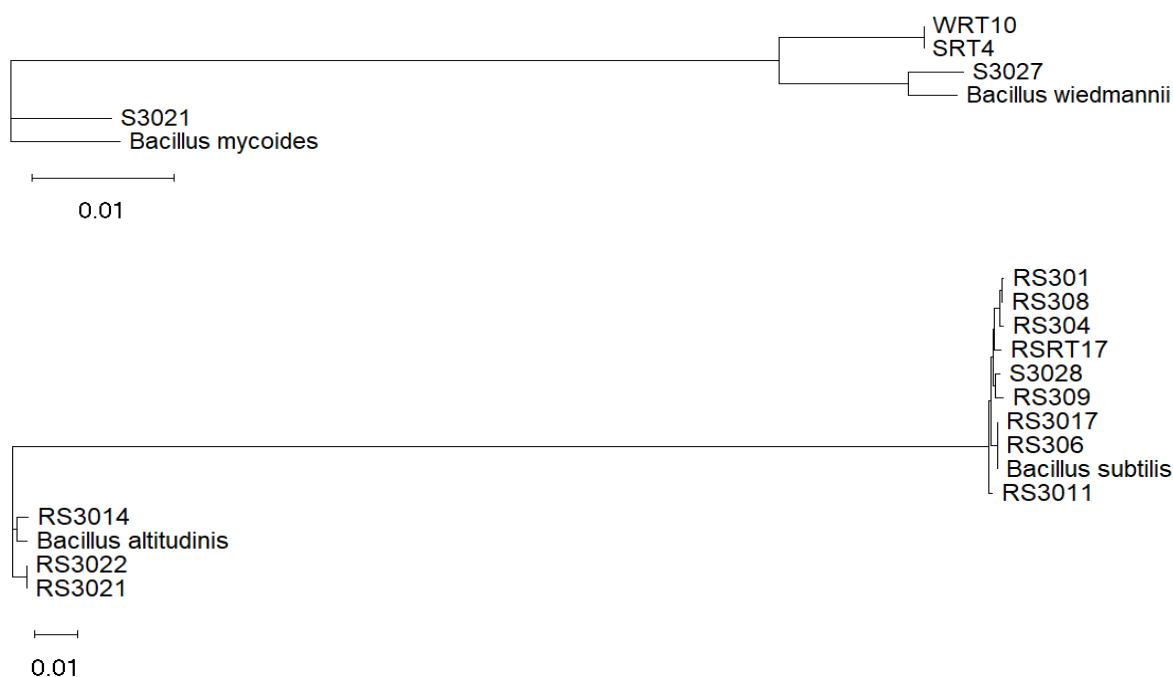


**Figure 2:** Phylogenetic trees resulting from the core genome analysis. For a better representation four type strain genomes were included in analysis (*B. mycooides* DSM2048, *B. wiedmannii* DSM102050; *B. altitudinis* 41KF2b<sup>T</sup>, *B. subtilis* DSM10).

Core genome analysis of all 16 isolates showed no common genes. After dividing the genomes into two major subgroups (*B. subtilis* and *B. cereus* group), the analysis revealed 71 core genes in the *B. subtilis* group and 1446 core genes in the *B. cereus* group.

#### 4 CONCLUSIONS

Identification of selected highly keratinolytic isolates by 16S rRNA gene sequencing or FAMES analysis was successful at genus level. All isolates belong to genus *Bacillus*. Final identification with WGS divided the isolates into four *Bacillus* species (*B. mycooides*, *B. subtilis*, *B. altitudinis* and *B. wiedmannii*). Core genome analysis clearly divided the isolates into two groups: *Bacillus subtilis* group (*B. subtilis* and *B. altitudinis*) and *Bacillus cereus* group (*B. mycooides* and *B. wiedmannii*).

#### 5 REFERENCES

- Andrews, S., Lindenbaum, P., Howard, B., Ewels, P. (2011–2014). FastQC high throughput sequence QC report Version 0.11.2. Retrieved from <http://www.bioinformatics.babraham.ac.uk/projects/fastqc>
- Bankevich, A., Nurk, S., Antipov, D., Gurevich, A.A., Dvorkin, M., Kulikov, A.S., ...Pevzner, P.A. (2012). SPAdes: A new genome assembly algorithm and its applications to single-cell sequencing. *Journal of Computational Biology*, 19(5), 455–477. <https://doi.org/10.1089/cmb.2012.0021>

- Church, D.L., Cerutti, L., Gürtler, A., Greiner, T., Zelazny, A., Emler, S. (2020). Performance and Application of 16S rRNA Gene Cycle Sequencing for Routine Identification of Bacteria in the Clinical Microbiology Laboratory. *Clinical Microbiology Reviews*, 33(4), e00053-19. <https://doi.org/10.1128/CMR.00053-19>
- Dawyndt, P., Vancanneyt, M., Snauwaert, C., De Baets, B., De Meyer, H., Swings, J. (2006) Mining fatty acid databases for detection of novel compounds in aerobic bacteria. *Journal of Microbiological Methods*, 66(3), 410–433. <https://doi.org/10.1016/j.mimet.2006.01.008>
- Lane, D.J. (1991). 16S/23S rRNA sequencing. In Stackebrandt, E. & Goodfellow, M. (Eds.), *Nucleic Acids Techniques in Bacterial Systematics* (pp. 115–148). Chichester, UK: John Wiley & Sons.
- Page, A.J., Cummins, C.A., Hunt, M., Wong, V.K., Reuter, S., Holden, M.T.G., ...Parkhill, J. (2015). Roary: Rapid large-scale prokaryote pan genome analysis. *Bioinformatics*, 31(22), 3691–3693. <http://doi.org/10.1093/bioinformatics/btv421>
- Pritchard, L., Glover, R.H., Humphris, S., Elphinstone, J.G., Toth, I.K. (2016). Genomics and taxonomy in diagnostics for food security: soft-rotting enterobacterial plant pathogens. *Analytical Methods*, 8(1), 12–24. <https://doi.org/10.1039/C5AY02550H>
- Richter, M., Rossello-Mora, R. (2009). Shifting the genomic gold standard for the prokaryotic species definition. *PNAS*, 106(45), 19126–19131. <https://doi.org/10.1073/pnas.0906412106>
- Rossen, J.W.A., Friedrich, A.W., Moran-Gilad, J. (2018). Practical issues in implementing whole-genome-sequencing in routine diagnostic microbiology. *Clinical Microbiology and Infection*, 24(4), 355–360. <https://doi.org/10.1016/j.cmi.2017.11.001>
- Sanguinetti, M., Posteraro, B. (2016). Mass spectrometry applications in microbiology beyond microbe identification: progress and potential. *Expert Review of Proteomics*, 13(10), 965–977. <https://doi.org/10.1080/14789450.2016.1231578>
- Santos, I.C., Smuts, J., Choi, W.S., Kim, Y., Kim, S.B., Schug, K.A. (2018). Analysis of bacterial FAMES using gas chromatography – vacuum ultraviolet spectroscopy for the identification and discrimination of bacteria. *Talanta*, 182, 536–543. <https://doi.org/10.1016/j.talanta.2018.01.074>
- Sasser, M. (1990). Identification of Bacteria by gas Chromatography of Cellular Fatty acids. MIDI Technical Note 101, Newark, ZDA: MIDI Inc.
- Seemann, T. (2014). Prokka: rapid prokaryotic genome annotation. *Bioinformatics*, 30(14), 2068–2069. <https://doi.org/10.1093/bioinformatics/btu153>
- Slabbinck, B., De Baets, B., Dawyndt, P., De Vos, P. (2009). Towards large-scale FAME-based bacterial species identification using machine learning techniques. *Systematic and Applied Microbiology*, 32(3), 163–176. <https://doi.org/10.1016/j.syapm.2009.01.003>
- Weisburg, W.G., Barns, S.M., Pelletier, D.A., Lane, D.J. (1991). 16S ribosomal DNA amplification for phylogenetic study. *Journal of Bacteriology*, 173(2), 697–703. <https://doi.org/10.1128/jb.173.2.697-703.1991>

# UPRAVLJANJE GOZDNIH EKOSISTEMOV/MANAGING FOREST ECOSYSTEMS

## Comparison of DEMATEL and WINGS method

Tjaša ŠMIDOVNIK<sup>1\*</sup>, Petra GROŠELJ<sup>1</sup>

<sup>1</sup> University of Ljubljana, Biotechnical Faculty, Department of Forestry and Renewable Forest Resources, Ljubljana, Slovenia

\*corresponding author: [tjasa.smidovnik@bf.uni-lj.si](mailto:tjasa.smidovnik@bf.uni-lj.si)

### Comparison of DEMATEL and WINGS method

**Abstract:** Interest in the use of multi-criteria decision-making methods is growing and so the number of different methods. These include the DEMATEL method (*Decision Making Trial and Evaluation Laboratory*) and the WINGS method (*Weighted Influence Non-linear Gauge System*). They are used to determine the relationships between the elements of the system. The WINGS method is descendant of DEMATEL method and include also the strength of each element. We selected an example from the literature to compare both methods. From the results we can see that the strength of the elements has a great influence on the final result (on the weights of the elements and on the position of the elements in the causal diagram).

**Key words:** DEMATEL; multi-criteria decision making. WINGS

### Primerjava metod DEMATEL in WINGS

**Izvelek:** Zanimanje za uporabo metod večkriterijskega odločanja narašča, s tem pa narašča tudi število različnih metod. V to skupino metodo sodita tudi metodi DEMATEL (*Decision Making Trial and Evaluation Laboratory*) in WINGS (*Weighted Influence Non-linear Gauge System*). Uporabljata se za določitev povezav med elementi v sistemu. Metoda WINGS je nadgradnja metode DEMATEL ter vključuje tudi moč posameznega elementa. Metodi smo primerjali na zgledu iz literature. Iz rezultatov lahko razberemo, da ima moč elementa velik vpliv na končne rezultate. Vpliva tako na uteži elementov kot tudi na njihovo postavitev v vzročnem diagramu.

**Ključne besede:** DEMATEL; večkriterijsko odločanje; WINGS

## 1 INTRODUCTION

Nowadays, many multi-criteria decision making method are used. Multi-criteria decision making (MCDM) is a collective term for mathematical methods, which used to solve decision problem with multiple (usually) conflicting goals (Eggers et al., 2019). Difrent methods such as AHP (*Analytic Hierarchical Process*), TOPSIS (*Technique for Order Performance by Similarity to Ideal Solutions*), VIKOR (*VIse Kriterijumska Optimizacija I Kompromisno Resenje*), DEMATEL (*Decision Making Trial and Evaluation Laboratory*) and WINGS (*Weighted Influence Non-linear Gauge System*) are used to deal with MCDM (Tavana, Mousavi, Khalili Nasr, & Mina, 2021).

DEMATEL (*Decision Making Trial and Evaluation Laboratory*) method was developed by the Geneva Research Centre of the Battelle Memorial Institute and is used to analyse the

relationships between the elements of the system. (Gabus & Fontela, 1972). It is one of the most widely used method in various fields such as ecology (Xu, Lu, & Zhang, 2021), energy (Wu et al., 2022), urbanization (Hanine et al., 2021), medicine (Song, Zhao, Mubarak, & Taresh, 2022) and others.

WINGS (*Weighted Influence Non-linear Gauge System*) method was proposed by Michnik (Michnik, 2013). WINGS is a descendant of the DEMATEL method and differs from it in that the strength of each element is considered in addition to its influence.

The aim of this paper is to compare the DEMATEL and WINGS methods on selected example from literature. We have looked how the strength of the elements in the WINGS method affect on the final results. In the Section 2, both methods are presented and applied to an example from the literature. Section 3 presents and compares the results. Section 4 provides the summary and conclusion of our study.

## 2 METHODS

### 2.1 DEMATEL (Decision Making Trial and Evaluation Laboratory)

Step 1: Generate the direct-influence matrix  $D$

Select the system of  $n > 2$  elements and examine the causal relations between them. It is advisable to create a map of influence that represents the system. The nodes in the graph represent the elements of the system, and the arrows represent the nonzero influence of one element on another (in the direction of the arrow). The decision makers assess all the influences of one element on another using scale from 0 to 4, where 0 represents no influence and 4 represents very high influence (Table 1). The assessments are arranged in the direct-influence matrix  $D$ . It is  $n \times n$  matrix with elements  $d_{ij}$  to the direct influence of element  $i$  on element  $j$ .

Step 2: Derive the normalized direct-relation matrix  $X$

$X = [x_{ij}]$  is the normalized direct-relation matrix and  $x_{ij}$  is calculated as follows

$$x_{ij} = \frac{d_{ij}}{\max(\max_{1 \leq i \leq n} \sum_{j=1}^n d_{ij}, \max_{1 \leq i \leq n} \sum_{i=1}^n d_{ij})}, i, j = 1, \dots, n.$$

Step 3: Derive the total relation matrix  $T$

Total relation matrix  $T$  is an infinitive sum of influences among factors.  $T = [t_{ij}]$  is calculated as follows

$$T = X + X^2 + \dots + X^n + \dots = X(I - X)^{-1}.$$

Step 4: Sum the rows and columns and construct the causal diagram

The row sums  $R_i$  (Eq. ) and the column sums  $C_j$  (Eq. ) are calculated for each elements.  $R_i$  represents direct and indirect effects of the factor  $i$  on other factors.  $C_j$  represents direct and indirect effects that the factor  $j$  receives from all other factors.

$$R_i = \sum_{j=1}^n t_{ij}, i = 1, \dots, n$$

$$C_j = \sum_{i=1}^n t_{ij}, j = 1, \dots, n$$

$R_i + C_i$ , also called prominence value, are calculated. It represents the importance of factor  $i$ . The net effect that factor  $i$  contributes to the system represents the difference  $R_i - C_i$  or relations value. The positive value means that an element effects on others, and the negative value means that it is influenced by other elements (Liu, Long, & Li, 2020). For better transparency and easier analysis, the result can be represented in the causal diagram. It consists of  $R_i + C_i$  on the horizontal axis, while  $R_i - C_i$  on the vertical axis divides the factors into cause (positive values) and effect (negative values) groups (Mao, Han, Deng, & Pelusi, 2020). The causal diagram is divided into four quadrants. In the first quadrant are key elements that have high importance, and in the second quadrant are driving elements. These two quadrants are separated by a vertical line that runs at the average value of  $R_i - C_i$ . The third quadrant has independent elements, while the elements in the fourth quadrant are influenced by other elements (Islam, Mustafa, & Sorooshian, 2019).

Step 5: Derive the weights of elements

The weights of elements are calculated as follow

$$\omega_i = \sqrt{(R_i + C_i)^2 + (R_i - C_i)^2}$$

## 2.2 WINGS (Weighted Influence Non-linear Gauge System)

Because WINGS is a descendant of the DEMATEL method has also similar steps. It differs in first step, where also the strength of the elements is determined.

Step 1: Generate the strength-influence matrix  $D$

Decision makers evaluate all influences between elements and determine the strength of each element (Table 1). A five-point scale is also used to determine the strength of the elements, where 0 means the element has no strength and 4 means the element has very high strength. It is recommended that a scale with the same levels be used for all assessments, as this maintains a balance of impacts. All values, influences and strengths of the elements, are then arranged in

the strength-influence matrix  $D$ . Values representing the strength of the elements are inserted into principal diagonal  $d_{ii}$  (strength of element  $i$ ). Values representing influences of elements are inserted in such a way that for  $i \neq j$ ,  $d_{ij}$  is influence of element  $i$  on element  $j$  (Michnik, 2013).

**Table 1:** Linguistic terms and their corresponding scalar numbers

Linguistic terms	Abbreviation	Corresponding scalar value
No influence/strength	NI/NS	0
Very low influence/strength	VLI/VLS	1
Low influence/strength	LI/LS	2
High influence/strength	HI/HS	3
Very high influence/strength	VHI/VHS	4

The other steps are the same as for the DEMATEL method.

### 3 RESULTS AND DISCUSSION

Example from the literature is selected (Radziszewska-Zielina & Śladowski, 2017). Five elements were compared. Element  $C_3$  has the highest strength and the element  $C_4$  has the lowest. Elements  $C_1$  and  $C_4$  effect on the three elements, while other elements effect on one or two elements. Elements  $C_3$ ,  $C_4$  and  $C_5$  are influenced by most elements, while the remaining two elements are influenced by only one element. Figure 1 shows the direct influences between the elements and the strength of the elements. In the calculation with the DEMATEL method, all elements have no strengths.

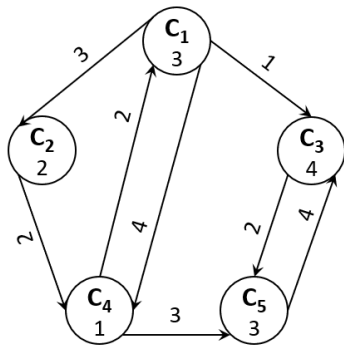


**Figure 1:** The graph of system (WINGS)

Two matrices are shown below. On the right side is the direct-influence matrix  $D$  (DEMATEL method) and on the left is the strength-influence matrix (WINGS method).

$$D_{DEMATEL} = \begin{pmatrix} 0 & 3 & 1 & 4 & 0 \\ 0 & 0 & 0 & 2 & 0 \\ 0 & 0 & 0 & 0 & 2 \\ 0 & 2 & 0 & 0 & 3 \\ 0 & 0 & 4 & 0 & 0 \end{pmatrix} \quad D_{WINGS} = \begin{pmatrix} 3 & 3 & 1 & 4 & 0 \\ 0 & 2 & 0 & 2 & 0 \\ 0 & 0 & 4 & 0 & 2 \\ 0 & 2 & 0 & 1 & 3 \\ 0 & 0 & 4 & 0 & 3 \end{pmatrix}$$

The following two tables (Table 2 and Table 3) show the results (row sums, column sums, prominence values and relations values, weights of the elements and their ranking) obtained by DEMATEL and WINGS methods.

**Table 2:** The results of DEMATEL, row sums (R), column sums (C), prominence values (Ri+Ci) and relations values (Ri-Ci), weights of element and theirs ranking

	T					R	C	R + C	R - C	weight (ranking)
	C <sub>1</sub>	C <sub>2</sub>	C <sub>3</sub>	C <sub>4</sub>	C <sub>5</sub>					
C <sub>1</sub>	0,00	0,53	0,28	0,63	0,31	1,75	0,00	1,75	1,75	0,25 (1)
C <sub>2</sub>	0,00	0,07	0,06	0,27	0,11	0,50	0,87	1,37	-0,36	0,14 (5)
C <sub>3</sub>	0,00	0,00	0,14	0,00	0,29	0,43	1,28	1,71	-0,85	0,19 (4)
C <sub>4</sub>	0,00	0,27	0,23	0,07	0,46	1,02	0,97	1,99	0,05	0,20 (3)
C <sub>5</sub>	0,00	0,00	0,57	0,00	0,14	0,71	1,31	2,02	-0,59	0,21 (2)

**Table 3:** The results of WINGS, row sums (R), column sums (C), prominence values (Ri+Ci) and relations values (Ri-Ci), weights of element and theirs ranking

	T					R	C	R + C	R - C	weight (ranking)
	C <sub>1</sub>	C <sub>2</sub>	C <sub>3</sub>	C <sub>4</sub>	C <sub>5</sub>					
C <sub>1</sub>	0,38	0,61	0,40	0,67	0,35	2,40	0,38	2,78	2,03	0,23 (3)
C <sub>2</sub>	0,00	0,28	0,06	0,26	0,11	0,71	1,14	1,85	-0,43	0,13 (5)
C <sub>3</sub>	0,00	0,00	0,83	0,00	0,46	1,29	2,50	3,79	-1,21	0,26 (1)
C <sub>4</sub>	0,00	0,26	0,29	0,15	0,50	1,20	1,08	2,28	0,12	0,15 (4)
C <sub>5</sub>	0,00	0,00	0,92	0,00	0,60	1,52	2,03	3,55	-0,51	0,24 (2)

The two tables above (Table 2 and Table 3) show that the weights of the elements depend on which method was used. We can see that the order of the elements also changes. The element C<sub>3</sub> is in the fourth position if the DEMATEL method was used and in the first position if the WINGS method was used. This is because the element has a very high strength, which is considered in the WINGS method.

For better transparency and comparison, the results of both methods (DEMATEL and WINGS) are shown in the causal diagram (Figure 2).

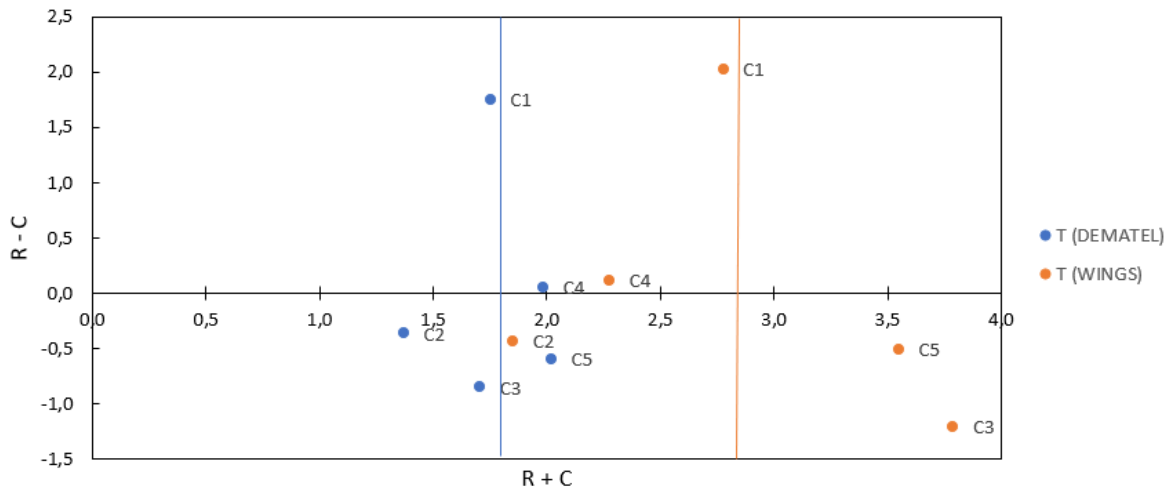


Figure 2: Cause and effect elements calculated with DEMATEL and WINGS method

Five elements were compared. We calculated the average values  $R + C$  for both methods. These two values are different, so that the quadrants do not overlap. The causal diagram (Figure 2) shows that the elements are evenly distributed among the quadrants, regardless of which method we use (DEMATEL or WINGS). In both cases, elements  $C_1$  and  $C_4$  are among the influencing elements, while elements  $C_2$ ,  $C_3$  and  $C_5$  are influenced by other elements. In the WINGS method, the elements are arranged slightly differently. The elements that have more impact are further to the right in the causal diagram. The largest shift to the right is observed for element  $C_3$ , which is expected since it is also assigned the maximum strength. Element  $C_1$  also gains influence (shifts to the right to element  $C_4$ ).

#### 4 CONCLUSIONS

Nowadays, multi-criteria decision making methods are widely used. One of them is also the DEMATEL and WINGS methods. The DEMATEL method is used to determine the relationships between elements in the system. The WINGS method is an upgrade of the DEMATEL method and also includes the strength of each element.

In this paper, the two multi-criteria methods (DEMATEL and WINGS) were compared using an example from literature. The results show that the strength of elements affects on element's weight and their position in the causal diagram. The results show that the WINGS method is more suitable for use, because the strength of each element plays an important role in the classification of elements. Although the DEMATEL method is already a well-known and is widely used method, the results show that it is more advisable to use the WINGS method.

#### ACKNOWLEDGEMENT

The authors acknowledge the financial support from the Slovenian Research Agency (ARRS) within the framework of research program P4-0059 and young researcher grant (Tjaša Šmidovnik).

## 5 REFERENCES

- Eggers, J., Holmgren, S., Nordström, E.-M., Lämås, T., Lind, T., & Öhman, K. (2019). Balancing different forest values: Evaluation of forest management scenarios in a multi-criteria decision analysis framework. *Forest Policy and Economics*, *103*, 55-69. doi:10.1016/j.forpol.2017.07.002
- Gabus, A., & Fontela, E. (1972). World Problems, An Invitation to Further Thought within the Framework of DEMATEL.
- Hanine, M., Boutkhom, O., El Barakaz, F., Lachgar, M., Assad, N., Rustam, F., & Ashraf, I. (2021). An Intuitionistic Fuzzy Approach for Smart City Development Evaluation for Developing Countries: Moroccan Context. *Mathematics*, *9*(21). doi:10.3390/math9212668
- Islam, A. S. M. T., Mustafa, S., & Sorooshian, S. (2019). An Error-Proof Approach for Decision Making Using DEMATEL. *KnE Social Sciences*. doi:10.18502/kss.v3i22.5054
- Liu, H., Long, H., & Li, X. (2020). Identification of critical factors in construction and demolition waste recycling by the grey-DEMATEL approach: a Chinese perspective. *Environ Sci Pollut Res Int*, *27*(8), 8507-8525. doi:10.1007/s11356-019-07498-5
- Mao, S., Han, Y., Deng, Y., & Pelusi, D. (2020). A hybrid DEMATEL-FRACTAL method of handling dependent evidences. *Engineering Applications of Artificial Intelligence*, *91*. doi:10.1016/j.engappai.2020.103543
- Michnik, J. (2013). Weighted Influence Non-linear Gauge System (WINGS) – An analysis method for the systems of interrelated components. *European Journal of Operational Research*, *228*(3), 536-544. doi:10.1016/j.ejor.2013.02.007
- Radziszewska-Zielina, E., & Śladowski, G. (2017). Supporting the selection of a variant of the adaptation of a historical building with the use of fuzzy modelling and structural analysis. *Journal of Cultural Heritage*, *26*, 53-63. doi:10.1016/j.culher.2017.02.008
- Song, P., Zhao, J., Mubarak, S. M. A., & Taresh, S. M. (2022). Critical success factors for epidemic emergency management in colleges and universities during COVID-19: A study based on DEMATEL method. *Saf Sci*, *145*, 105498. doi:10.1016/j.ssci.2021.105498
- Tavana, M., Mousavi, H., Khalili Nasr, A., & Mina, H. (2021). A fuzzy weighted influence non-linear gauge system with application to advanced technology assessment at NASA. *Expert Systems with Applications*, *182*. doi:10.1016/j.eswa.2021.115274
- Wu, Y., Liu, F., Wu, J., He, J., Xu, M., & Zhou, J. (2022). Barrier identification and analysis framework to the development of offshore wind-to-hydrogen projects. *Energy*, *239*. doi:10.1016/j.energy.2021.122077
- Xu, D., Lu, C., & Zhang, X. (2021). An Ecological Development Level Evaluation of the Forestry Industry in China Based on a Hybrid Ensemble Approach. *Forests*, *12*(9). doi:10.3390/f1209128

## ZNANOST O CELICI/CELL SCIENCES

### Ultrastructure of septate junctions in arthropod epithelia: comparative analysis of junctions in the hindgut and digestive glands of *Porcellio scaber*

Katja KUNČIČ<sup>1\*</sup>, Polona MRAK<sup>1</sup>, Urban BOGATAJ<sup>1</sup>, Nada ŽNIDARŠIČ<sup>1</sup>

<sup>1</sup> University of Ljubljana, Biotechnical Faculty, Department of Biology, Ljubljana, Slovenia

\* corresponding author: [katja.kuncic@bf.uni-lj.si](mailto:katja.kuncic@bf.uni-lj.si)

#### **Ultrastructure of septate junctions in arthropod epithelia: comparative analysis of junctions in the hindgut and digestive glands of *Porcellio scaber***

**Abstract:** Epithelia function as selectively permeable barriers in various organs. Complex regulation of paracellular fluxes in transporting epithelia depends on cell-cell junctions. In invertebrates, the occluding function is performed by septate junctions (SJs). Arthropods have two types of SJs: pleated SJs in ectodermal epithelia and smooth SJs in endodermal epithelia. In this study, we analysed and compared the ultrastructural characteristics of SJs in the ectodermal hindgut epithelia of the anterior chamber and papillate region and SJs in the endodermal digestive glands' epithelium of the isopod *Porcellio scaber* (Latreille, 1804). SJs in the analysed epithelia differ primarily in the architecture, extensiveness, and the presence of microtubules. Consecutive arrays of septa and short segments of the intercellular space without septa are characteristic for the architecture of SJs in the hindgut. They are more extensive and are associated with abundant microtubules in the papillate region compared with SJs in the anterior chamber. In the anterior chamber and digestive glands, the SJs occupy about one-tenth of the lateral cell membranes apposed, whereas in the papillate region they occupy about one-third of the interface. The results are evaluated and discussed in the perspective of the morphological diversity and common features of SJs in arthropod epithelia.

**Key words:** cytoskeleton; digestive system; isopods; septate junctions; transporting epithelia

#### **Ultrastruktura septiranih stikov v epitelih členonožcev: primerjalna analiza stikov v zadnjem črevesu in prebavnih žlezah *Porcellio scaber***

**Izveček:** Epitelna tkiva delujejo kot selektivno prepustne bariere v različnih organih. Kompleksna regulacija paracelularnih pretokov v transportnih epitelih je odvisna od medceličnih stikov. Paracelularni transport v epitelih nevretenčarjev regulirajo septirani stiki (SS). Pri členonožcih ločimo dva tipa SS: nagubane SS v ektodermalnih epitelih in gladke SS v endodermalnih epitelih. V tej študiji smo analizirali in primerjali ultrastrukturne značilnosti SS v ektodermalnih epitelih anterirone komore in papilatne regije zadnjega črevesa ter SS v endodermalnem epitelu prebavnih žlez enakonožca *Porcellio scaber* (Latreille, 1804). SS v teh epitelih se razlikujejo predvsem po arhitekturi in obsegu ter prisotnosti mikrotubulov. SS v črevesu obsegajo zaporedne nize sept, ločene z odseki medceličnega prostora brez sept. SS v papilatni regiji so najbolj obsežni in pod membrano je vidnih veliko mikrotubulov. V epitelu anterirone komore in prebavnih žlez obsegajo SS približno desetino lateralne stične površine celic, v epitelu papilatne regije pa kar tretjino. Evalvacija rezultatov je osredotočena na razpravo o morfološki raznolikosti in univerzalnih značilnostih SS pri členonožcih.

**Ključne besede:** citoskelet; prebavni sistem; raki enakonožci; septirani stiki; transportni epiteli

## 1 INTRODUCTION

Epithelia function as selectively permeable barriers between the internal and the external environment of the organism and between physiologically distinct compartments in various organs. The architecture and function of epithelia crucially depend on cell-cell junctions (Fristrom, 1988; Baum & Georgiou, 2011; Varadarajan et al., 2019). Invertebrate epithelial cells are attached to each other by adherens junctions (AJs), while septate junctions (SJs) are essential for the regulation of transepithelial transport in between cells, i.e. the paracellular pathway, and prevent pathogens from crossing epithelial barriers (Tepass & Hartenstein, 1994; Izumi & Furuse, 2014; Jonusaite et al., 2016). SJs of invertebrates functionally correspond to tight junctions in vertebrates. The morphology of SJs varies depending on invertebrate species and type of epithelium (Jonusaite et al., 2016). In ectodermal and endodermal arthropod epithelia, pleated SJs and smooth SJs surround the subapical region of the cell, respectively, but the significance of two types of SJs is not explained (Flower & Filshie, 1975; Noirot-Timothee et al., 1978; Fristrom, 1988; Tepass & Hartenstein, 1994; Izumi & Furuse, 2014; Jonusaite et al., 2016). In SJs electron-dense septa span the intercellular space of constant width, resulting in a "ladder-like" ultrastructural appearance in sections perpendicular to the septa. Information on SJs' molecular architecture, formation during development, function in the paracellular flux regulation and in the immune barrier, mainly derives from studies of *Drosophila melanogaster*.

The digestive system of arthropods is the site of nutrient and water absorption and serves as a barrier to pathogens. With respect to these functions, the regulation of paracellular transport by SJs in the epithelia of the digestive system is crucial (Fristrom, 1988; Tepass & Hartenstein, 1994; Jonusaite et al., 2016). To better understand the structural diversity and roles of SJs, it is advantageous to analyse the ultrastructural characteristics of SJs in epithelia with different functions. We have analysed SJs in the epithelia of the digestive system of the isopod crustacean *Porcellio scaber* because comprehensive data are available on the functional anatomy of its digestive system (Hames & Hopkin, 1989; Storch & Štrus, 1989; Štrus et al., 1995; Štrus et al., 2019) and the ultrastructure of cells in different epithelia of its digestive system (Hames & Hopkin, 1991; Žnidaršič et al., 2003; Bogataj et al., 2018). The digestive system of terrestrial isopods consists of the ectodermal foregut and hindgut and the endodermal digestive glands (hepatopancreas). The foregut and hindgut form the alimentary canal, which is covered by a chitinous cuticle on the luminal surface. The hindgut consists of the anterior chamber, papillate region, and rectum. The apical surfaces of the cells in the anterior chamber are enlarged by infoldings of the cell membrane, indicating pronounced transport between the cells and the lumen of the hindgut. In the papillate region, very deep apical and basal membrane labyrinths indicate pronounced transport across both surfaces, consistent with roles in ion transport and osmoregulation (Bogataj et al., 2018). The digestive glands comprise four blind-ending tubules connected to the foregut. The cells of the digestive glands secrete digestive enzymes and play a role in nutrient absorption and storage. Their apical and basal surfaces are increased by microvilli and a basal labyrinth, respectively (Hames & Hopkin, 1989, 1991; Žnidaršič et al., 2003; Štrus et al., 2019).

The aim of this study is the ultrastructural characterisation of SJs in the epithelium of the anterior chamber and papillate region of the hindgut and in the epithelium of digestive glands in adult *P. scaber*. The results are evaluated and discussed in the perspective of the morphological diversity and common features of SJs in arthropod epithelia.

## 2 MATERIALS AND METHODS

### 2.1 Tissue samples

Specimens of *P. scaber* (Latreille, 1804) were collected in Slovenia and reared in a glass terrarium with soil and leaf litter. The animals were maintained at 22-25 °C, high humidity, and a 12-16 h light cycle. The hindguts and digestive glands were isolated from anaesthetized adult animals.

### 2.2 Preparation of sections and imaging by transmission electron microscopy

The isolated tissues were fixed in aldehydes, postfixed in 1% OsO<sub>4</sub>, dehydrated in a graded series of aqueous ethanol and embedded in resin (Agar 100 or Spurr's). Semithin sections (0.5 µm) and ultrathin sections (~70 nm) were cut with a glass and a diamond knife, respectively, using a Reichert Ultracut S ultramicrotome (Leica). Semithin sections were stained with Azure II – Methylene Blue (Richardson stain), dried, mounted in Ultrakitt (J.T. Baker), and inspected with an Axioscope Opton (Zeiss) light microscope. Ultrathin sections were contrasted and imaged with the CM100 (Philips) transmission electron microscope, equipped with an Orius SC200 (Gatan) digital camera and Digital Micrograph software.

Measurements of selected structural characteristics of SJs were performed using ImageJ/Fiji software with the "straight line" tool. The following characteristics were measured: (i) the width of the intercellular space in the SJ region, (ii) the thickness of individual septa, and (iii) the distance between consecutive septa. For the hindgut, six SJs from the anterior chamber of three animals and eight SJs from the papillate region of three animals were included in the analysis. For the digestive glands, measurements were performed on three SJs from two animals. Each characteristic was measured at least four times in each SJ and the median of these measurements is reported in the results.

## 3 RESULTS AND DISCUSSION

### 3.1 Ultrastructure of the pleated septate junctions in the epithelia of anterior chamber and papillate region in the hindgut of *P. scaber*

In the hindgut, AJs are subapical and SJs are basal to them (Fig. 1). Consecutive arrays of septa and short segments of the intercellular space without septa are characteristic for the architecture of SJs in the hindgut (discontinuous SJ). In the anterior chamber, the lateral cell membranes are moderately interdigitated (Fig. 1A). The pleated SJs occupy about one tenth of the lateral membranes. The intercellular space in the junction region is ~18 nm wide. Electron-dense septa are ~6.1 nm thick and the distance between consecutive septa is ~6.7 nm (Fig 1B). In the papillate region, the lateral membranes are intensely interdigitated (Fig. 1C), and the SJs are approximately five times more extensive than in the anterior chamber and occupy about one-third of the lateral membranes. The short segments of the intercellular space without septa are expanded and alternate with the arrays of septa (Fig. 1C). Abundant microtubules are seen close to the SJs. The intercellular space is ~16.6 nm wide, septa are ~6 nm thick and consecutive septa are ~7.3 nm apart.

The intercellular space width, septa thickness and distance between septa in the pleated SJs measured in this study are approximately in the range of values reported for various ectodermal epithelia of arthropods. The intercellular space width of about 15 nm was measured in different arthropod epithelia: in the epidermis of the same species (Kunčič et al., 2022), in the hindgut of a termite (Noirot-Timothee & Noirot, 1980), and in the tracheole investment of the eye of the locust (Lane & Skaer, 1980). The values for individual septa thickness are quite variable in the literature: 5 nm was reported for *P. scaber* epidermis (Kunčič et al., 2022), 8 – 9 nm and 2 – 9 nm were reported by Lane & Skaer (1980) and by Noirot-Timothee & Noirot (1980), respectively. The distance between consecutive septa in *P. scaber* hindgut is roughly in the range of previous measurements in the epidermis, i.e., 6 nm (Kunčič et al., 2022).

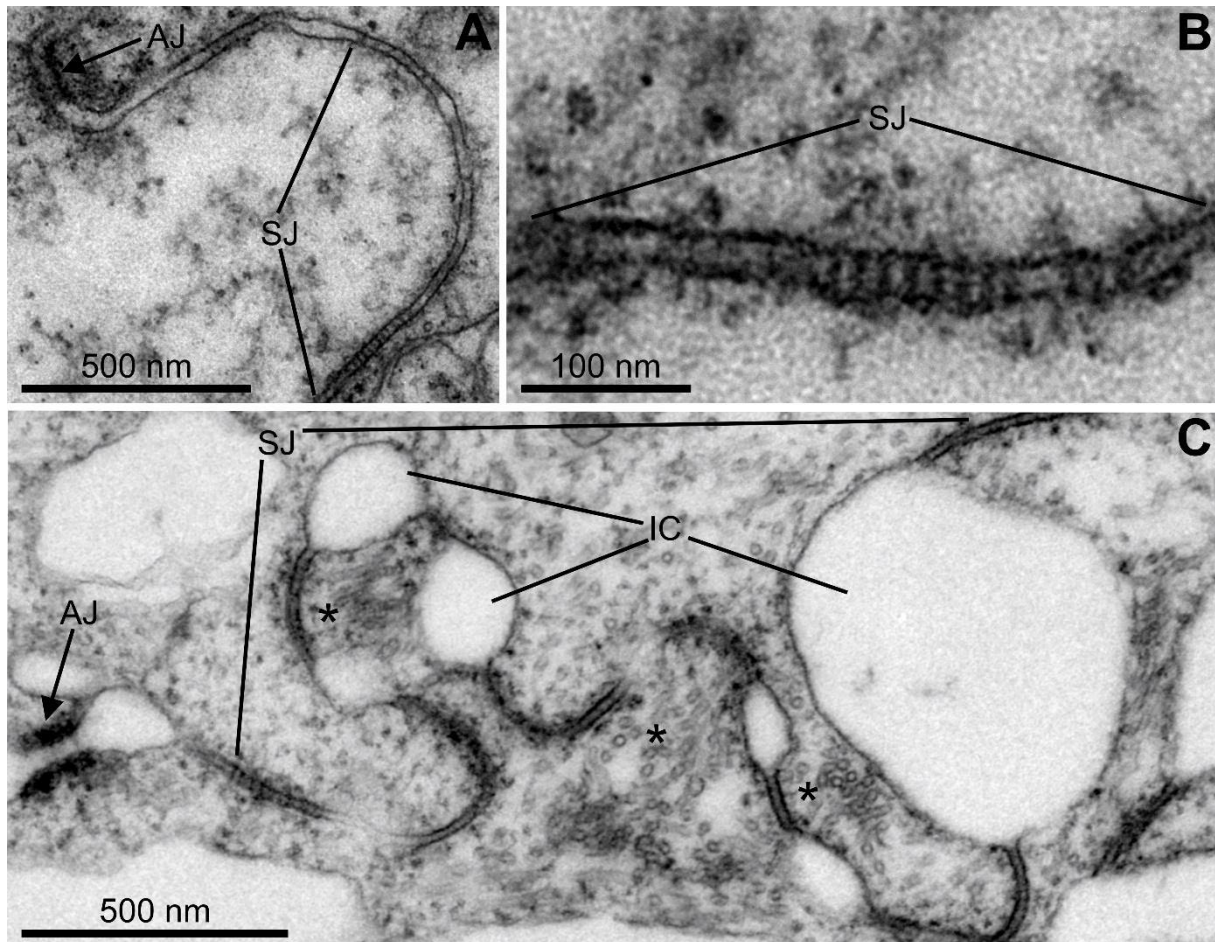


**Figure 1:** Ultrastructure of the subapical junctional complex in the epithelium of the anterior chamber (A-B) and papillate region (C) of the adult *P. scaber* hindgut. The adherens junction (AJ) is located subapically, and the septate junction (SJ) is located basal to the AJ. C. Extensive SJ in the papillate region epithelium, segments of expanded intercellular space without septa and numerous microtubules in the cytosol near the SJ are evident (asterisks). Abbreviations: AJ – adherens junction, IC – intercellular space, SJ – septate junction.

### 3.2 Ultrastructure of the smooth septate junctions in the digestive gland epithelium of *P. scaber*

The septa of the smooth SJs in the digestive glands of *P. scaber* are generally hardly discernible (Fig. 2). The intercellular space in the junction region is ~16.3 nm wide and generally contains a homogeneous, electron-dense material (Fig. 2C). The lateral cell membranes are not intensely interdigitated. The previously reported data for the intercellular space width in the smooth SJs are variable: 20 nm (Beyenbach et al., 2010), 17.5 nm (Hudspeth & Revel, 1971), 11 – 15 nm

for the american cockroach midgut (Noirot-Timothee & Noirot, 1980), 14 – 17 nm for housefly midgut (Lane & Skaer, 1980), and 15 nm for caterpillar (Flower & Filshie, 1975). Smooth SJs in digestive glands of *P. scaber* are continuous, i.e., no electron lucent regions are visible in the intercellular space. SJs occupy about one-tenth of the lateral cell membranes and are up to 4  $\mu\text{m}$  long, which is shorter than previously reported length of 10  $\mu\text{m}$  for smooth SJs in the hepatic caeca of a water flea (Hudspeth & Revel, 1971) and the Malpighian tubules of a mosquito (Beyenbach et al., 2010). Septa measured in this study are  $\sim 4.9$  nm thick and the distance between septa is  $\sim 5.1$  nm. In the junction region electron-dense material is present in the cytosol near the membranes (Figs 2B, C), but no microtubules are discerned. The septa thickness of 8 nm was reported previously for caterpillar by Flower & Filshie (1975).

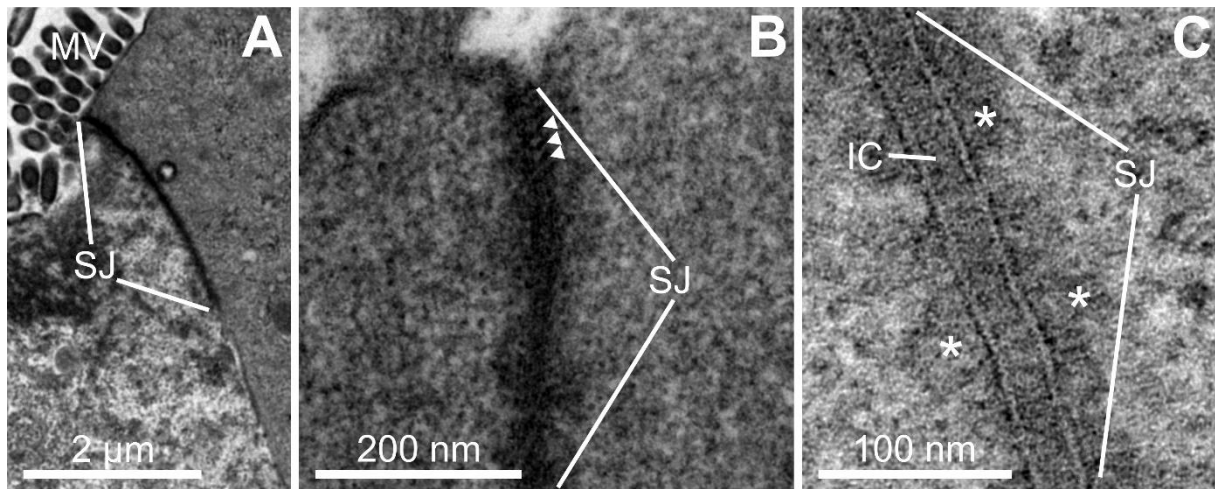


**Figure 2:** Ultrastructure of the subapical junctional complex between neighbouring epithelial cells of the digestive glands in adult *P. scaber*. A. Microvilli are present on the apical surface of the cells. A smooth septate junction (SJ) is located subapically. B. Smooth SJ ultrastructure with resolved septa (arrowheads). C. A homogeneous material in the intercellular space in the region of the junction. Electron-dense material is seen near the membranes in the cytosol (asterisks). Abbreviations: IC - intercellular space, MV - microvilli, SJ - septate junction.

#### 4 CONCLUSIONS

The most distinctive feature of SJs in different epithelia of digestive system in *P. scaber* is the overall extent of SJ. In the anterior chamber and digestive glands, the SJs occupy about one-tenth of the lateral membranes apposed, whereas in the papillate region they occupy about one-third. The extent of pleated SJs was reported to differ with regard to differences in osmotic stress in the gill epithelium of four species of gammarids (Shires, 1995). In Malpighian tubules of the mosquito, SJs occupy lateral cell membranes from apical to basal poles (Beyenbach et al., 2010). These data indicate that very extensive SJs are characteristic for epithelia with a pronounced role in the transport of ions. The absolute length of SJs indicates this also, as pleated SJs in the papillate region are about five times as long as pleated SJs in the anterior chamber or smooth SJs in the digestive glands of adult *P. scaber*. The SJs in the hindgut papillate region occupy extremely intense interdigitations of lateral cell membranes, compared to moderately interdigitated membranes in the anterior chamber. The intense interdigitations of cells in the papillate region may therefore play a role in increasing the SJ area (Bogataj et

al., 2018) and associated complexity of the paracellular pathway, which likely contributes to the tight regulation of paracellular transport in this osmoregulatory epithelium.

The pleated SJs in the hindgut comprise septa arrays and regions of intercellular space devoid of septa in between, which is in accordance with some previous reports on the architecture of arthropod SJs (Noirot-Timothee and Noirot 1980), including the epidermis of *P. scaber* (Kunčič et al., 2022), but the significance of this feature is not explained.

Cell junctions are usually associated with the cytoskeleton, but this has been rarely investigated in invertebrates. Microtubules are abundant near the pleated SJs in the hindgut papillate region, which was previously reported also by Bogataj et al. (2018). Microtubules were observed in the vicinity of pleated SJs also in the study of the gill epithelium of gammarids under changing osmotic conditions by Shires et al. (1995). They suggested that connections between microtubules and membranes in the SJ region may contribute to the stability of the junctions under osmotic stress. We observed accumulations of electron-dense material adjacent to the cell membrane at SJs in the digestive glands, but no microtubules. Studies by Lane and Flores (1988) on the epithelium of the mesenteric caeca and accessory glands of the american cockroach, suggest that actin filaments are associated with smooth and pleated SJs.

#### ACKNOWLEDGEMENT

The authors acknowledge financial support from the Slovenian Research Agency (core funding for the Integrative Zoology and Speleobiology Programme No. P1-0184) and funding for Young Researchers for KK. The equipment of the infrastructure centres 'Microscopy of biological samples' MRIC I0-0022 (Biotechnical Faculty, University of Ljubljana) and I0-0004 IC NIB was used.

#### 5 REFERENCES

- Baum, B., & Georgiou, M. (2011). Dynamics of adherens junctions in epithelial establishment, maintenance, and remodeling. *Journal of Cell Biology*, 192(6), 907–917. <https://doi.org/10.1083/jcb.201009141>
- Beyenbach, K. W., Skaer, H., & Dow, J. A. T. (2010). The developmental, molecular, and transport biology of Malpighian tubules. *Annual Review of Entomology*, 55(1), 351–374. <https://doi.org/10.1146/annurev-ento-112408-085512>
- Bogataj, U., Praznik, M., Mrak, P., Štrus, J., Tušek-Žnidarič, M., & Žnidaršič, N. (2018). Comparative ultrastructure of cells and cuticle in the anterior chamber and papillate region of *Porcellio scaber* (Crustacea, Isopoda) hindgut. *ZooKeys*, 801, 427–458. <https://doi.org/10.3897/zookeys.801.22395>
- Flower, N. E., & Filshie, B. K. (1975). Junctional structures in the midgut cells of lepidopteran caterpillars. *Journal of Cell Science*, 17(1), 221–239. <https://doi.org/10.1242/jcs.17.1.221>
- Fristrom, D. (1988). The cellular basis of epithelial morphogenesis. A review. *Tissue and Cell*, 20(5), 645–690. [https://doi.org/10.1016/0040-8166\(88\)90015-8](https://doi.org/10.1016/0040-8166(88)90015-8)
- Hames, C. A. C., & Hopkin, S. P. (1989). The structure and function of the digestive system of terrestrial isopods. *Journal of Zoology*, 217(4), 599–627. <https://doi.org/10.1111/j.1469-7998.1989.tb02513.x>

- Hames, C. A. C., & Hopkin, S. P. (1991). A daily cycle of apocrine secretion by the B cells in the hepatopancreas of terrestrial isopods. *Canadian Journal of Zoology*, 69(7), 1931–1937. <https://doi.org/10.1139/z91-267>
- Hudspeth, A. J., & Revel, J. P. (1971). Coexistence of gap and septate junctions in and invertebrate epithelium. *Journal of Cell Biology*, 50(1), 92–101. <https://doi.org/10.1083/jcb.50.1.92>
- Izumi, Y., & Furuse, M. (2014). Molecular organization and function of invertebrate occluding junctions. *Seminars in Cell & Developmental Biology*, 36, 186–193. <https://doi.org/10.1016/j.semcdb.2014.09.009>
- Jonusaite, S., Donini, A., & Kelly, S. P. (2016). Occluding junctions of invertebrate epithelia. *Journal of Comparative Physiology B*, 186(1), 17–43. <https://doi.org/10.1007/s00360-015-0937-1>
- Kunčič, K., Mrak, P., & Žnidaršič, N. (2022). Formation and remodelling of septate junctions in the epidermis of isopod *Porcellio scaber* during development. *ZooKeys*, 1101, 159–181. <https://doi.org/10.3897/zookeys.1101.78711>
- Lane, N. J., & Flores, V. (1988). Actin filaments are associated with the septate junctions of invertebrates. *Tissue and Cell*, 20(2), 211–217. [https://doi.org/10.1016/0040-8166\(88\)90042-0](https://doi.org/10.1016/0040-8166(88)90042-0)
- Lane, N. J., & Skaer, H. IeB. (1980). Intercellular junctions in insect tissues. *Advances in Insect Physiology*, 15, 35–213. [https://doi.org/10.1016/s0065-2806\(08\)60141-1](https://doi.org/10.1016/s0065-2806(08)60141-1)
- Noirot-Timothee, C., & Noirot, C. (1980). Septate and scalariform junctions in arthropods. *International Review of Cytology*, 63, 97–140. [https://doi.org/10.1016/s0074-7696\(08\)61758-1](https://doi.org/10.1016/s0074-7696(08)61758-1)
- Noirot-Timothee, C., Smith, D. S., Cayer, M. L., & Noirot, C. (1978). Septate junctions in insects: Comparison between intercellular and intramembranous structures. *Tissue and Cell*, 10(1), 125–136. [https://doi.org/10.1016/0040-8166\(78\)90011-3](https://doi.org/10.1016/0040-8166(78)90011-3)
- Shires, R., Lane, N. J., Inman, C. B. E., & Lockwood, A. P. M. (1995). Microtubule systems associated with the septate junctions of the gill cells of four gammarid amphipods. *Tissue and Cell*, 27(1), 3–12. [https://doi.org/10.1016/s0040-8166\(95\)80003-4](https://doi.org/10.1016/s0040-8166(95)80003-4)
- Storch, V., & Štrus, J. (1989). Microscopic anatomy and ultrastructure of the alimentary canal in terrestrial isopods. *Monografia. Monitore Zoologico Italiano*, 4, 105–126.
- Štrus, J., Drobne, D., & Ličar, P. (1995). Comparative anatomy and functional aspects of the digestive system in amphibious and terrestrial isopods (Isopoda: Oniscidea). In M. A. Alikhan (Ed.), *Terrestrial Isopod Biology* (pp. 15–23). A. A. Balkema.
- Štrus, J., Žnidaršič, N., Mrak, P., Bogataj, U., & Vogt, G. (2019). Structure, function and development of the digestive system in malacostracan crustaceans and adaptation to different lifestyles. *Cell and Tissue Research*, 377(3), 415–443. <https://doi.org/10.1007/s00441-019-03056-0>
- Tepass, U., & Hartenstein, V. (1994). The development of cellular junctions in the *Drosophila* embryo. *Developmental Biology*, 161(2), 563–596. <https://doi.org/10.1006/dbio.1994.1054>
- Varadarajan, S., Stephenson, R. E., & Miller, A. L. (2019). Multiscale dynamics of tight junction remodeling. *Journal of Cell Science*, 132(22). <https://doi.org/10.1242/jcs.229286>

Žnidaršič, N., Štrus, J., & Drobne, D. (2003). Ultrastructural alterations of the hepatopancreas in *Porcellio scaber* under stress. *Environmental Toxicology and Pharmacology*, 13(3), 161–174. [https://doi.org/10.1016/s1382-6689\(02\)00158-8](https://doi.org/10.1016/s1382-6689(02)00158-8)

## Experimental models for studying migratory potential of astrocytes

Maja ŽUGEČ<sup>1\*</sup>, Maja POTOKAR<sup>1,2\*</sup>

<sup>1</sup> Laboratory of Neuroendocrinology – Molecular Cell Physiology, Institute of Pathophysiology, Faculty of Medicine, University of Ljubljana, Ljubljana, Slovenia

<sup>2</sup> Celica Biomedical, Ljubljana, Slovenia

\*Corresponding authors: [maja.zugec@mf.uni-lj.si](mailto:maja.zugec@mf.uni-lj.si), [maja.potokar@mf.uni-lj.si](mailto:maja.potokar@mf.uni-lj.si)

### Experimental models for studying migratory potential of astrocytes

**Abstract:** Astrocytes are one of the most abundant cell types in the central nervous system, providing signalling, metabolic, immunologic support to neurons; therefore, it is important to understand underlying processes that enable astrocytes to reach their final destinations in order to exert proper signalling to the surrounding tissue. Cell migration is a crucial process in the development of the central nervous system, governing tissue homeostasis in physiological conditions, and enabling cellular redistribution in various pathologies. Astrocytes develop in early embryonal stages, proliferate and distribute to their designated destinations and continue to migrate in early postnatal life. We compared migratory properties of primary mouse astrocytes, immortalized mouse astrocytes lacking p53 protein, and human glioblastoma U-251 MG cell line, which derives from astrocytes. Our findings are the following: 1. time lapse images in the wound healing assay, recorded with the confocal microscope with differential interference contrast (DIC), enabled accurate measurements of the cell free area, which is important for calculating cell migration parameters, 2. neonatal mouse astrocytes retain a certain degree of migratory potential, 3. mouse immortalized *p53*<sup>-/-</sup> astrocytes, which lack the expression of p53 protein, migrate significantly faster than primary astrocytes, 4. human glioblastoma cells with genetic drift migrate faster than primary neonatal astrocytes, but slower than immortalized *p53*<sup>-/-</sup> astrocytes.

**Key words:** astrocytes; cell migrations; glioblastoma; microscopy; U-251 MG

### Ekperimentalni modeli za preučevanje migracijskega potenciala astrocitov

**Izveček:** Astroцитi so ena najpogostejših tipov celic v centralnem živčnem sistemu in uravnavajo delovanje nevronov prek procesov signaliziranja, ter presnovne in imunološke podpore. Zato je pomembno razumeti procese, ki astroцитom omogočajo, da dosežejo ustrezna območja, kjer lahko lokalno uravnavajo delovanje tkiva. Migracije celic so v razvoju centralnega živčnega sistema ključnega pomena, saj uravnavajo homeostazo tkiv v fizioloških razmerah, v različnih patoloških stanjih pa omogočajo prerazporejanje celic. Astroцитi se v embrionalnem razvoju razvijejo že v zgodnjih fazah, nato pa se razmnožijo in prerazporedijo na ustrezna območja ter ohranijo sposobnost migriranja še v zgodnjem postnatalnem obdobju. V raziskavi smo primerjali lastnosti migracij primarnih mišjih astroцитov, imortaliziranih mišjih astroцитov z izbitim genom za protein p53, in humanih glioblastomskih U-251 MG celic, ki izvirajo iz astroцитov. Naše ugotovitve so sledeče: 1. časovno zajemanje slik s konfokalnim mikroskopom v tehniki diferencialni interferenčni kontrast (DIC) v poskusu preučevanja zapiranja poškodbe, omogoča natančne meritve površine brez celic, iz katere lahko izračunamo migracijski potencial celic, 2. mišji astroцитi, izolirani iz neonatalnih mišk, deloma ohranijo sposobnost migracije, 3. imortalizirani mišji astroцитi (*p53*<sup>-/-</sup>) migrirajo izrazito hitreje kot

primarni astrociti, 4. humane glioblastomske celice migrirajo hitreje kot primarni neonatalni astrociti, vendar počasneje kot imortalizirani astrociti (*p53*<sup>-/-</sup>).

**Ključne besede:** astrociti; glioblastom; migracije celic; mikroskopija, U-251 MG

## 1 INTRODUCTION

Astrocytes are one of the most abundant cell types in the central nervous system (CNS) (Bass et al., 1971). For several decades they have been considered to have a secondary and passive role in providing support to neuronal distribution and interactions, however, recent studies have revealed that they actively regulate the physiological functions of the brain, and that their dysfunction can lead to different disorders (Burda & Sofroniew, 2014; Molofsky et al., 2012; Sloan & Barres, 2014).

During embryonal development astrocytes derive from astrocyte precursor cells, which at around 16th-18th day of embryonic development in rodents undergo the “gliogenic switch” from neural stem cells in the subventricular zone (Felix et al., 2021; Ge et al., 2012). These newly formed astrocytes reach their designated destinations within the cortex by migrating along radial glia cells (Felix et al., 2021; Kriegstein & Alvarez-Buylla, 2009). Their migration, along with neuronal and glial precursors, is a crucial process in the brain development, where cells migrate over significant distances (Cayre et al., 2009; Jacobsen & Miller, 2003). During early postnatal development the migration of astrocytes is not complete (Kriegstein & Alvarez-Buylla, 2009), and they still translocate to a certain extent during the process when radial glia are losing their guiding processes before differentiation (Felix et al., 2021; Kriegstein & Alvarez-Buylla, 2009). Data on this type of migration are scarce. In contrast, astrocytes in the adult brain are quiescent under physiological conditions, but they may reversibly become engaged in a migration (Zhang et al., 2018). Since cell migration is involved in the majority of cellular processes implicated in maintaining cellular homeostasis and tissue morphogenesis in normal physiological conditions (Vicente-Manzanares & Horwitz, 2011), the research of migratory properties of astrocytes in different settings is of crucial importance.

It is generally accepted that in pathological conditions cell migration affects wound healing, immune response, and the spread of cancer metastasis (Friedl & Wolf, 2010; Ridley et al., 2003). Astrocytes become reactive under pathological conditions such as infections, trauma, ischemia, and neurodegenerative diseases, meaning that their genetic profile changes to resemble the undifferentiated one. Such astrocytes proliferate, migrate and form a dense network of hypertrophic cells known as the astroglial scar (Rolls et al., 2009; Silver et al., 2014; Sun & Jakobs, 2012). Astrocyte migration after injury or inflammation is specific and may involve only migration (redistribution) of their processes (Wang & Hamilton, 2009).

In contrast, astrocyte migration is reinduced in malignant gliomas, the most common primary brain tumors originating from astrocytes, where glioblastoma (GBM) is the most malignant and highly aggressive. Patients, diagnosed with GBM, have life expectancy of only 12-15 months even with treatment combining resection, radiation therapy, and chemotherapy (Ostrom et al., 2013; Furnari et al., 2007; Gieryng et al., 2017). The major reason for treatment failure is diffuse invasion of GBM cells into the surrounding brain tissue (Cuddapah et al., 2014; Hwang et al., 2008) by migrating along different pathways such as blood vessels or myelinated nerves (Hamadi et al., 2014).

To unravel the migratory properties of astrocytes and to understand the signalling pathways that regulate their expansion and migration in different developmental and pathological conditions, it is necessary to evaluate the migratory potential of astrocytes, which enables them to develop, and to use an appropriate model with an adequate interpretation of the data. Here we describe the migratory properties of astrocytes in several experimental models, including immortalized astrocytes, which are genetically transformed cells with infinite proliferation ability (Frisa & Jacobberger, 2002; Furihata et al., 2016; Morikawa et al., 2001).

## 2 MATERIALS AND METHODS

Unless stated otherwise, all chemicals used were obtained from Sigma-Aldrich (Merck KGaA, Germany).

### 2.1 Cell cultures

Primary mouse astrocytes were isolated from cerebral cortices of neonatal (1 day old) C57BL/6 mice, as previously described (Schwartz & Wilson, 1992), and maintained in high-glucose Dulbecco's modified Eagle's medium supplemented with 10 % fetal bovine serum, 1 mM sodium pyruvate, 2 mM L-glutamine, 5 U/ml penicillin, and 5 µg/ml streptomycin in 5 % CO<sub>2</sub>/95 % air at 37 °C. All procedures involving animals were carried out in accordance with Animal Protection Act (Official Gazette of the RS, No.38/2013 and official consolidated text 21/18, 92/20 and 159/21).

Immortalized (p53<sup>-/-</sup>) mouse astrocytes were obtained from Professor Gerhard Wiche (University of Vienna, Austria) and maintained as primary mouse astrocytes. They were isolated from cerebral cortices of neonatal (1 day old) mice which do not express p53 protein.

Human glioblastoma cell line U-251 MG is a widely used GBM model. This cell line, derived from a male patient with malignant astrocytoma, was established at the Wallenberg laboratory, Uppsala, Sweden (Pontén & Westermarck, 1978; Westermarck et al., 1973). We obtained it from Professor Nunzio Vicario (University of Catania, Italy) and maintained essentially in the same way as primary astrocytes, with the only modification in the concentration of antibiotics (100 U/ml penicillin, and 100 µg/ml streptomycin).

### 2.2 Astrocyte migration (wound healing) assay and confocal laser scanning microscopy

Cells were plated on 2 well inserts, which were kept in 35 mm dish (Ibidi GmbH, Germany) in an optimised concentration to reach confluence. 24 h later the insert was removed, and the feeding medium was replaced with the medium with reduced (2 %) fetal bovine serum to minimize the effect of cell proliferation in repopulation of insert free area (Kniss & Burry, 1988). Images of migrating cells were recorded in the heating chamber (37 °C), at 10 × air objective (Plan-Apochromat 10x/0.45 M27) with the confocal microscope LSM800 (Zeiss, Germany) at the time of insert removal (0 h) and at regular intervals of 4 h for the total period of 24 h. In between respective recordings cells were incubated at 37 °C, 5 % CO<sub>2</sub>/95 %. Migration assays were performed on primary mouse astrocytes (8 replicates isolated from 2 animals), on immortalized mouse astrocytes (11 replicates from 2 animals), and on human glioblastoma U-251 MG cells (8 replicates).

### 2.3 Data analysis

Image analysis was conducted in Fiji (Schindelin et al., 2012) with modifications of previously described procedure (Jonkman et al., 2014; Pijuan et al., 2019). Briefly, in DIC images edges of the cell free area were contrasted and delineated, to select all the areas devoid of cells. Then the area (in  $\mu\text{m}^2$ ) and the gap width (in  $\mu\text{m}$ ) were measured and used in MS Excel (Microsoft, USA) to calculate the cell migration rate ( $v_{migration}$ ) and the time of 50 % gap closure ( $t_{1/2}$ ), as described (Jonkman et al., 2014):

$$v_{migration} = \frac{|slope|}{2 \times l} \quad (1)$$

and  $t_{1/2}$  as:

$$t_{1/2} = \frac{Initial\ Gap\ Area}{2 \times |slope|} \quad (2).$$

Statistical analysis was performed in SigmaPlot (Systat Software Inc, USA). For the comparison of two groups t-test was used, and statistically significant differences were observed at value  $p < 0.05$ . Results are presented as mean  $\pm$  standard error.

## 3 RESULTS AND DISCUSSION

Cell migration is a process, important in the brain development (Cayre et al., 2009) and in various pathological conditions such as infections, trauma, ischemia, and neurodegenerative diseases and cancer (Rolls et al., 2009; Sun & Jakobs, 2012).

In this study we evaluated migration of different types of astrocytes in wound healing assay. First, we compared the migration rate of primary mouse astrocytes and immortalized mouse astrocytes. The latter are proposed to have a higher proliferative rate (Frisa & Jacobberger, 2002; Furihata et al., 2016; Morikawa et al., 2001). Time lapse recordings of confluent cells was performed at 0 h, 4 h, 8 h, 12 h, and 24 h after insert removal and the cell free area was used to calculate migratory properties of confluent cells (Figure 1A). The results show that the average speed of primary mouse astrocytes is almost  $12 \times$  slower than the speed of immortalized astrocytes (Figure 1B<sub>i</sub>). The time that is needed for cells to close half of the gap ( $t_{1/2}$  (h)) is almost  $9 \times$  longer in the case of primary astrocytes in comparison to immortalized astrocytes (Figure 1B<sub>ii</sub>).  $t_{1/2}$  is influenced by the wound area ( $500 \pm 100 \mu\text{m}$ ) at the start of the experiment ( $t = 0$  h), with larger or smaller wound areas taking longer or shorter periods to reach  $t_{1/2}$ , respectively (Jonkman et al., 2014).

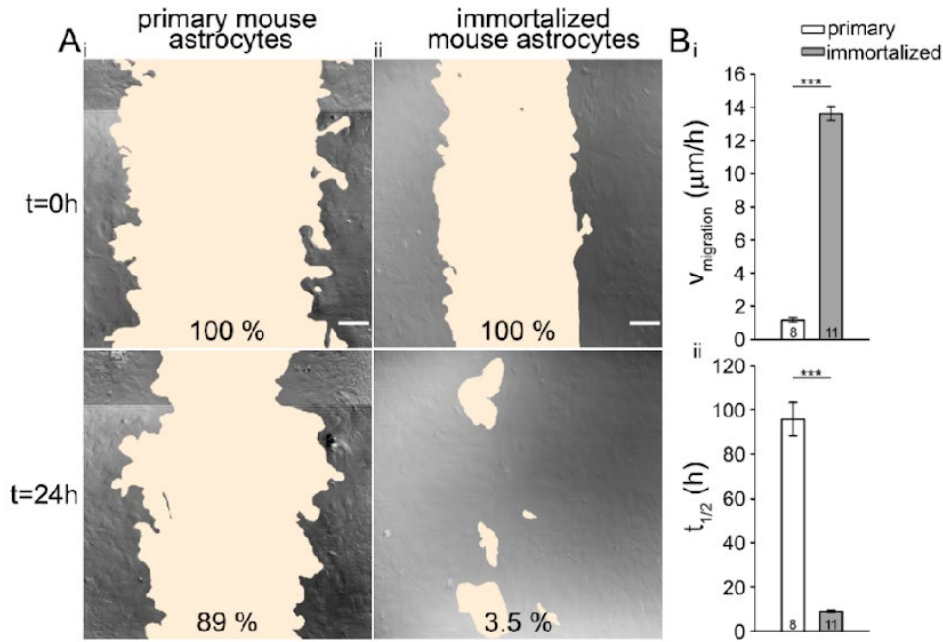


**Figure 1:** Migration of primary mouse astrocytes is slower than migration of immortalized mouse astrocytes. Time-lapse images of primary (A<sub>i</sub>) and immortalized (A<sub>ii</sub>) mouse astrocytes recorded in wound healing assay. Differences in gap closures are depicted in beige, while cell-covered area is grey; percentages denote cell free areas at 0 h and 24 h after insert removal. Scale bars: 100  $\mu\text{m}$ . The average speed of primary mouse astrocytes is slower than that of immortalized astrocytes (B<sub>i</sub>).  $t_{1/2}$  (h) is longer in primary astrocytes in comparison to immortalized astrocytes (B<sub>ii</sub>). Statistical analysis was performed by Student's t-test (\*\*\*)  $p < 0.001$ . Number of replicates is shown in the bars.

The results are in accordance with the proposition that migration of astrocytes is not yet complete during early postnatal development, when radial glia are in the process of losing their guiding processes before differentiation (Felix et al., 2021; Kriegstein & Alvarez-Buylla, 2009). Moreover, the results are also in line with the assumption that neonatal astrocytes travel shorter distances than embryonal astrocytes (Kriegstein & Alvarez-Buylla, 2009). For example, the migratory speed of neonatal astrocytes was roughly  $10 \times$  slower from embryonal astrocytes from E17 rat embryos (De Pascalis et al., 2018).

On the other hand, significantly faster migration was measured in immortalized astrocytes lacking the expression of p53, which plays a central role in maintaining cellular homeostasis and is frequently deregulated in cancer. These results are in line with the properties of GBM cells, which invade into the surrounding brain tissue (Cuddapah et al., 2014; Hwang et al., 2008), and their migratory ability has already been shown (Diao et al., 2019). Deregulated p53 pathway components have been implicated in GBM cell invasion, migration, proliferation, evasion of apoptosis, and cancer cell stemness (Zhang et al., 2018).

While U-251 MG cells migrate approximately two times faster than primary mouse astrocytes, the migratory speed of human glioblastoma U-251 MG cell line (Figure 2) is roughly one third of the speed of immortalized mouse astrocytes. While it is expected that glioblastoma cells migrate faster than primary astrocytes, they are unexpectedly slower from immortalized astrocytes. The differences in the speed might be attributed to the different species, different passage number (high passage number in the case of U-251 MG), and genotype modifications that affect several processes involved in migratory properties of cells. Namely, it is well known that *in vitro* subculturing conditions impose a selection pressure on cell lines, and over time

this may result in a genetic drift in the cancer cells U-251 MG. For example, only the original low-passaged U-251 cells, established in the 1960s, maintain a DNA copy number resembling a typical GBM profile, whereas all long-term subclones lost the typical GBM profile. During long-term subculture the cell lines seem to lose much of the typical GBM signature, and they gain a large number of local duplications and/or deletions that probably accumulates over time (Torsvik et al., 2014).

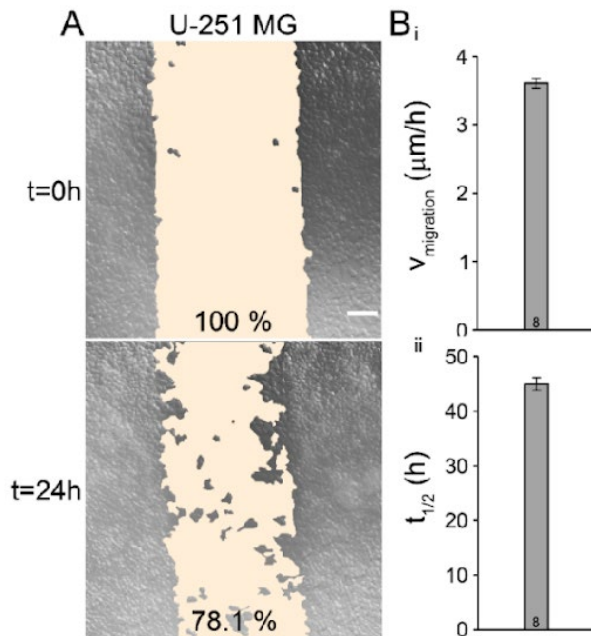


**Figure 2:** Migration of human glioblastoma U-251 MG cells. Time-lapse images of confluent U-251 MG cells recorded in wound healing assay at time 0 h and 24 h after insert removal (A). The migration rate ( $B_i$ ) and the time for the gap closure to 50 % ( $B_{ii}$ ).

#### 4 CONCLUSIONS

In the present research we measured collective migration properties of three different developmental and/or genetically diverse astrocytes; i.e., primary mouse astrocytes, immortalized mouse astrocytes lacking p53 protein, and human glioblastoma U-251 MG cell line, which derives from astrocytes. Cell migrations were monitored at 4 h intervals until the gap closure time in immortalized astrocytes. As expected, primary neonatal mouse astrocytes migrated significantly slower than immortalized mouse astrocytes. Moreover, human glioblastoma U-251 MG cell line shows an ability to migrate, as expected. The migration rate of U-251 MG was lower than the migration rate of immortalized mouse astrocytes, but higher than that of primary mouse astrocytes. The differences may be attributed to dissimilar developmental stages and subculturing conditions that induce genetic drift. These facts should be considered when interpreting the data on migratory properties of astrocytes in normal physiological and pathological conditions. Wound healing migration assay in combination with DIC imaging provides images with clearly discernible boundary between cells and cell free area, which is of crucial importance for the analysis of migratory properties of migrating cells.

## ACKNOWLEDGEMENT

The study was funded by the Slovenian Research Agency (ARRS) (source No.: P3-0310). We thank prof. Wiche from Department of Biochemistry and Cell biology, University of Vienna, Austria for providing immortalized mouse astrocytes, and to prof. Vicario, from Department of Biomedical and Biotechnological Sciences, University of Catania, Italy for providing human glioblastoma U-251 MG cell line.

## 5 REFERENCES

- Bass, N. H., Hess, H. H., Pope, A., & Thalheimer, C. (1971). Quantitative cytoarchitectonic distribution of neurons, glia, and DNA in rat cerebral cortex. *J Comp Neurol*, *143*(4), 481-490. doi:10.1002/cne.901430405
- Burda, J. E., & Sofroniew, M. V. (2014). Reactive gliosis and the multicellular response to CNS damage and disease. *Neuron*, *81*(2), 229-248. doi:10.1016/j.neuron.2013.12.034
- Cayre, M., Canoll, P., & Goldman, J. E. (2009). Cell migration in the normal and pathological postnatal mammalian brain. *Prog Neurobiol*, *88*(1), 41-63. doi:10.1016/j.pneurobio.2009.02.001
- Cuddapah, V. A., Robel, S., Watkins, S., & Sontheimer, H. (2014). A neurocentric perspective on glioma invasion. *Nat Rev Neurosci*, *15*(7), 455-465. doi:10.1038/nrn3765
- De Pascalis, C., Perez-Gonzalez, C., Seetharaman, S., Boeda, B., Vianay, B., Burute, M., et al. (2018). Intermediate filaments control collective migration by restricting traction forces and sustaining cell-cell contacts. *J Cell Biol*, *217*(9), 3031-3044. doi:10.1083/jcb.201801162
- Diao, W., Tong, X., Yang, C., Zhang, F., Bao, C., Chen, H., et al. (2019). Behaviors of Glioblastoma Cells in in Vitro Microenvironments. *Sci Rep*, *9*(1), 85. doi:10.1038/s41598-018-36347-7
- Felix, L., Stephan, J., & Rose, C. R. (2021). Astrocytes of the early postnatal brain. *Eur J Neurosci*, *54*(5), 5649-5672. doi:10.1111/ejn.14780
- Friedl, P., & Wolf, K. (2010). Plasticity of cell migration: a multiscale tuning model. *J Cell Biol*, *188*(1), 11-19. doi:10.1083/jcb.200909003
- Frisa, P. S., & Jacobberger, J. W. (2002). Cell density related gene expression: SV40 large T antigen levels in immortalized astrocyte lines. *BMC Cell Biol*, *3*, 10. doi:10.1186/1471-2121-3-10
- Furihata, T., Ito, R., Kamiichi, A., Saito, K., & Chiba, K. (2016). Establishment and characterization of a new conditionally immortalized human astrocyte cell line. *J Neurochem*, *136*(1), 92-105. doi:10.1111/jnc.13358
- Furnari, F. B., Fenton, T., Bachoo, R. M., Mukasa, A., Stommel, J. M., Stegh, A., et al. (2007). Malignant astrocytic glioma: genetics, biology, and paths to treatment. *Genes Dev*, *21*(21), 2683-2710. doi:10.1101/gad.1596707

- Ge, W. P., Miyawaki, A., Gage, F. H., Jan, Y. N., & Jan, L. Y. (2012). Local generation of glia is a major astrocyte source in postnatal cortex. *Nature*, *484*(7394), 376-380. doi:10.1038/nature10959
- Giering, A., Pszczolkowska, D., Walentynowicz, K. A., Rajan, W. D., & Kaminska, B. (2017). Immune microenvironment of gliomas. *Lab Invest*, *97*(5), 498-518. doi:10.1038/labinvest.2017.19
- Hamadi, A., Giannone, G., Takeda, K., & Ronde, P. (2014). Glutamate involvement in calcium-dependent migration of astrocytoma cells. *Cancer Cell Int*, *14*, 42. doi:10.1186/1475-2867-14-42
- Hwang, J. H., Smith, C. A., Salhia, B., & Rutka, J. T. (2008). The role of fascin in the migration and invasiveness of malignant glioma cells. *Neoplasia*, *10*(2), 149-159. doi:10.1593/neo.07909
- Jacobsen, C. T., & Miller, R. H. (2003). Control of astrocyte migration in the developing cerebral cortex. *Dev Neurosci*, *25*(2-4), 207-216. doi:10.1159/000072269
- Jonkman, J. E., Cathcart, J. A., Xu, F., Bartolini, M. E., Amon, J. E., Stevens, K. M., et al. (2014). An introduction to the wound healing assay using live-cell microscopy. *Cell Adh Migr*, *8*(5), 440-451. doi:10.4161/cam.36224
- Kniss, D. A., & Burry, R. W. (1988). Serum and fibroblast growth factor stimulate quiescent astrocytes to re-enter the cell cycle. *Brain Research*, *439*(1-2), 281-288. doi:10.1016/0006-8993(88)91485-0
- Kriegstein, A., & Alvarez-Buylla, A. (2009). The glial nature of embryonic and adult neural stem cells. *Annu Rev Neurosci*, *32*, 149-184. doi:10.1146/annurev.neuro.051508.135600
- Molofsky, A. V., Krencik, R., Ullian, E. M., Tsai, H. H., Deneen, B., Richardson, W. D., et al. (2012). Astrocytes and disease: a neurodevelopmental perspective. *Genes Dev*, *26*(9), 891-907. doi:10.1101/gad.188326.112
- Morikawa, M., Asai, K., Kokubo, M., Fujita, K., Yoneda, K., Yamamoto, N., et al. (2001). Isolation and characterization of a new immortal rat astrocyte with a high expression of NGF mRNA. *Neuroscience Research*, *39*(2), 205-212. doi:10.1016/s0168-0102(00)00217-0
- Ostrom, Q. T., Gittleman, H., Farah, P., Ondracek, A., Chen, Y., Wolinsky, Y., et al. (2013). CBTRUS statistical report: Primary brain and central nervous system tumors diagnosed in the United States in 2006-2010. *Neuro Oncol*, *15 Suppl 2*, ii1-56. doi:10.1093/neuonc/not151
- Pijuan, J., Barcelo, C., Moreno, D. F., Maiques, O., Siso, P., Marti, R. M., et al. (2019). In vitro Cell Migration, Invasion, and Adhesion Assays: From Cell Imaging to Data Analysis. *Front Cell Dev Biol*, *7*, 107. doi:10.3389/fcell.2019.00107
- Pontén, J., & Westermarck, B. (1978). Properties of human malignant glioma cells in vitro. *Med Biol*, *56*(4), 184-193.

- Ridley, A. J., Schwartz, M. A., Burridge, K., Firtel, R. A., Ginsberg, M. H., Borisy, G., et al. (2003). Cell migration: integrating signals from front to back. *Science*, *302*(5651), 1704-1709. doi:10.1126/science.1092053
- Rolls, A., Shechter, R., & Schwartz, M. (2009). The bright side of the glial scar in CNS repair. *Nat Rev Neurosci*, *10*(3), 235-241. doi:10.1038/nrn2591
- Schindelin, J., Arganda-Carreras, I., Frise, E., Kaynig, V., Longair, M., Pietzsch, T., et al. (2012). Fiji: an open-source platform for biological-image analysis. *Nat Methods*, *9*(7), 676-682. doi:10.1038/nmeth.2019
- Schwartz, J. P., & Wilson, D. J. (1992). Preparation and characterization of type 1 astrocytes cultured from adult rat cortex, cerebellum, and striatum. *Glia*, *5*(1), 75-80. doi:10.1002/glia.440050111
- Silver, J., Schwab, M. E., & Popovich, P. G. (2014). Central nervous system regenerative failure: role of oligodendrocytes, astrocytes, and microglia. *Cold Spring Harb Perspect Biol*, *7*(3), a020602. doi:10.1101/cshperspect.a020602
- Sloan, S. A., & Barres, B. A. (2014). Mechanisms of astrocyte development and their contributions to neurodevelopmental disorders. *Curr Opin Neurobiol*, *27*, 75-81. doi:10.1016/j.conb.2014.03.005
- Sun, D., & Jakobs, T. C. (2012). Structural remodeling of astrocytes in the injured CNS. *Neuroscientist*, *18*(6), 567-588. doi:10.1177/1073858411423441
- Torsvik, A., Stieber, D., Enger, P. O., Golebiewska, A., Molven, A., Svendsen, A., et al. (2014). U-251 revisited: genetic drift and phenotypic consequences of long-term cultures of glioblastoma cells. *Cancer Med*, *3*(4), 812-824. doi:10.1002/cam4.219
- Vicente-Manzanares, M., & Horwitz, A. R. (2011). Cell migration: an overview. *Methods Mol Biol*, *769*, 1-24. doi:10.1007/978-1-61779-207-6\_1
- Wang, Y. F., & Hamilton, K. (2009). Chronic vs. acute interactions between supraoptic oxytocin neurons and astrocytes during lactation: role of glial fibrillary acidic protein plasticity. *ScientificWorldJournal*, *9*, 1308-1320. doi:10.1100/tsw.2009.148
- Westermarck, B., Pontén, J., & Hugosson, R. (1973). Determinants for the establishment of permanent tissue culture lines from human gliomas. *Acta Pathol Microbiol Scand A*, *81*(6), 791-805. doi:10.1111/j.1699-0463.1973.tb03573.x
- Zhang, Y., Dube, C., Gibert, M., Jr., Cruickshanks, N., Wang, B., Coughlan, M., et al. (2018). The p53 Pathway in Glioblastoma. *Cancers (Basel)*, *10*(9). doi:10.3390/cancers10090297

## ZNANOST O ŽIVALIH/ANIMAL SCIENCE

### Effect of vitamins E, C and selenium supplementation on gut fermentative activity and gut histology of broiler chickens exposed to cyclic heat stress

Manca PEČJAK<sup>1\*</sup>, Vida REZAR<sup>1</sup>, Milka VRECL<sup>2</sup>, Alenka LEVART<sup>1</sup>, Jakob LESKOVEC<sup>1</sup>, Janez SALOBIR<sup>1</sup>, Tatjana PIRMAN<sup>1</sup>

<sup>1</sup> University of Ljubljana, Biotechnical Faculty, Department of Animal Science, Ljubljana, Slovenia

<sup>2</sup> University of Ljubljana, Veterinary Faculty, Institute of Preclinical Sciences, Ljubljana, Slovenia

\*corresponding author: [manca.pecjak@bf.uni-lj.si](mailto:manca.pecjak@bf.uni-lj.si)

#### **Effect of vitamins E, C and selenium supplementation on gut fermentative activity and gut histology of broiler chickens exposed to cyclic heat stress**

**Abstract:** Environmental changes associated with high ambient temperatures cause heat stress in poultry production, which affects animal health and performance. The aim of our study was to determine whether dietary supplementation with vitamins E, C, and selenium (Se) affects the histological structure of the gastrointestinal tract of broilers exposed to cyclic heat stress. In addition, we wanted to determine if the most commonly used nutritional specifications for vitamins and minerals from NRC and Aviagen for broilers were sufficient to cover the antioxidant needs under heat stress conditions, or if more vitamin E, C, and Se should be added under these conditions. In the study, a total of 60-day-old broilers were randomly divided into 3 experimental groups (NRC, Ross, and Ross+ECSe). Body weight, feed intake, and conversion ratio were monitored weekly. At the end of the experiment, 12 birds per group were slaughtered, the small intestine, caecum, colon and the contents of the small intestine were collected. The results showed that dietary supplementation with the combination of vitamins E, C, and Se had no effect on intestinal histology. In addition, the NRC and Aviagen nutritional recommendations appear to be sufficient to meet the antioxidant needs of broilers even under heat stress conditions.

**Key words:** antioxidants; broiler chicken; heat stress; intestine histology; short chain fatty acids

#### **Vpliv dodatka vitaminov E, C in selena na fermentativno aktivnost in histološko zgradbo prebavil pitovnih piščancev v pogojih cikličnega vročinskega stresa**

**Izveček:** Podnebne spremembe, ki povzročajo visoke okoljske temperature, izzovejo vročinski stres v reji perutnine, kar vpliva na zdravje in prirejo živali. Namen naše študije je bil preučiti, ali prehranski dodatek vitaminov E, C in selena (Se) vpliva na histološko zgradbo prebavil pitovnih piščancev, izpostavljenih cikličnemu vročinskemu stresu. Prav tako smo želeli preučiti, ali najpogosteje uporabljena prehranska priporočila za vitamine in rudninske snovi za pitovne piščance, NRC in Aviagen, zadoščajo za pokrivanje potreb po antioksidantih v pogojih

vročinskega stresa ali je treba v teh pogojih dodati še več vitamina E, C in Se. V poskus smo vključili 60-dni stare piščance, ki smo jih naključno razdelili v 3 poskusne skupine (NRC, Ross, Ross+ECSe). Tedensko smo spremljali telesno maso živali, zauživanje in izkoriščanje krme. Na koncu poskusa smo žrtvovali 12 živali na skupino in jim odvzeli tanko, debelo črevo ter slepo črevo in vsebino tankega črevesa. Glede na dobljene rezultate lahko sklepamo, da dodatek vitaminov E, C in Se ni vplival na histološko zgradbo prebavil. Prav tako lahko sklepamo, da NRC in Aviagen priporočila zadostujejo za pokrivanje potreb pitovnih piščancev po vitaminih in rudninskih snoveh tudi v pogojih vročinskega stresa.

**Ključne besede:** antioksidanti; histološka zgradba prebavil; hlapne maščobne kisline; pitovni piščanci; vročinski stres

## 1 INTRODUCTION

Heat stress is a major problem in poultry production worldwide, particularly in tropical and subtropical regions with hotter climates, as well as in other climate zones during the spring and summer months (Akbarian et al., 2016). Among all farm animals, poultry appears to be particularly susceptible to the negative effects of heat stress (Lara & Rostagno, 2013), as birds do not have sweat glands and their feather cover acts as an extremely good insulator, making heat exchange difficult (Ajakaiye et al., 2011). Heat stress is expressed when the amount of heat produced by the animal exceeds the body's ability to release it to the environment. This leads to various behavioural, immunological and physiological reactions such as endocrine disorders, respiratory alkalosis and electrolyte imbalance (Nawab et al., 2018). The intestinal tract has an important role in the absorption of nutrients and works as a physical barrier to prevent the invasion of various pathogens from external environment (Xiaofang et al., 2018). Heat stress (HS) affects morphological changes in the intestinal tract, resulting in smaller absorption surface, poorer nutrient absorption, reduced villus height and crypt depth, and lower villus height to crypt depth ratio in the small intestine (Deng et al., 2012; Mishra & Jha, 2019). This in turn is also reflected in reduced feed intake, increased feed conversion ratio (FCR), and lower body weight (BW) of birds reared under HS (Fouad et al., 2016; Habibian et al., 2016). Exposure of birds to high temperatures is also reflected in damage of intestinal epithelial cells, which causes the loss of integrity of tight junctions between enterocytes in the epithelium, allowing pathogens to damage the intestinal mucosa (Song et al., 2013) and impair digestion and absorption of nutrients, facilitating translocation of pathogenic bacteria and toxins from the intestinal tract into the bloodstream and triggering the inflammatory immune response (Slawinska et al., 2016).

To minimize the negative effects of heat stress in poultry, several nutritional strategies have been proposed, mainly related to supplementing the diet with different vitamins, minerals, and electrolytes. Vitamins E and C, as well as selenium (Se), are known to be among the most effective antioxidants in mitigating the negative effects of heat stress (Shakeri et al., 2020). Vitamin E is the major lipid-soluble antioxidant that protects cell membranes and tissues from oxidative damage, while vitamin C regenerates oxidized vitamin E (Traber & Stevens, 2011). Selenium is involved in antioxidant defence mechanisms as a cofactor for antioxidant enzymes involved in maintaining redox balance and is known to restore the antioxidant activity of vitamin C (Lykkesfeldt & Svendsen, 2007). The combination of these antioxidants may be

even more effective than supplementation alone in alleviating heat stress symptoms by acting synergistically against oxidative damage to lipids (Shakeri et al., 2020).

The aim of our study was to investigate the effects of dietary supplementation with vitamins E, C, and Se on growth performance, intestinal contents characteristics, and histological parameters in different parts of the intestine of broilers exposed to cyclic HS. In addition, we aim to determine whether the NRC (NRC, 1994) minimal nutrient requirements and Aviagen (Aviagen, 2019) commercial nutritional recommendations for vitamin E and Se are sufficient to mitigate the negative effects of HS on broiler intestinal histology.

## 2 MATERIALS AND METHODS

Sixty male Ross 308 broiler chickens were reared from day 1 to day 43 of age and randomly divided into 3 experimental groups corresponding to the dietary treatments. The experimental diets were formulated according to two different nutritional specifications, the first met the National Research Council (NRC) (NRC, 1994) minimal nutrient requirements for poultry and the second met the commercial nutritional recommendations for Ross 308 (Ross) (Aviagen, 2019). The third experimental diet was additionally supplemented with a combination of 200 IU vitamin E, 250 mg vitamin C, and 0.20 mg Se kg feed<sup>-1</sup> (Ross+ECSe) when Ross 308 specifications were met. Chickens were fed a starter diet for the first 10 days of housing, a grower diet from day 10 to day 24, and a finisher diet from day 25 to the end of the trial (day 43). The ingredients and calculated nutrient contents of the experimental starter, grower and finisher diets are shown in Table 1.

**Table 1:** Composition and calculated nutrient content of experimental diets for broiler chickens.

<b>Composition of diets (g kg<sup>-1</sup>)</b>			
<b>Ingredients<sup>1</sup></b>	<b>Starter (day 1-10)</b>	<b>Grower (day 11-24)</b>	<b>Finisher (day 25-43)</b>
Maize	314.0	360.0	515.0
Wheat	200.0	200.0	100.0
Wheat bran	30.0	15.0	0.00
Soya meal	274.0	234.0	193.0
Corn gluten meal	85.0	91.2	93.0
Plant oil	50.8	56.1	57.2
<b>Calculated energy (MJ kg<sup>-1</sup>) and calculated nutrient content (g kg<sup>-1</sup>)<sup>2</sup></b>			
Metabolizable energy	12.6	13.0	13.4
Crude protein	228.0	214.0	194.0
Crude fat	75.0	81.0	85.0
Crude fiber	24.0	23.0	21.0
Digestible lysine	12.9	11.5	10.3
Digestible methionine	5.12	5.61	5.19
Calcium	8.95	8.70	7.89
Phosphorus - available	5.45	4.36	4.38
Sodium	1.90	2.00	2.00

<sup>1</sup> Experimental diets also contain salt, monocalcium phosphate, limestone, L-lysine, DL-methionine, L-threonine, coccidiostat (Maxiban® G160, Elanco Products Co., UK), and mineral-vitamin mixture calculated to meet mineral and vitamin requirements for NRC or Ross 308 diets. <sup>2</sup> Energy and the content of individual nutrients were calculated according to nutrient content of the individual components of the diet.

Diet and fresh water were provided *ad libitum* and their growth performance was measured weekly. Chickens were reared under a standard lighting program. Until the 26<sup>th</sup> day of the housing, ambient temperature was regulated according to the recommendations for Ross 308 broiler chickens (Aviagen, 2018). On day 26, the ambient temperature was adjusted to daily fluctuations between 23.5 and 31 °C to trigger the daily temperature under heat stress conditions. Therefore, chickens were exposed to a temperature of 31 °C for 7 h per day and 23.5 °C for the remainder of the day.

On day 43, 12 birds per group were randomly selected, weighed, and sacrificed by stunning and bleeding. Small intestine, caecum and colon were weighed, and the small intestine was further divided into duodenum, jejunum, and ileum. Tissue samples for histological measurements were taken from different parts of the small intestine. All tissue samples were fixed in 5% buffered formalin solution before further analysis. The contents of the caecum were collected by finger squeezing, then collected in plastic Eppendorf tubes and stored at -20 °C for further analysis of short-chain fatty acids (SCFAs).

The viscosity of the small intestinal contents was determined on the same day using a separate aliquot of the small intestinal contents and performed according to the method described by Bedford & Classen (1992). In the contents of caecum, the concentrations of SCFAs were determined by gas chromatography according to the method described by Pirman et al. (2021) using an Agilent 6890A GC system with DB-FASTWAX UI capillary column (30 m x 0.25mm x 0.25 µm) and FID detector (Agilent, USA). Collected parts of small intestine tissue fixed in 5% buffered formalin solution were embedded in paraffin and evenly distributed histological sections with a size of 5 µm were cut and stained with a combination of hematoxylin and eosin (H&E). Histomorphometric analysis of the stained tissue sections was performed as described by Pirman et al. (2021). The crypt depth was measured from the crypt-villus junction to the base, and the villus height was measured from the tip to the crypt-villus junction, as shown in Figure 1.

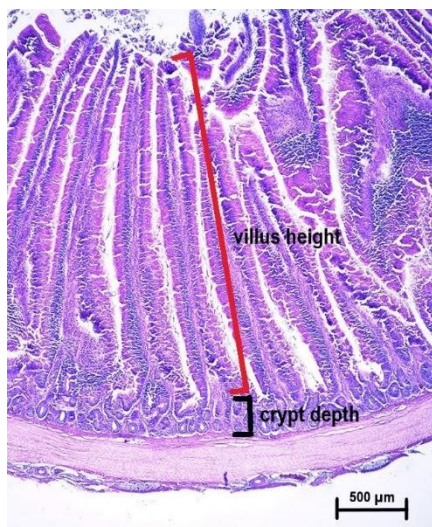


**Figure 1:** Histological cross-section of small intestine (10× magnification).

Data were statistically evaluated using the mixed procedure of the SAS/STAT module (SAS Institute Inc., Cary, NC, 2002-2010), with dietary treatment used as a fixed effect and pens as a random effect. Least square means (LSM) of the experimental diets for each variable were determined using the Tukey-Kramer multiple comparison test.

## 3 RESULTS AND DISCUSSION

Heat stress has negative effects on growth performance and welfare of broilers. It is also reported to alter gut morphology by inducing intestinal injury and consequently affect nutrient absorption. To minimize the negative effects of HS, several nutritional strategies have been suggested, with dietary supplementation of feed additives such as vitamins E, C, and Se being one of the most effective. In the present study no differences in BW of broilers and feed conversion were observed between the experimental groups (Table 2), although throughout the trial, higher BW tended to be observed in the Ross+ECSe group compared to the other experimental groups. This is consistent with other studies in which no differences in growth performance were observed in broilers under heat stress receiving a combination of vitamins E and C or vitamin E and Se (Ghazi Harsini et al., 2012; Zeferino et al., 2016). On the other hand, Calik et al. (2022) reported that dietary supplementation with vitamin E (250 mg kg<sup>-1</sup>) and Se (1 mg kg<sup>-1</sup>) improved body weight gain and feed intake of broilers exposed to cyclic HS.

**Table 2:** Body weight (BW) of broilers from day 21 to 42 and feed conversion through the trial.

	NRC	Ross	Ross+ECSe	SEM	p -Value
BW 21 <sup>st</sup> day (g)	814.9	906.2	915.0	23.65	0.1005
BW 28 <sup>th</sup> day (g)	1257.3	1396.6	1452.3	43.08	0.1005
BW 35 <sup>th</sup> day (g)	1735.6	1975.1	1983.0	55.48	0.0824
BW 42 <sup>th</sup> day (g)	2174.6	2504.9	2582.8	97.85	0.1096
Feed conversion*(g g <sup>-1</sup> )	2.30	2.06	1.90		

NRC – minimal nutrient requirement of NRC, no supplementation, Ross - recommended levels of Aviagen for Ross 308 broilers, no supplementation, Ross+ECSe - Ross+vitE+vitC+Se. \*Expressed as an average value in group, since the birds were housed in a group and individual consumption could not be determined.

There were no differences in the relative weights of different parts of the intestine (Table 3) among groups. On the other hand, Jahejo et al. (2016) reported that dietary supplementation with vitamin C (150 mg kg<sup>-1</sup>) improved the weight and length of duodenum, jejunum, ileum, and colon in broilers under HS. The viscosity of the intestinal contents depends largely on the type of dietary fiber and its content in the feed, which consequently affect the digestion and absorption of nutrients (Ndelekwute et al., 2018). High viscosity in the small intestine results in slower movement of digesta, providing more substrate for the microbiota and accelerating fermentation (Pirman et al., 2021). In our study, the viscosity of the small intestine contents was not affected by dietary supplements (Table 3). The latter indicates that fermentation in the small intestine was similar in all groups, where mainly the degradation of carbohydrates with endogenous enzymes occur. SCFAs have important role in modulating intestinal microflora, promoting epithelial cell proliferation, inhibit proliferation of pathogens in the intestine, and serve as an important source of energy (Yadav & Jha, 2019). The supplements increased the levels of SCFAs in the caecum, especially ethanoic and butanoic acids, and also the total levels of SCFAs, but no significant differences were found between the groups (Table 3). Similarly, Gružauskas et al. (2014) reported that dietary supplementation with vitamin E and Se had no significant effect on acetic, propionic, and butyric acid levels.

**Table 3:** Effect of different dietary treatments on relative weight (%) of different parts of intestine, viscosity of small intestine contents and short chain fatty acids (SCFAs) concentration in caecum contents.

	NRC	Ross	Ross+ECSe	SEM	p -value
<b>Relative weight (%)</b>					
Small intestine	1.82	1.69	1.67	0.06	0.2580
Caecum	0.16	0.13	0.12	0.02	0.2622

Colon	0.28	0.27	0.25	0.02	0.4728
<b>Viscosity (cP)</b>					
Small intestine contents	2.28	1.86	2.15	0.08	0.0717
<b>SCFAs in caecum (<math>\mu\text{mol g}^{-1}</math>)</b>					
Ethanoic acid	64.48	62.63	69.64	4.59	0.6035
Propanoic acid	6.65	5.29	5.41	0.47	0.2168
2-methylpropanoic acid	0.85	0.77	0.76	0.05	0.5984
Butanoic acid	14.49	17.32	18.01	1.72	0.4099
3-methylbutanoic acid	1.10	0.90	0.80	0.08	0.1541
Pentanoic acid	1.49	1.29	1.40	0.11	0.5298
Sum of SCFAs	89.13	86.76	97.15	5.09	0.4417

Nomenclature of experimental groups as in Table 2. SCFAs – short chain fatty acids.

Heat stress has been reported to cause histological damage in the intestinal tract of poultry, mainly related to decreased villus height and increased crypt depth, resulting in a lower villus height:crypt depth (VH:CD) ratio, with the small intestine being more sensitive compared to caecum (Rostagno, 2020). In addition, villus height, crypt depth, and VH:CD ratio are important parameters to determine intestinal mucosal injury. In the present study, no differences were observed between the experimental groups in villus height, crypt depth, and VH:CD ratio in the small intestine (Table 4). In contrast, Yoo et al. (2016) reported that broilers supplemented with combination of vitamins E, C, and alpha-lipoic acid had higher villus height and improved VH:CD ratio. In addition, Amer et al. (2021) observed an increase in villus height and width, crypt depth, and improved VH:CD ratio in the small intestine of broilers when they received a combination of vitamin C and safflower oil.

**Table 4:** Effect of different dietary treatments on villus height ( $\mu\text{m}$ ), crypt depth ( $\mu\text{m}$ ) and VH:CD ratio in the small intestine

	<b>NRC</b>	<b>Ross</b>	<b>Ross+ECSe</b>	<b>SEM</b>	<b>p -value</b>
Villus height ( $\mu\text{m}$ )	1617	1660	1668	55.59	0.7857
Crypt depth ( $\mu\text{m}$ )	183	180	173	4.34	0.3461
VH:CD ratio	8.86	9.47	9.49	9.49	0.3684

Nomenclature of experimental groups as in Table 2. VH – villus height, CD – crypt depth.

#### 4 CONCLUSIONS

The results of our study indicate that dietary supplementation with the combination of vitamins E, C, and Se had no effect on growth performance, gut fermentative activity, and gut histology of broilers under HS. Furthermore, the widely used NRC and Aviagen nutritional recommendations for antioxidants appear to be sufficient to mitigate the negative effects of HS on the intestinal health. Although the addition of higher levels of vitamin E, vitamin C, and Se to broiler diets did not show synergistic effects, neither was a negative effect observed on the intestinal histology of broilers under HS. Nevertheless, further studies under different environmental conditions and considering different types of stressors would be of great importance to better highlight the mechanisms of potential synergistic effects of dietary antioxidants on intestinal histology.

## 5 REFERENCES

- Ajakaiye, J. J., Perez-Bello, A. & Mollineda-Trujillo A. (2011). Impact of heat stress on egg quality in layer hens supplemented with l-ascorbic acid and dl-tocopherol acetate. *Veterinarski arhiv*, 81(1), 119-132.
- Akbarian, A., Michiels, J., Degroote, J., Majdeddin, M., Golian, A. & De Smet, S. (2016). Association between heat stress and oxidative stress in poultry; mitochondrial dysfunction and dietary interventions with phytochemicals. *Journal of Animal Science and Biotechnology*, 7, 37.
- Amer, S. A., Mohamed, W. A. M., Gharib, H. S. A., Al-Gabri, N. A., Gouda, A., Elabbasy, M. T., ... Omar, A. E. (2021). Changes in the growth, ileal digestibility, intestinal histology, behavior, fatty acid composition of the breast muscles, and blood biochemical parameters of broiler chickens by dietary inclusion of safflower oil and vitamin C. *BMC Veterinary Research*, 17(68), 1-18.
- Aviagen. (2018). *Ross Broiler Management Handbook*. Retrieved from: [https://en.aviagen.com/assets/Tech\\_Center/Ross\\_Broiler/Ross-BroilerHandbook2018-EN.pdf](https://en.aviagen.com/assets/Tech_Center/Ross_Broiler/Ross-BroilerHandbook2018-EN.pdf).
- Aviagen. (2019). *Ross 308 Broiler: Nutrition Specifications*. Retrieved from: [https://en.aviagen.com/assets/Tech\\_Center/Ross\\_Broiler/RossBroilerNutritionSpecs2019-EN.pdf](https://en.aviagen.com/assets/Tech_Center/Ross_Broiler/RossBroilerNutritionSpecs2019-EN.pdf).
- Bedford, M. R. & Classen, H. L. (1992). Reduction in intestinal viscosity through manipulation of dietary rye and pentosanase concentration is effected through changes in the carbohydrate: composition in the intestinal aqueous phase and results in improved growth rate and food conversion efficiency of broiler chicks. *Journal of Nutrition*, 122(3), 560-569.
- Calik, A., Emami N. K., White, M. B., Walsh, M. C., Romero, L. F. & Dalloul, R. A. (2022). Influence of dietary vitamin E and selenium supplementation on broilers subjected to heat stress, Part I: Growth performance, body composition and intestinal nutrient transporters. *Poultry Science*, doi: <https://doi.org/10.1016/j.psj.2022.101857>
- Deng, W., Dong, X. F., Tong, J. M. & Zhang, Q. (2012). The probiotic *Bacillus licheniformis* ameliorates heat stress-induced impairment of egg production, gut morphology, and intestinal mucosal immunity in laying hens. *Poultry Science*, 91(3), 575-582.
- Fouad, A. M., Chen, W., Ruan, D., Wang, S., Xia, W. G. & Zheng, C. T. (2016). Impact of heat stress on meat, egg quality, immunity and fertility in poultry and nutritional factors that overcome these effects: A review. *International Journal of Poultry Science*, 15(3), 81-95.
- Ghazi Harsini, S., Habibiyan, M., Moeini, M. M. & Abdolmohammadi, A. R. (2012). Effects of dietary selenium, vitamin E, and their combination on growth, serum metabolites, and antioxidant defense system in skeletal muscle of broilers under heat stress. *Biological Trace Element Research*, 148, 322-330.

- Gružauskas, R., Barštys, T., Racevičiūtė-Stupelienė, A., Kliševičiūtė, V., Buckiūnienė, V. & Bliznikas, S. (2014). The effect of sodium selenite, selenium methionine and vitamin E on productivity, digestive processes and physiologic condition of broiler chickens. *Veterinarija Ir Zootechnika*, 65(87), 22-29.
- Habibian, M., Ghazi, S. & Moeini, M. M. (2016). Effects of dietary selenium and vitamin E on growth performance, meat yield, and selenium content and lipid oxidation of breast meat of broilers reared under heat stress. *Biological Trace Element Research*, 169(1), 142-152.
- Jahejo, A. R., Leghari, I. H., Sethar, A., Rao, M. N., Nisa M. & Sethar G. H. (2016). Effect of heat stress and ascorbic acid on gut morphology of broiler chicken. *Sindh University Research Journal (Science Series)*, 48(4), 829-832.
- Lara, L. J. & Rostagno, M. H. (2013). Impact of heat stress on poultry production. *Animals*, 3(2), 356-369.
- Lykkesfeldt, J. & Svendsen, O. (2007). Oxidants and antioxidants in disease: Oxidative stress in farm animals. *The Veterinary Journal*, 173(3), 502-511.
- Mishra, B. & Jha, R. (2019). Oxidative stress in the poultry gut: potential challenges and interventions. *Frontiers in Veterinary Science*, 6, 60.
- Nawab, A., Ibtisham, F., Li, G., Kieser, B., Wu, J., Liu, W., ... An, L. (2018). Heat stress in poultry production: Mitigation strategies to overcome the future challenges facing the global poultry industry. *Journal of Thermal Biology*, 78: 131-139.
- Ndelekwute, E. K., Assam, E. D., Assam, E. M. (2018). Apparent nutrient digestibility, gut pH, and digesta viscosity of broiler chickens fed acidified water. *MOJ Anatomy & Physiology*. 5(4), 250-253.
- NRC. (1994). *Nutrient Requirements of Poultry*. National Academic Press, Washington, DC.
- Pirman, T., Rezar, V., Vrecl, M., Salobir, J. & Levart, A. (2021). Effect of olive leaves or marigold petal extract on oxidative stress, gut fermentative activity, and mucosa morphology in broiler chickens fed a diet rich in n-3 polyunsaturated fats. *Japan Poultry Science Association*, 58(2), 119-130.
- Rostagno, M. H. (2020). Effects of heat stress on the gut health of poultry. *Journal of Animal Science*, 98(4), skaa090.
- Shakeri, M., Oskoueian, E., Le, H. H. & Shakeri, M. (2020). Strategies to combat heat stress in broiler chickens: Unveiling the roles of selenium, vitamin E and vitamin C. *Veterinary Sciences*, 7(2), 71.
- Slawinska, A., Hsieh, J. C., Schmidt, C. J., Lamont, S. J. (2016). Heat stress and lipopolysaccharide stimulation of chicken macrophage-like cell line activates expression of distinct sets of genes. *PLOS one*, 11(10): e0164575.
- Song, J., Jiao, L. F., Xiao, K., Luan, Z. S., Hu, C. H., Shi, B. & Zhan, X. A. (2013). Cello-oligosaccharide ameliorates heat stress-induced impairment of intestinal microflora, morphology and barrier integrity in broilers. *Animal Feed Science and Technology*, 184(3-4), 175-181.

- Traber, M. G. & Stevens, J. F. (2011). Vitamins C and E: Beneficial effects from a mechanistic perspective. *Free Radical Biology & Medicine*, 51(5), 1000-1013.
- Xiaofang, H., Lu, Z., Ma, B., Zhang, L., Li, J., Jiang, Y., ... Gao F. (2018). Chronic heat stress damages small intestinal epithelium associated with AMPK pathway in broilers. *Journal of Agricultural and Food Chemistry*, 66, 7301-7309.
- Yadav, S. & Jha, R. (2019). Strategies to modulate the intestinal microbiota and their effects on nutrient utilization, performance, and health of poultry. *Journal of Animal Science and Biotechnology*, 10, 2.
- Yoo, J., Young J. Y., Koo, B., Jung, S. Yoon, U. Y., Kang, H. B., ... Heo, J. M. (2016). Growth performance, intestinal morphology, and meat quality in relation to alpha-lipoic acid associated with vitamin C and E in broiler chickens under tropical conditions. *Revista Brasileira de Zootecnia*, 45(3), 113-120.
- Zeferino, C. P., Komiyama, C. M., Pelícia, V. C., Fascina, V. B., Aoyagi, M. M., Coutinho, L.L., ... Moura, A. S. A. M. T. (2016). Carcass and meat quality traits of chickens fed diets concurrently supplemented with vitamins C and E under constant heat stress. *Animal*, 10(1), 163-171.

## ŽIVILSTVO/FOOD SCIENCE

### Effect of enzymatic treatment on phenolics content and antioxidant activity from spelt (*Triticum spelta* L.) seeds

Marjeta MENCIN<sup>1</sup>, Petra TERPINC<sup>1\*</sup>

<sup>1</sup> University of Ljubljana, Biotechnical Faculty, Department of Food Science and Technology, Ljubljana, Slovenia

\*corresponding author: [petra.terpinc@bf.uni-lj.si](mailto:petra.terpinc@bf.uni-lj.si)

#### **Effect of enzymatic treatment on phenolics content and antioxidant activity from spelt (*Triticum spelta* L.) seeds**

**Abstract:** The aim of this study was to explore the impact of treatment with different enzymes and their combination on the accessibility of spelt phenolics. Enzymatic treatment had a significant effect on extractable phenolics and their reactivity towards FC reagent, DPPH<sup>•</sup> and ABTS<sup>•+</sup> radicals. Samples treated with all five enzymes together had the highest extractable phenolic content and antioxidant activity. At the same time, treatment with feruloyl esterase and combination of cellulase, xylanase and feruloyl esterase had negative effect on the bound phenolics content. Our *in vitro* study suggests that enzymatic treatment significantly improves the ratio between extractable and bound phenolics and is also a good way to improve the accessibility and subsequent activity of bound antioxidants in spelt seeds. Principal component analysis (PCA) revealed similarities and differences between groups of samples in our study.

**Key words:** antioxidant activity; cellulase; extractable and bound phenolics; feruloyl esterase; PCA; xylanase

#### **Vpliv encimskega tretiranja na vsebnost fenolov in antioksidativno aktivnost iz semen pire (*Triticum spelta* L.)**

**Izvelek:** Namen te študije je bil raziskati vpliv tretiranja z različnimi encimi in njihovimi kombinacijami na dostopnost pirinih fenolov. Encimsko tretiranje je imelo pomemben učinek na ekstraktibilne fenole in njihovo reaktivnost v reakciji s FC reagentom ter DPPH<sup>•</sup> in ABTS<sup>•+</sup> radikali. Vzorci, obdelani z vsemi petimi encimi, so pokazali največjo vsebnost ekstraktibilnih fenolov in antioksidativno aktivnost. Hkrati je tretiranje s feruloil esterazo in s kombinacijo celulaze, ksilanaze in feruloil esteraze negativno vplivalo na vsebnost vezanih fenolov. Naša *in vitro* študija kaže, da encimsko tretiranje bistveno izboljša razmerje med ekstraktibilnimi in vezanimi fenoli in nudi dobro priložnost za izboljšanje dostopnosti in kasnejše aktivnosti vezanih antioksidantov v semenih pire. Metoda glavnih komponent (PCA) je pokazala podobnosti in razlike med skupinami vzorcev v naši raziskavi.

**Ključne besede:** antioksidativna aktivnost; celulaza; ekstraktibilni in vezani fenoli; feruloil esteraza; PCA; ksilanaza

## 1 INTRODUCTION

Spelt (*Triticum spelta* L.) is an ancient subspecies of common wheat. *Triticum* bran is a good source of dietary fiber, consisting mainly of arabinoxylans, cellulose, and  $\beta$ -glucan (Bautista-Expósito et al., 2020). The most abundant phenolics generally occur in spelt in insoluble bound form. *p*-Coumaric and ferulic acids, which are predominant structural components in spelt seeds and are found both ester-bound to polysaccharides (especially to arabinoxylans) and ether-bound to lignin in plant cell walls (Bei et al., 2018; Mencin et al., 2021). Kern et al. (2003) reported that only extractable phenolic acids are available for absorption in the human small or large intestine, meanwhile human absorption of the predominantly bound phenolic acids in wheat bran has been shown to be minimal. With this in mind, releasing the bound phenolic acids in spelt seeds prior to consumption by bioprocessing techniques such as enzymatic treatment could be a strategy to improve their bioaccessibility in humans. Enzymatic treatment is a specific and effective method for releasing bound phenolic acids from cell wall materials (Chen et al., 2015). Cell wall hydrolyzing enzymes (cellulases, xylanases, etc.) have been effectively used to release bound phenolics by breaking up cell wall materials from wheat bran (Acosta-Estrada et al., 2014; Bei et al., 2018). Feruloyl esterases are a subclass of carboxylesterases that hydrolyze the ester bond between hydroxycinnamic acids (e.g. ferulic acid) and hemicellulose present in plant cell wall. Moreover, feruloyl esterase should also act in synergy with xylanases by cleaving diferulic bridges between xylan chains, opening the structures and releasing lignin. Proteins constitute up to 17% of the bran layer; therefore, protease has been explored for bran degradation (Singh et al., 2016). Phenolic acids, with their carboxyl and hydroxyl groups, are able to bond with starch and other polysaccharides via hydrogen bonds, chelation, or covalent bonds (Yu et al., 2001). Therefore, hydrolysis of starch by  $\alpha$ -amylase can release phenolic acids. The aim of this study was to investigate the effect of different enzymes (alone or in combination), on the enhanced release of phenolics from spelt seeds, as well as to demonstrate the effect of enzymes on the distribution of phenolics between extractable and bound forms in the spelt seed.

## 2 MATERIALS AND METHODS

### 2.1 Enzymatic treatments of seeds

Milled and freeze-dried raw spelt seeds were treated with different enzymes (cellulase (EC 3.2.1.4); xylanase (EC 3.2.1.8); feruloyl esterase (EC 3.1.1.73); protease (EC 232-752-2) and  $\alpha$ -amylase (EC 232-560-9)). The enzymatic treatment was performed at 40 °C for 4 h in 50 mL centrifuge tubes with continuous stirring. The most suitable conditions for each enzyme were taken from the manufacturers' recommendations, namely, 100 mM sodium acetate buffer (pH 4.5) for cellulase and xylanase; in 100 mM sodium phosphate buffer (pH 6) for feruloyl esterase,  $\alpha$ -amylase and protease. The optimised conditions for enzymatic treatment were the sample-to-buffer ratio 1:4 (w/v), the optimal enzyme concentrations were for cellulase 25 U/g DW, xylanase 5 U/g DW, feruloyl esterase 10 U/g DW,  $\alpha$ -amylase 50 U/g DW and protease 50 U/g DW. The optimal concentrations of enzymes, time of enzymatic treatments and sample-to-buffer ratio for each enzyme, were selected based on preliminary experiments (data not shown). After this treatment, the sample was collected and freeze-dried.

### 2.2 Preparation of extractable and bound phenolics

Aliquots of the homogenised and freeze-dried treated seeds were mixed with 99.9% methanol at a ratio of 1:9 (w/v). After shaking for 2 h at room temperature, the samples were centrifuged ( $9793.9\times g$ , 10 min) and filtered (pore size,  $0.45\ \mu\text{m}$ ). These filtered supernatants from the extractions contained the extractable phenolics. The solid residues after methanol extraction were treated by adding 2 M sodium hydroxide (20 mL) and shaking for 4 h at room temperature. After hydrolysis, the samples containing the released phenolics were acidified to pH 3 with concentrated formic acid. These filtered hydrolysates represented solution of bound phenolics.

### 2.3 Determination of total phenolics content (TPC) and antioxidant activities

The TPCs were determined using the Folin–Ciocalteu (FC) method and antioxidant activities were determined using DPPH $\cdot$  and ABTS $^{+\cdot}$  scavenging activities, according to the method described in our previous publication (Mencin et al., 2021). A standard curve was prepared with Trolox, and the data were expressed as mg Trolox equivalents per g dry weight (mg TE/g DW).

### 2.4 Statistical analysis

The difference among various enzymatic treatments of spelt seeds was analysed with One-way analysis of variance (ANOVA) and Duncan's post-hoc test. The level of statistical significance was set as  $p < 0.05$ . The statistical analysis was performed using SPSS programme, as version 22 for Windows. Principal component analysis [PCA] was performed to interpret the differences in all of the analysed samples by OriginPro 2015.

## 3 RESULTS AND DISCUSSION

### 3.1 Effect of enzymatic treatment on total phenolic content

The non-treated spelt seeds were used as a control sample. Following the preparation of the extracts, the TPC of the extractable fraction was 2.95 mg TE/g DW and of the bound fraction was 6.00 mg TE/g DW. All samples treated with different enzymes improved the extractable and bound TPCs of spelt seeds compared to the control sample. Here, the treatment with feruloyl esterase (F) showed the lowest increase in extractable and bound TPCs by 159% and 62%, respectively, while the highest increase in extractable and bound TPCs showed simultaneous treatment with all five enzymes (C+X+F+A+P) (642%) and treatment with amylase (225%), respectively (Table 1). All three experiments that included combination of cellulase, xylanase and feruloyl esterase showed a greater ability to release bound TPCs into extractable TPCs compared to treatment with these enzymes alone (Table 1). This result suggests that feruloyl esterase in synergism can hydrolyze the ester- or ether- bond between phenolics and the cell wall structure of spelt seeds and transform bound phenolics into extractable form, which is consistent with Acosta-Estrada et al. (2014).

Regardless of the enzymatic treatment, bound phenolics represented a prevalent proportion of total phenolics, the only exception are treatments with protease and C+X+F+A+P. Treatment with C+X+F+A+P resulted in the highest increase in the proportion of extractable TPCs over the total phenolics (extractable + bound) from 33% (non-treated seeds) to 60%, while treatment

with amylase resulted in the lowest increase in the proportion of extractable TPCs over the total phenolics, which amounted to 37%.

Interestingly, protease was able to significantly increase the release of extractable TPCs from seeds, suggesting that this enzyme preparation may be included in hydrolysis of ester and/or glycosidic bonds. Our TPC values may be overestimated since Everette et al. (2010) showed that many non-phenolic compounds exhibit considerable reactivity toward the FC reagent, including proteins. Contrary to our expectations, we found that treatments with xylanase, feruloyl esterase and cellulase, alone or in combination with each other, were less efficient than protease or amylase. Similar data were reported by Sungsopha (2009), implying that after treatment of rice bran with  $\alpha$ -amylase and protease, the extractable TPCs was increased by 476% compared to non-treated samples. The increase in extractable TPCs is likely due to the increased release of bound phenolics (Bei et al., 2018). However, enzymatic treatment could not completely convert bound phenolics to the extractable form because cell wall matrix of spelt seeds might contain arabinoxylans, which cannot be hydrolysed by enzymes (Moore et al., 2006).

### 3.2 Antioxidant activities of spelt seeds treated with different enzymes

The antioxidant activities of extractable and bound fractions from the different treated spelt seeds were determined using two assays, referred to as DPPH<sup>•</sup> and ABTS<sup>•+</sup> scavenging activities. The DPPH<sup>•</sup> and ABTS<sup>•+</sup> assays are based on electron or hydrogen radical transfer mechanisms, and involve reduction of a coloured oxidant; as such, they are similar to the FC assay (Dawidowicz & Olszowy, 2013).

In general, in comparison to control, these free radical scavenging activities of the extractable phenolics were significantly higher for the samples treated with enzymes (Table 1). Simultaneous treatment with all five enzymes (C+X+F+A+P) showed the greatest increase in DPPH<sup>•</sup> (1182%) and ABTS<sup>•+</sup> (914%) scavenging activities of extractable fractions compared to control sample. The lowest increase in DPPH<sup>•</sup> and ABTS<sup>•+</sup> scavenging activities was showed by treatment with cellulase (32%) and feruloyl esterase (217%), respectively.

Here, amylase treatment showed the greatest increases in DPPH<sup>•</sup> scavenging activity (45%) while protease treatment showed the greatest increase in ABTS<sup>•+</sup> scavenging activity (132%) of the bound fraction, compared to control sample. Interestingly, treatment with feruloyl esterase (F) or treatment with combination of cellulase, xylanase and feruloyl esterase (C+X+F) showed decrease in bound DPPH<sup>•</sup> (25%) and ABTS<sup>•+</sup> (8% and 13%, respectively) scavenging activities.

The enzymatic treatment increased the antioxidant activity of the seeds probably by releasing polar antioxidants bounded to the cell wall and/or by hydrolyzing biopolymers, such as polypeptides and polysaccharides (Azmir et al., 2013). There are two possible explanation for improving the antioxidant activity: one was to increase the solubility of the TPCs from spelt seeds and the other was to obtain more phenolics with higher bioactivities using the biotransformation method (Wang et al., 2018).

Meanwhile, the antioxidant activity determined by an ABTS<sup>•+</sup> scavenging activity was significantly higher than the antioxidant activity determined by a DPPH<sup>•</sup> scavenging activity. Floegel et al. (2011) showed that the ABTS<sup>•+</sup> assay is based on the generation of a blue-green ABTS<sup>•+</sup>, which is applicable to both hydrophilic and lipophilic antioxidant systems, whereas the DPPH<sup>•</sup> assay uses a radical dissolved in organic media and is applicable to hydrophobic systems. Due to the high content of *p*-coumaric and ferulic acids in spelt seeds (Mencin et al.,

2021), a higher ABTS<sup>+</sup> than DPPH<sup>•</sup> scavenging activity was expected. It appears that enzymatic treatments had a significantly positive impact on the antioxidant activities of the extractable and bound TPCs.

**Table 1.** Total phenolic content (TPC) and antioxidant activities (DPPH and ABTS assays) for the extractable and bound phenolics from the spelt seeds treated with different enzymes. Data are means  $\pm$  standard deviation and are expressed as mg Trolox equivalents per g dry weight (mg TE/g DW). Different letters within the same fraction (extractable or bound) indicate significant differences ( $P < 0.05$ ; Duncan's Multiple Range Test).

Enzymatic treatment	TPC		DPPH		ABTS	
	mg TE / g DW		mg TE / g DW		mg TE / g DW	
	Extractable	Bound	Extractable	Bound	Extractable	Bound
Non-treated	2.95 $\pm$ 0.09 <sup>a</sup>	6.00 $\pm$ 0.10 <sup>A</sup>	0.22 $\pm$ 0.02 <sup>a</sup>	1.55 $\pm$ 0.07 <sup>B</sup>	1.67 $\pm$ 0.07 <sup>a</sup>	3.20 $\pm$ 0.09 <sup>B</sup>
C	9.50 $\pm$ 0.27 <sup>d</sup>	13.45 $\pm$ 0.23 <sup>EF</sup>	0.29 $\pm$ 0.02 <sup>b</sup>	1.75 $\pm$ 0.05 <sup>C</sup>	8.48 $\pm$ 0.11 <sup>g</sup>	3.81 $\pm$ 0.11 <sup>C</sup>
X	8.60 $\pm$ 0.20 <sup>c</sup>	12.78 $\pm$ 0.07 <sup>D</sup>	0.68 $\pm$ 0.01 <sup>e</sup>	1.51 $\pm$ 0.06 <sup>B</sup>	7.20 $\pm$ 0.18 <sup>e</sup>	4.46 $\pm$ 0.24 <sup>E</sup>
F	7.65 $\pm$ 0.15 <sup>b</sup>	9.73 $\pm$ 0.45 <sup>B</sup>	0.89 $\pm$ 0.02 <sup>f</sup>	1.16 $\pm$ 0.06 <sup>A</sup>	5.30 $\pm$ 0.32 <sup>b</sup>	2.93 $\pm$ 0.13 <sup>A</sup>
C + X	10.21 $\pm$ 0.16 <sup>ef</sup>	13.49 $\pm$ 0.26 <sup>F</sup>	0.37 $\pm$ 0.01 <sup>c</sup>	1.75 $\pm$ 0.02 <sup>C</sup>	8.95 $\pm$ 0.08 <sup>h</sup>	4.22 $\pm$ 0.15 <sup>D</sup>
X + F	10.48 $\pm$ 0.20 <sup>f</sup>	12.94 $\pm$ 0.21 <sup>DE</sup>	0.51 $\pm$ 0.01 <sup>d</sup>	1.73 $\pm$ 0.06 <sup>C</sup>	6.60 $\pm$ 0.09 <sup>c</sup>	3.74 $\pm$ 0.13 <sup>C</sup>
C+X+F	9.63 $\pm$ 0.15 <sup>de</sup>	11.80 $\pm$ 0.15 <sup>C</sup>	0.54 $\pm$ 0.01 <sup>d</sup>	1.16 $\pm$ 0.05 <sup>A</sup>	6.95 $\pm$ 0.17 <sup>d</sup>	2.78 $\pm$ 0.11 <sup>A</sup>
P	19.67 $\pm$ 0.38 <sup>h</sup>	15.89 $\pm$ 0.16 <sup>H</sup>	2.64 $\pm$ 0.06 <sup>g</sup>	2.03 $\pm$ 0.02 <sup>E</sup>	7.57 $\pm$ 0.11 <sup>f</sup>	7.42 $\pm$ 0.10 <sup>H</sup>
A	11.28 $\pm$ 0.48 <sup>g</sup>	19.48 $\pm$ 0.83 <sup>I</sup>	0.93 $\pm$ 0.03 <sup>f</sup>	2.25 $\pm$ 0.05 <sup>F</sup>	6.62 $\pm$ 0.12 <sup>c</sup>	5.61 $\pm$ 0.05 <sup>F</sup>
C+X+F+A+P	21.88 $\pm$ 1.08 <sup>i</sup>	14.82 $\pm$ 0.27 <sup>G</sup>	2.82 $\pm$ 0.13 <sup>h</sup>	1.92 $\pm$ 0.04 <sup>D</sup>	16.94 $\pm$ 0.14 <sup>i</sup>	6.57 $\pm$ 0.09 <sup>G</sup>

C: cellulase; X: xylanase; F: feruloyl esterase; P: protease; A:  $\alpha$ -amylase.

### 3.3 Multivariate analysis

Principal component analysis (PCA) is one of the most classical and widely used techniques to reduce dimensionality and increase interpretability of large datasets. PCA was performed to evaluate the extractable and bound fractions of spelt seeds treated with different combinations of enzymes based on their TPCs, and their antioxidant activities (DPPH<sup>•</sup>, ABTS<sup>+</sup>) (Fig. 1). Principal component 1 (PC1) explained up to 72.3% of total variance and PC2 explained 24.4%. Thus, the presented two-dimensional graph was able to explain 96.7% of the variability in the experimental data (Fig. 1). Samples were separated along the first PC by differences observed in TPC and DPPH<sup>•</sup>, while the second PC separated the samples based on ABTS<sup>+</sup>. As can be seen in Fig. 1, there are three groups of samples and two samples that cannot be assigned to any group. It can be observed that the groups do not overlap, so a clear separation can be observed between samples treated with different enzymes and their combinations.

Extractable fractions of samples treated with individual enzymes or in combination are positioned in the left upper side of the graph. These samples showed lower TPC and DPPH<sup>•</sup> scavenging activity compared to extractable fractions of C+X+F+A+P and protease treated samples, while showed significantly higher levels of TPC, DPPH<sup>•</sup> and ABTS<sup>+</sup> scavenging activities than non-treated extractable fraction. The extractable fractions of samples treated with protease alone or in combination (C+X+F+A+P) are positioned in the right side of the graph (Fig. 1). These samples had the highest extractable TPCs, DPPH<sup>•</sup> and ABTS<sup>+</sup> scavenging.

The second group represents the bound fractions of samples treated with cellulase, xylanase and feruloyl esterase alone or in combination (C+X; X+F; C+X+F) and non-treated bound

fraction. These samples showed lower bound TPCs, DPPH<sup>•</sup> and ABTS<sup>•+</sup> scavenging activities compared to other group containing bound fractions of protease, amylase and C+X+F+A+P treated samples. The last group represents the bound fraction of samples treated with protease, amylase and combination of all five enzymes (C+X+F+A+P). These samples showed the highest TPCs, DPPH<sup>•</sup> and ABTS<sup>•+</sup> scavenging activities among bound fractions (Fig. 1). It is interesting to note that extractable fraction of sample treated with all five enzymes has significantly different position in the graph than other extractable fractions and the corresponding bound fraction, suggesting that there are much greater differences between these samples (Fig. 1). Extractable fraction of sample treated with protease positioned closer to the bound fractions, indicating that there are certain similarities between these samples, mainly because of the increase in extractable phenolics due to the release of bound phenolics.

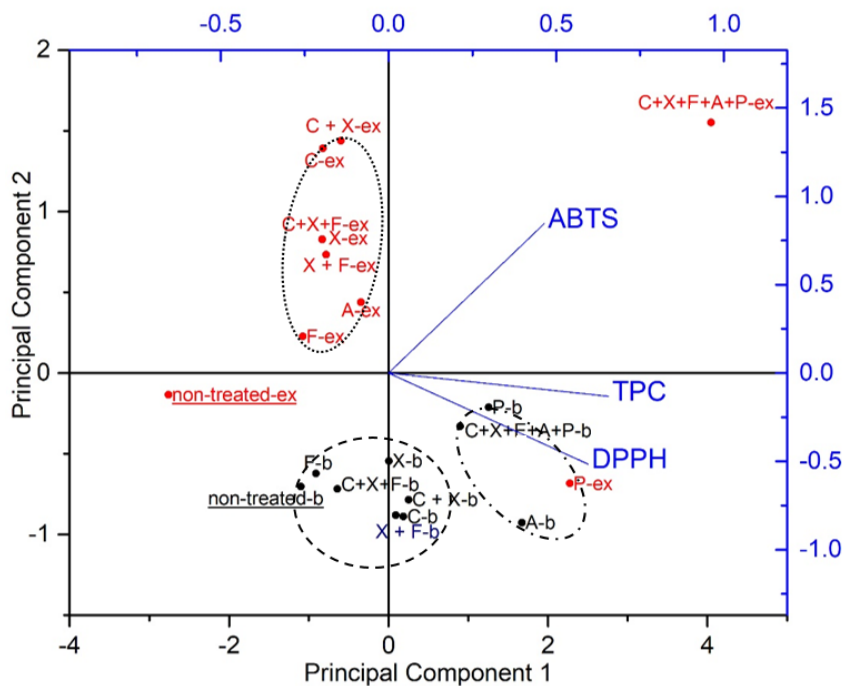


**Figure 1:** PCA biplot of the first two principal components from analysis of extractable (ex) and bound (b) fractions of spelt seeds treated with different enzymes. TPC: total phenolic content; DPPH: DPPH<sup>•</sup> scavenging activity; ABTS: ABTS<sup>•+</sup> scavenging activity; C: cellulase; X: xylanase; F: feruloyl esterase; P: protease; A:  $\alpha$ -amylase.

#### 4 CONCLUSIONS

This study demonstrates an approach where treatments with enzymes alone or in combinations significantly improves the extractable TPCs and their antioxidant activities of spelt seeds. Additionally, treatment with combining all enzymes was clearly the most efficient way to release a large amount of bound phenolics in the extractable form and improve their accessibility. Enzymatic treatment significantly improves extractable TPC in all cases, but the bound TPC still represented a prevalent proportion, except for protease and C+X+F+A+P treatments. Our results showed that enzymatic treatment could be used to enhance the extractable antioxidant activities and the potential bioaccessibility of antioxidants in spelt seeds. Further studies are needed to explore the specific pathway of enzymatic modification of phenolics to their more potent antioxidant compounds.

## 5 REFERENCES

- Acosta-Estrada, B. A., Gutiérrez-Urbe, J. A., Serna-Saldívar, S. O. (2014). Bound phenolics in foods, a review. *Food Chemistry*, 152, 46-55. <https://doi.org/10.1016/j.foodchem.2013.11.093>
- Azmir, J., Zaidul, I. S. M., Rahman, M. M., Sharif, K. M., Mohamed, A., Sahena, F., Jahurul, M. H. A., Ghafoor, K., Norulaini, N. A. N., & Omar, A. K. M. (2013). Techniques for extraction of bioactive compounds from plant materials: a review. *Journal of Food Engineering*, 117(4), 426–436. <https://doi.org/10.1016/j.jfoodeng.2013.01.014>
- Bautista-Expósito, S., Tomé-Sánchez, I., Martín-Diana, A. B., Frias, J., Peñas, E., Rico, D., Casas, M. J. G., & Martínez-Villaluenga, C. (2020). Enzyme selection and hydrolysis under optimal conditions improved phenolic acid solubility, and antioxidant and anti-inflammatory activities of wheat bran. *Antioxidants*, 9(10), 984. <https://doi.org/10.3390/antiox9100984>
- Bei, Q., Chen, G., Liu, Y., Zhang, Y., & Wu, Z. (2018). Improving phenolic compositions and bioactivity of oats by enzymatic hydrolysis and microbial fermentation. *Journal of Functional Foods*, 47, 512–520. <https://doi.org/10.1016/j.jff.2018.06.008>
- Chen, P. X., Tang, Y., Marcone, M. F., Pauls, P. K., Zhang, B., Liu, R., & Tsao, R. (2015). Characterization of free, conjugated and bound phenolics and lipophilic antioxidants in regular- and non-darkening cranberry beans (*Phaseolus vulgaris* L.). *Food Chemistry*, 185, 298–308. <https://doi.org/10.1016/j.foodchem.2015.03.100>
- Dawidowicz & Olszowy, M. (2013). The importance of solvent type in estimating antioxidant properties of phenolic compounds by ABTS assay. *European Food Research and Technology*, 236(6), 1099–1105.
- Everette, J. D., Bryant, Q. M., Green, A. M., Abbey, Y. A., Wangila, G. W., & Walker, R. B. (2010). Thorough study of reactivity of various compound classes toward the Folin–Ciocalteu reagent. *Journal of Agricultural and Food Chemistry*, 58(14), 8139–8144. <https://doi.org/10.1021/jf1005935>
- Floegel, A., Kim, D.-O., Chung, S.-J., Koo, S. I., & Chun, O. K. (2011). Comparison of ABTS/DPPH assays to measure antioxidant capacity in popular antioxidant-rich US foods. *Journal of Food Composition and Analysis*, 24(7), 1043–1048. <https://doi.org/10.1016/j.jfca.2011.01.008>
- Kern, S. M., Bennett, R. N., Mellon, F. A., Kroon, P. A., & Garcia-Conesa, M.-T. (2003). Absorption of hydroxycinnamates in humans after high-bran cereal consumption. *Journal of Agricultural and Food Chemistry*, 51(20), 6050–6055. <https://doi.org/10.1021/jf0302299>
- Mencin, M., Abramovič, H., Jamnik, P., Mikulič Petkovšek, M., Veberič, R., & Terpinč, P. (2021). Abiotic stress combinations improve the phenolics profiles and activities of extractable and bound antioxidants from germinated spelt (*Triticum spelta* L.) seeds. *Food Chemistry*, 344, 128704. <https://doi.org/10.1016/j.foodchem.2020.128704>

- Moore, J., Cheng, Z., Su, L., & Yu, L. (2006). Effects of solid-state enzymatic treatments on the antioxidant properties of wheat bran. *Journal of Agricultural and Food Chemistry*, 54(24), 9032–9045. <https://doi.org/10.1021/jf0616715>
- Singh, A., Sharma, V., Banerjee, R., Sharma, S., & Kuila, A. (2016). Perspectives of cell-wall degrading enzymes in cereal polishing. *Food Bioscience*, 15, 81–86. <https://doi.org/10.1016/j.fbio.2016.05.003>
- Sungsopha, J., Moongngarm, A., & Kanesakoo, R. (2009). Application of germination and enzymatic treatment to improve the concentration of bioactive compounds and antioxidant activity of rice bran. *Australian Journal of Basic and Applied Sciences*, 3, 3653–3661
- Wang, L., Luo, Y., Wu, Y., Liu, Y., & Wu, Z. (2018). Fermentation and complex enzyme hydrolysis for improving the total soluble phenolic contents, flavonoid aglycones contents and bio-activities of guava leaves tea. *Food Chemistry*, 264, 189–198. <https://doi.org/10.1016/j.foodchem.2018.05.035>
- Yu, J., Vasanthan, T., & Temelli, F. (2001). Analysis of phenolic acids in barley by high-performance liquid chromatography. *Journal of Agricultural and Food Chemistry*, 49(9), 4352–4358. <https://doi.org/10.1021/jf0013407>

POKROVITELJI DOGODKA / SPONSORS

**barcaffé**



omegac

**WRIGLEY**